SKELETAL MUSCLE REGULATORY FACTORS WITH ALTERATIONS IN MUSCLE MASS

by

Jennifer Michele Litt Miller
B.Sc. (Kinesiology), University of Waterloo, 2001

DISSERTATION SUBMITTED IN PARTIAL FULFILLMENT OF
THE REQUIREMENTS FOR THE DEGREE OF

DOCTOR OF PHILOSOPHY

In the
School of Kinesiology
Faculty of Applied Sciences

SIMON FRASER UNIVERSITY

Spring 2007

Your file Votre référence
ISBN: 978-0-494-38188-5
Our file Notre référence
ISBN: 978-0-494-38188-5

APPROVAL

Name: **Jennifer Michele Litt Miller**

Degree: **Doctor of Philosophy**

Title of Dissertation: **Skeletal Muscle Regulatory Factors with Alterations in Muscle Mass**

Examining Committee:

Chair: **Dr. Parveen Bawa**
Professor, School of Kinesiology

Dr. Wade Parkhouse
Senior Supervisor
Professor, School of Kinesiology

Dr. Charles Krieger
Supervisor
Professor, School of Kinesiology

Dr. Neil Watson
Internal Examiner
Professor, Department of Psychology

Dr. Don McKenzie
External Examiner
Professor, Human Kinetics, UBC

Date Defended: April 5, 2007

ABSTRACT

Given that maintenance of skeletal muscle mass is essential for overall health, functionality and quality of life, it is critical to elucidate the fundamental mechanisms underlying the maintenance of muscle mass which likely vary as a function of muscle status (i.e. healthy or diseased). This thesis examined key skeletal muscle regulatory factors (smRFs) that are known to affect skeletal muscle mass, including components of the PI3K/Akt and MAPK(ERK) pathways, calcineurin, the myogenic regulatory factors and myostatin, following administration of a β_2-adrenergic agonist, Clenbuterol, and with progressive denervation.

Although it is known that Clenbuterol induces hypertrophy and attenuates atrophy of skeletal muscle, its mechanism of action is unclear. In this thesis, I have demonstrated that Clenbuterol induces PKA-independent stimulation of smRFs (cAMP, p-Akt, p-ERK), and additional phospho-kinases (PKCa, PAK1/2/3, FAK and Pyk2) that are also thought to be involved in regulating muscle mass. These changes occur relatively rapidly, often within 10 minutes of administration.

Using a G93A mouse model of progressive denervation, I found an up-regulation of smRFs involved in growth/survival (Akt, calcineurin, ERK1/2), and decreases in the myogenic regulatory factor, MyoD, in skeletal muscle of these mice. These alterations occurred in conjunction with the onset of later-stage (i.e. severe) symptoms but prior to significant muscle atrophy. I was therefore interested in determining if Clenbuterol would attenuate the onset of disease symptoms and muscle atrophy accompanying the

progressive denervation by altering these smRFs. Akt and MyoD levels in the G93A mouse were similar to wild-type muscle after six weeks of Clenbuterol treatment. Clenbuterol also attenuated the progression of symptoms in G93A mice which may account for the levels of smRFs observed. Increases in G93A mouse body mass, improved motor coordination (RotoRod) and strength (PaGE, females only) were also observed with Clenbuterol treatment without significant increases in muscle mass.

This thesis suggests that alterations in smRFs, including the PI3K/Akt and MAPK(ERK) pathways, calcineurin, and the myogenic regulatory factors occur prior to any observable changes in muscle mass. Identification of these muscle-specific factors has clinical relevance for the characterization and treatment of skeletal muscle atrophy associated with chronic diseases.

Keywords: skeletal muscle mass, cell signalling, Clenbuterol, progressive denervation

Subject Terms: Striated muscle – physiology;
Cellular signal transduction;
Neuromuscular Diseases – research;
Muscle Proteins

STATEMENT OF ETHICS APPROVAL

The author, whose name appears on the title page of this work, has obtained, for the research described in this work, either:

(a) Human research ethics approval from the Simon Fraser University Office of Research Ethics,

or

(b) Advance approval of the animal care protocol from the University Animal Care Committee of Simon Fraser University;

or has conducted the research

(c) as a co-investigator, in a research project approved in advance,

or

(d) as a member of a course approved in advance for minimal risk human research, by the Office of Research Ethics.

A copy of the approval letter has been filed at the Theses Office of the University Library at the time of submission of this thesis or project.

The original application for approval and letter of approval are filed with the relevant offices. Inquiries may be directed to those authorities.

ACKNOWLEDGEMENTS

I would like to thank my senior supervisor, Dr. Wade Parkhouse for sharing an incredible wealth of knowledge and offering support throughout my graduate experience. I could not have become the researcher or person I am today without your guidance. Thank you to Dr. Charles Krieger for offering insight and support during the course of my degree. I would also like to acknowledge NSERC and SFU for funding I received to support my graduate research activities.

Thank you to all of the friends I have made during my time at SFU – I could not have navigated this roller coaster ride without your assistance with lab protocols, trips to Renaissance, the Highland Pub and Terry Fox field, and the many conversations (scientific or not) we've had in the last 5+ years. To Shona and Susie, you are godsends to any graduate student and I could never have survived without you both. To Laurie, Marilyn and Van – thank you for your support during my time here. Thank you to the gang down at ACF for your assistance and making my job much easier.

To my Mom and Dad, my deepest thanks for always being there for me with never-ending love and support no matter what road I chose to follow. To Sonya and Dave, my extended family who have adopted me as one of your own, thank you. Finally, to Aaron, from the bottom of my heart I thank you for being there for me everyday, for never questioning why, and for your understanding and love that helped get me through this chapter in my life.

TABLE OF CONTENTS

LIST OF FIGURES

LIST OF TABLES

CHAPTER 1: REVIEW OF LITERATURE

Skeletal Muscle Mass

Maintenance of skeletal muscle mass is essential for overall health, functionality and quality of life. Loss of muscle mass results in substantial decreases in muscular strength; declines in muscle are predictive of increased rates of incident disability and mortality (Metter et al., 2002). Information regarding the elements that regulate mass, specifically the expression and/or content of muscle-specific signalling factors, is critical in elucidating the fundamental mechanisms underlying the maintenance of muscle mass. It is also of clinical relevance for the characterization and treatment of declines in skeletal muscle mass associated with chronic diseases.

For more than 50 years, researchers have investigated a number of different factors hypothesized to be involved in the regulation of skeletal muscle mass and overall muscular health (Glass, 2005; Sartorelli and Fulco, 2004). More recent literature has suggested that muscle quality and not necessarily absolute mass may be the best predictor of muscular health and functionality (Goodpaster et al., 2006). The condition of skeletal muscle or *muscle mass status* may ultimately reflect the overall health and well-being of the muscle. This status can be thought of as an interplay of many morphological, functional and biochemical characteristics including not only the muscle's size (cross-sectional area) and degree of functionality, but also the composition and/or expression of key muscle-specific signalling factors thought to be involved with the maintenance of skeletal muscle mass.

Skeletal Muscle Atrophy

Atrophy is most often caused by disuse/inactivity and is associated with aging, poor nutrition/starvation, and chronic diseases resulting from genetic abnormality or systemic disease (McKinnell and Rudnicki, 2004). Regardless of its etiology, atrophy is characterized by decreases in muscle fibre diameter, total protein content, force generation, and fatigue resistance (Jackman and Kandarian, 2004). Anabolic and catabolic imbalances exist when muscle atrophies, where rates of protein degradation exceed those of protein synthesis. This imbalance leads to decreases in total muscle protein, muscle mass and impaired functional capacity. Because of this impairment, atrophied muscle is often referred to as compromised or abnormal muscle tissue.

Hypoactivity of skeletal muscle results in muscle atrophy within days of short-term experimental models including hindlimb suspension, immobilization, nerve transection, or denervation (Mercier et al., 1999; Dupont-Versteegden et al., 2004). Denervation-induced atrophy is characterized by a decrease in mean muscle cross-sectional area and increase in the proportion of angulated fibres (Pachter and Eberstein, 1992). Atrophy is also associated with ultrastructural changes within the muscle including extensive proteolysis (Goldberg, 1969), disorganization of sarcomeres via actin and myosin filament disruption (Lu et al., 1997) and a progressive loss of mitochondria (Borisov et al., 2001). Denervation also leads to the accumulation of connective tissue, a decrease in the number of satellite cells, and apoptosis of myonuclei (Carlson et al., 2002). Acute denervation models do not necessarily parallel chronic models such as aging, chronic deconditioning, progressive denervation, or chronic disease.

Progressive denervation of skeletal muscle is often associated with aberrant reinnervation, aging and neuromuscular disorders (Solomon and Bouloux, 2006). Individuals with amyotrophic lateral sclerosis (ALS) are troubled by progressive denervation and subsequent atrophy of skeletal muscle tissue. Although the cause of ALS, a progressively debilitating and fatal neurodegenerative disease, is unknown, it is characterized by a progressive loss of both upper and lower motor neurons (Corbett et al., 1982) followed by extensive denervation and significant skeletal muscle atrophy (Frey et al., 2000). This continuous loss of functional motor neurons, particularly of larger, fast type motor units (Theys et al., 1999), prevents the capacity to sprout and regenerate denervated muscle tissue (Chiu et al., 1995). Research had shown cellular (protein) alterations of nervous tissue with models of progressive denervation (Hu et al., 2003), however, the effects of progressive denervation on muscle-specific signalling factors is currently unclear.

Skeletal Muscle Hypertrophy

Muscle hypertrophy is accompanied by an increase in net protein turnover, whereby muscle protein synthesis exceeds protein degradation. Increases in protein synthesis occur via increases in transcription, translation or through the addition of myonuclei (Bodine, 2006). Mechanical (i.e. stretch or contraction of the muscle) and chemical (i.e. hormonal or metabolic elements acting on the muscle) stimuli have been shown to induce muscle hypertrophy and are often dependent upon the nature of the stimulus (i.e. its intensity, frequency and specificity) (Baldwin and Haddad, 2002). Significant muscle hypertrophy is observed with resistance training in humans and in overloaded rodent skeletal muscle (Alway et al., 2005). Compensatory overload and

continuous stretch of muscle fibres have also been shown to hypertrophy muscle of animals (Booth and Thomason, 1991).

Targeted genetic manipulation of specific growth-related factors within skeletal muscle cells has been shown to induce hypertrophy, reflected in increases in myotube area, width, and rates of protein synthesis (Semsarian et al., 1999a). Cellular changes associated with hypertrophy can be induced and examined with as little as a single dose of selective pharmacological agents. Among other anabolic agents, the β_2-adrenergic agonist, Clenbuterol, has been shown to increase protein synthesis (Horne and Hesketh, 1990) and muscle hypertrophy in both cardiac and skeletal muscle tissue (MacLennan and Edwards, 1989). Increases in both slow and fast-twitch muscle mass (per kg wet weight) have been observed with Clenbuterol treatment in both normal and compromised/abnormal rat muscle (Hinkle et al., 2002; Herrera et al., 2001; Sneddon et al., 2001; Murphy et al., 1996; Carter and Lynch, 1994b; Carter et al., 1991; Zeman et al., 1987). As such, Clenbuterol could be a potential therapeutic agent for the prevention/treatment of skeletal muscle atrophy. However, the mechanism by which this drug acts, including its effect on muscle-specific signalling factors is unclear at this time.

Cellular Regulation of Muscle Mass: smRFs

Recent investigations regarding the regulation of myogenesis and skeletal muscle mass have resulted in the identification of key muscle-specific signalling pathways and proteins (Figure 1). These factors, hereon referred to as *skeletal muscle regulatory factors* (smRFs), have been shown to turn on/off with a variety of stimuli, including muscle hypertrophy and/or atrophy, organism development and differential loading conditions. Changes occur within the muscle itself at a cellular level long before

observable alterations in mass, rates of protein synthesis and/or levels of circulating growth factors. smRFs that have been previously shown to be involved with skeletal muscle hypertrophy and/or atrophy include PI3-kinase/Akt/p70s6k (Rommel et al., 2001), ERK1/2 (Widegren et al., 2000; Williamson et al., 2003), calcineurin (Michel et al., 2004), the myogenic regulatory factors (Lowe et al., 1998), myostatin (McPherron et al., 1997), and the β_2-adrenergic (AC/cAMP/PKA) pathway (Zeman et al., 1987).

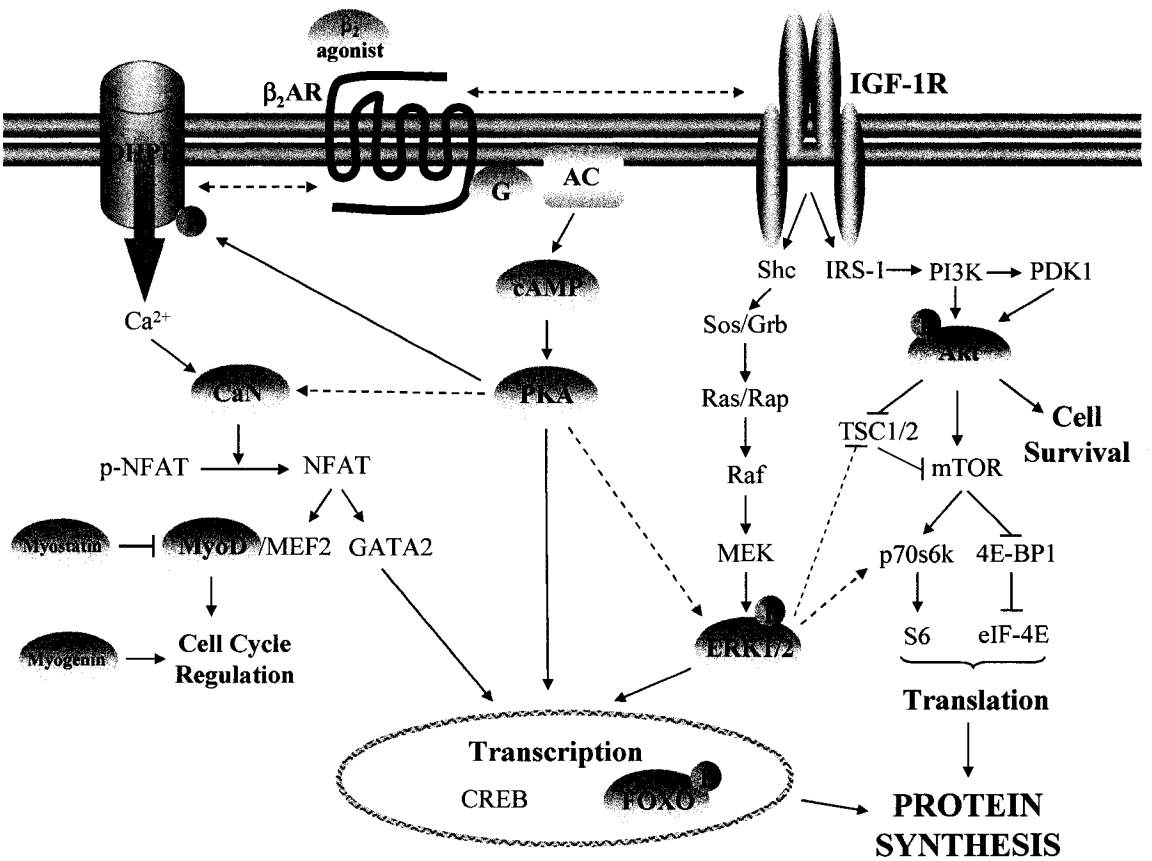

Figure 1: Simplified schematic of key skeletal muscle regulatory factors (smRFs) known to be involved in the regulation of skeletal muscle mass.
Factors shown are defined within text [note: Ca^{2+}- calcium ion; CREB - cAMP response element-binding protein; DHPR - dihydropyradine receptor (L-type calcium channel)]. Solid arrows refer to confirmed pathways/interactions. Dotted arrows refer to speculated pathways/interactions. Those factors examined within the context of this dissertation are highlighted in orange.

smRFs: Muscle-specific Signalling Factors Involved in the Regulation of Muscle Mass

A number of smRFs have been shown to be linked to insulin-like growth factor-1 (IGF-1). IGF-1 is an anabolic hormone that is released from the muscle itself and acts through a variety of protein kinase intermediates to promote DNA synthesis, satellite cell proliferation, amino acid uptake, and glycogen and protein synthesis (Adams, 1998). In skeletal muscle, IGF-1 mRNA increases three-fold within two days of functional overload in rodents (DeVol et al., 1990) and within a single bout of eccentric exercise in humans (Bamman et al., 2001). Transgenic mice that over-express IGF-1 using a muscle-specific promoter possess muscles that are double in mass compared to wild-type control mice (Shavlakadze et al., 2005; Musaro et al., 2001; Coleman et al., 1995) and demonstrate accelerated muscle regeneration (Rabinovsky et al., 2002; Musaro et al., 2001).

The biological actions of IGF-1 are initiated via the binding of IGF-1 to the extra cellular α-subunit of its own tyrosine-kinase receptor (IGF-1R) on the cell membrane and subsequent activation/phosphorylation of a number of intracellular substrates, including Shc (src homology-containing domain) and IRS-1 (Myers et al., 1994; Coolican et al., 1997). Insulin receptor substrate-1 (IRS-1) is the major cytosolic substrate of the IGF-1 receptor and serves as a docking protein to support the assembly of protein complexes and to initiate additional myogenic, intracellular signalling pathways such as the phosphatidylinositol 3-kinase (PI3K) cascade (Myers et al., 1994; Butler et al., 1998; Coolican et al., 1997).

PI3K/Akt

When phosphorylated by IGF-1, the cytosolic docking protein, IRS-1, binds to and activates the p85 regulatory subunit of a lipid kinase, phosphatidylinositol 3-kinase (PI3K). PI3K exists ubiquitously in various tissues but is known to play a key role in skeletal muscle proliferation/differentiation, protein synthesis, and muscle cell survival (Glass, 2003a). It is activated by a variety of growth factors, including IGF-1 (Halevy and Cantley, 2004; Rommel et al., 2001), fibroblast growth factor (Katoh and Katoh, 2006), and vascular endothelial growth factor (Li et al., 2003; Kosmidou et al., 2001). Levels of PI3K increase in hypertrophied skeletal muscle and decrease with atrophy (Rommel et al., 2001; Bodine et al., 2001). Inactive PI3K leads to decreases in organ size (both cell size and number) (Weinkove and Leevers, 2000).

PI3K acts through a variety of membrane-phospholipids, including phosphatidylinosital-4,5-biphosphate (PtdIns-4,5-P_2), phosphatidylinositol-3,4,5-triphosphate (PtdIns-3,4,5-P_3), and phosphatidylinositol-3,4-biphosphate (PtdIns-3,4-P_2) (Woscholski et al., 1995). PtdIns-3,4,5-P_3 acts as a binding site for two protein kinases associated with PI3K: Akt (also protein kinase B, PKB) and phophoinositide-dependent protein kinase (PDK1). These two downstream kinases subsequently initiate a signalling cascade of kinase intermediates involved in protein synthesis, gene transcription, glucose metabolism, and cell proliferation (Glass, 2003a).

Akt, which exists primarily as the isoform Akt1 in skeletal muscle, is a serine/threonine kinase that is activated by both PI3K-dependent and -independent mechanisms (Sakamoto and Goodyear, 2002). Akt was originally observed to display similar physical and functional properties to those of protein kinase A (PKA) and protein

kinase C (PKC), resulting in its PKB designation (Scheid and Woodgett, 2001). After binding to PtdIns-3,4,5-P_3, Akt translocates to the cell membrane and is activated (phosphorylated) by PDK1 at two specific amino acid residues on the kinase (Thr^{308} and Ser^{473}) (Alessi et al., 1996). Phosphorylation of both sites is required for full activation of the kinase, although this process is not yet fully understood (Toker and Newton, 2000).

Akt has been shown to have critical roles in hypertrophy and the prevention of muscle atrophy *in vivo* (Bodine et al., 2001) and it is activated by muscle contraction in a rapid and transient fashion (Sakamoto and Goodyear, 2002). Over-expression of a constitutively active form of Akt1 (c.a. Akt) in rodent skeletal muscle via transfection (Pallafacchina et al., 2002) or genetic manipulation (Lai et al., 2004) has been shown to promote a 2-fold increase in muscle fibre diameter in both healthy and atrophied muscle (Bodine et al., 2001). In cardiac muscle tissue, over-expression of Akt leads to a significant increase in cardiomyocyte size and left ventricular hypertrophy (Condorelli et al., 2002).

Akt-deficient mice demonstrate a marked impairment in organism and skeletal muscle growth (Cho et al., 2001). Ten to fourteen days of muscle unloading via hindlimb suspension in rats results in a decrease in Akt content and activity (phosphorylated Akt, p-Akt) and muscle atrophy (Bodine et al., 2001; Sugiura et al., 2005). Akt activity increases in innervated muscles when compared to denervated muscles in parallel with muscle growth (Pallafacchina et al., 2002). In the G93A mouse, a model of progressive denervation, there are conflicting reports regarding levels of Akt in progressively denervated skeletal muscle. Whereas increases in Akt protein content has been found in progressively denervated skeletal muscle of G93A mice (Cunningham L, thesis), other

studies have cited decreases in the pAkt/Akt ratio in these mice (Leger et al., 2006). Clarification of this discrepancy is needed.

Downstream of this kinase, Akt phosphorylates and activates the mammalian target of rapamycin (mTOR) that is critical to the regulation of proliferation and skeletal muscle growth (Bodine, 2006). mTOR, a serine/threonine kinase, has also been shown to be activated following functional overload (Bodine et al., 2001) and treatment with insulin, IGF-1 (Parkington et al., 2003) and essential amino acids (Rennie et al., 2004). Recently literature has identified mTOR as a key junction point for different signalling pathways aside from PI3K/Akt, including the MAPK (ERK) pathway (discussed in the next section). Although mTOR signalling appears to be complex, it is thought to primarily regulate protein translation through two distinct mechanisms: 1) phosphorylation of the ribosomal protein S6 kinase (p70s6k) and 2) phosphorylation of the eukaryotic initiation factor (eIF) binding protein, eIF 4E-BP1. Together, p70s6k and 4E-BP1 coordinate the translation of proteins, the behaviour of eukaryotic initiation factors and ribosomes (Shah et al., 2000b).

p70s6k is thought to play a critical role in regulating the translation of a class of mRNA transcripts that contain a 5' TOP (terminal oligopyrimidine tract) at their transcriptional start site (Sakamoto and Goodyear, 2002) and therefore is an important signalling intermediate that leads to the activation of protein synthesis and muscle hypertrophy. Activated p70s6k hyperphosphorylates the ribosomal protein, S6, and enables the up-regulation of 5' TOP mRNAs for encoding translational (elongation) machinery and ribosomal proteins (Alessi et al., 1998). Treatment of cells with rapamycin (a blocker of mTOR) eliminates the phosphorylation and activation of p70s6k

(Jefferies et al., 1997) and almost completely inhibits muscle hypertrophy (Bodine et al., 2001).

Activation of p70s6k is increased following *in situ* contraction (Baar and Esser, 1999; Haddad and Adams, 2002), high frequency stimulation (Nader and Esser, 2001; Baar and Esser, 1999), and resistance exercise *in vivo* (Hernandez et al., 2000). This activation is often found to be delayed and transient (Bodine et al., 2001) but remains elevated in hypertrophied skeletal muscle 36 hours following electrical stimulation (Hernandez et al., 2000). The degree of p70s6k phosphorylation (activation) is correlated with increase in muscle weight (Baar and Esser, 1999). In contrast, irradiated muscle demonstrates decreases in p70s6k phosphorylation, impacting protein synthetic rates (Adams et al., 2002).

mTOR also exerts its effects on protein translation through phophorylating the translation repressor, 4E-BP1 (also known as PHAS-I, phosphorylatable heat- and acid-stable inhibitor) (Shah et al., 2000b) which is predominantly expressed in skeletal, cardiac muscle and adipose tissue (Hu et al., 1994). When demand for translation is low, 4E-BP1 exists in a dephosphorylated form and acts as a strong translational inhibitor by binding and forming a relatively stable complex with eukaryotic initiation factor (eIF)-4E (Jackman and Kandarian, 2004; Shah et al., 2000a). Phosphorylation of 4E-BP1 leads to its release from the inhibitory complex (Bodine, 2006). For example, when the receptor tyrosine kinase (RTK) family of growth factor receptors are stimulated, the (eIF)-4E--4E-BP1 complex is disturbed and (eIF)-4E is free to associate with additional scaffolding proteins (i.e. eIF-4G) to increase protein translational capacity (Shah et al., 2000a). 4E-BP1 phosphorylation is both LY294002 (a PI3K inhibitor) and rapamycin sensitive (Shah

et al., 2000a). The amount of (eIF)-4E--4E-BP1 complex and/or level of 4E-BP1 mRNA has been found to be increased in atrophied gastrocnemius muscle due to hindlimb unloading (Bodine et al., 2001) and starvation (Jagoe et al., 2002), reflecting decreased rates of protein translation. As is expected, the stability of the inhibitory (eIF)-4E--4E-BP1 complex is favoured in these compromised situations (Shah et al., 2000a).

Recent evidence points to the important role of PI3K/Akt in modulating muscle cell survival (Lawlor and Rotwein, 2000), through associations with many pro-survival molecules. The various functions of Akt may be due to a number of different downstream signalling intermediates through which it exerts its growth and/or survival effects (Downward, 1998). For example, increased levels of apoptosis (programmed cell death) have been shown in neuronal cells transfected with an inactive form of Akt (Dudek et al., 1997). A variety of researchers have investigated the pathway's impact on cellular survival via its interactions with different signalling proteins, including the ability of Akt to inactivate anti-apoptotic proteins Bcl-2 and Bcl-X_L (Yang et al., 1995) and the forkhead (FKHR) family of transcription factors (Brunet et al., 1999).

Members of the FKHR or winged helix transcription factor family regulate transcription of genes important in metabolism (Nakae et al., 2001), cell cycle progression (Dijkers et al., 2000; Shi and Garry, 2006), and apoptosis (Brunet et al., 1999). Previous research has identified three mammalian homologues: FKHR (FOXO1), FKHRL1 (FOXO3a), and AFX (FOXO4) (Furuyama et al., 2002). In the regulation of muscle mass, phosphorylation of FKHR (p-FKHR) by Akt results in exclusion from the nucleus and away from their target, pro-apoptotic genes (Brunet et al., 1999). Conversely, dephosphorylation of FKHR factors results in their entry into the nucleus

followed by activation of pro-apoptotic factors (Sandri et al., 2004). Dephosphorylated FKHR has been shown to negatively regulate skeletal muscle mass and function (Kamei et al., 2004). Members of the FKHR family have been shown to regulate the fate of muscle precursor cells, including the cell cycle kinetics of satellite cells (Shi and Garry, 2006). As the PI3K/Akt pathway stimulates a variety of different signalling proteins in skeletal muscle, it plays significant roles in regulating protein synthesis and cell survival, this combination of functions subsequently influences skeletal muscle mass.

Extra-cellular Signal-Regulated Kinases (ERKs)

In addition to the PI3K/Akt pathway, IGF-1 also activates the extra-cellular signal-regulated kinase (ERK) pathway (Figure 1). The ERK pathway, a component of the more general group of the mitogen-activated protein kinase (MAPK) signalling pathways, is ubiquitously expressed, plays a primary role in cell proliferation or mitogenesis and has been shown to regulate cell development, differentiation and survival (Chuderland and Seger, 2005).

Binding of IGF-1 to its receptor attracts SH2 binding domains of the docking protein Shc to the receptor's intracellular surface. Shc binds with small G-proteins, Grb1 and Sos, to activate further downstream components of the ERK pathway. As with other MAPK pathways, the ERK pathway consists of a series of kinase intermediates that phosphorylate and activate in a specific order (ERK-specific signalling proteins are shown in parentheses): MAPKKKK (Ras and Rap), MAPKKK (Raf), MAPKK (MEK), and MAPK (ERK). Two isoforms of ERK exist in skeletal muscle tissue, ERK1 (or p44MAPK) and ERK2 (or p42MAPK), with numerical reference indicative of the protein's molecular weight (in kDa). ERK1 and ERK2 have only a 17% divergence in

their amino acid sequence and elicit similar regulatory function with respect to phosphorylation and location within the cell (Chuderland and Seger, 2005). As such, references to the two isoforms within muscle are often written as a single ERK (ERK1/2) term. Activation of ERK via phosphorylation at two sites (Thr^{202} and Tyr^{204}) induces conformational changes that exposes a catalytic pocket and allows ERK to phosphorylate downstream targets such as specific transcription factors Elk-1, CREB, c-jun and c-fos, involved in modulating protein synthesis (Chuderland and Seger, 2005).

The interactions between the PI3K/Akt and MAPK(ERK) pathways in skeletal muscle contribute to the complexity of cellular regulation of muscle mass. Cross-talk between the two pathways has been demonstrated in skeletal muscle (Wang et al., 2001) as ERK phosphorylation is induced by activating Akt (Campbell et al., 2004). Much of this cross-talk evidence suggests that the two signalling pathways converge at mTOR, with more recent literature pointing to a protein complex upstream of mTOR, the tuberous sclerosis complex (TSC), which consists of the proteins tuberin, the product of the TSC2 gene, and hamartin, the product of the TSC1 gene (Williamson et al., 2006). Tuberin is a GTPase-activator protein (GAP) that binds to and inhibits mTOR function in its dephosphorylated state (Castro et al., 2003). Co-expression of both TSC1 and TSC2 have been shown to dephosphorylate downstream targets of mTOR, such as 4E-BP1 and S6K (Tee et al., 2002), leading to inhibition of protein translation. Phosphorylation of tuberin results in the inactivation of the tuberin-hamartin complex, a decreased tuberin-GAP activity and stimulation of mTOR signalling (Williamson et al., 2006). Tuberin has been shown to be phosphorylated by Akt (Potter et al., 2003) as well as ERK1 and ERK2

(Ma et al., 2005), which enhances mTOR signalling by inhibiting GAP-mTOR interactions.

The ERK pathway is activated by IGF-1 administration (Adi et al., 2002), β_2-adrenergic agonists (Shi et al., 2006), acute and chronic exercise (Williamson et al., 2006; Widegren et al., 2001), muscle contraction and mechanical stretch (Rennie et al., 2004). However, whereas growth factor administration normally increases the activation of the ERK pathway, it's activation has also been shown to be attenuated in aged cells (Hutter et al., 2000), indicating that the ERK pathway may not promote muscle growth in situations of compromised muscle mass.

Calcineurin

Calcineurin is a serine/threonine protein phosphatase 2B that is important in calcium signalling and also thought to act as a key regulatory second messenger involved with skeletal muscle hypertrophy (Dunn et al., 1999; Bodine et al., 2001; Mitchell and Pavlath, 2002; Schiaffino and Serrano, 2002). Until recently, few studies have focused on the role that calcineurin plays in the regulation skeletal muscle mass.

The 61 kDa calmodulin-binding catalytic subunit of calcineurin (calcineurin A) is activated in overloaded muscles (Dunn et al., 2000; Mitchell and Pavlath, 2002). Once activated, calcineurin signals downstream to additional proteins and genes involved in the regulation of muscle fibre size and myofibrillar protein phenotype. Calcineurin dephosphorylates transcription factors, including GATA-2, nuclear factor of activated T cells (NFAT) and myocyte enhancer factor 2 (MEF2) (Dunn et al., 2000; Musaro et al., 1999). These transcription factors, when dephosphorylated, translocate to the nucleus

where they activate the transcription of various genes involved in protein synthesis (Mitchell and Pavlath, 2002).

Although calcineurin's role in muscle growth has been well established in cardiac muscle, its influence in skeletal muscle is less clear. Calcineurin has been found to be highly correlated with muscle mass as well as changes in contractile and metabolic components of skeletal muscle (Mitchell et al., 2002). Early *in vitro* studies with skeletal muscle cell lines have suggested that calcineurin may influence muscle hypertrophy (Bodine et al., 2001; Semsarian et al., 1999b) as both hypertrophy and protein transcription are inhibited by cyclosporin A, a calcineurin blocker (Dunn et al., 1999; Mitchell and Pavlath, 2002; Mitchell et al., 2002). However, transgenic mice that over-express activated calcineurin do not exhibit skeletal muscle hypertrophy (Dunn et al., 2000; Naya et al., 2000). It is speculated that sufficient levels of calcineurin (for growth) are present in normal, healthy skeletal muscle (Rennie et al., 2004). Recent literature suggests that calcineurin's influence on skeletal muscle hypertrophy may require additional signalling intermediates, potentially factors associated with the PI3K/Akt pathway (Rommel et al., 2001).

Calcineurin's role in the regulation of muscle mass may depend on muscle phenotype and the stage of myofibre growth (Mitchell et al., 2002). Calcineurin plays a key role in the promotion of the slow-twitch muscle gene programme (Stewart and Rittweger, 2006; Schiaffino and Serrano, 2002) as a ten-fold over-expression of a constitutively active form of calcineurin (c.a. CaN) has been shown to promote fast-to-slow fibre type transformations (Naya et al., 2000; Serrano et al., 2001). Inhibition and/or lack of calcineurin genetically leads to a reduction in slow, oxidative skeletal

muscle fibres (Bassel-Duby and Olson, 2003) and the up-regulation of a faster phenotype (Spangenburg and Booth, 2003). However, many of these studies have also shown this transformation in the absence of observable muscle fibre hypertrophy. Further studies are needed to clarify the role of calcineurin in the regulation of muscle mass.

Calcineurin levels are elevated rapidly (3-10 days) during recovery from a 10-day hindlimb suspension protocol (Childs et al., 2003; Sugiura et al., 2005). Stupka et al. (2004) also found that calcineurin is essential for muscle regeneration in *mdx* mice, a model that is characterized by progressive muscle degeneration. These results imply that calcineurin's role in muscle growth may depend on the system studied including its muscle mass status. It has also been suggested that calcineurin plays a role in muscle regeneration following injury (Sakuma et al., 2003). Calcineurin may possess clinically relevant therapeutic properties for the prevention and/or treatment of muscle atrophy, since up-regulation of a slow muscle phenotype could have superior fatigue-resistance. In situations of muscle denervation or atrophy, it is hypothesized that calcineurin may attenuate the targeted atrophy of faster fibres and prolonging muscular survival.

Myogenic Regulatory Factors (MRFs)

Development and maturation of skeletal muscle (i.e. myogenesis) depends on a multitude of signals, including a family of closely related proteins called myogenic regulatory factors (MRFs). The MRFs, a group of transcription factors expressed solely in skeletal muscle cells, are responsible in part, for switching on the muscle cell lineage during development (Rescan, 2001). More recently, it has been suggested that regenerating muscle exhibits similar morphological and biochemical alterations to the developing embryonic muscle (Launay et al., 2001; Charge and Rudnicki, 2004) and

therefore MRFs may play key roles in regeneration following muscle injury/atrophy (Rescan, 2001).

The MRF proteins belong to a group of larger proteins that have a basic DNA-binding motif and a helix-loop-helix (bHLH) dimerization domain (Rescan, 2001). MRFs regulate gene expression, myoblast proliferation and differentiation (Musaro and Rosenthal, 1999). Although MRFs have been primarily implicated in the recruitment and activation of muscle precursor cells, such as satellite cells, they may also promote the proliferation and differentiation of skeletal muscle cells into mature myofibres. Their role in modulating muscle mass during postnatal development and in compromised tissue is unclear.

Four MRFs: MyoD, Myf5, Myogenin, and MRF4, have been identified in studies of embryogenesis and cell culture models of differentiation (Stewart and Rittweger, 2006). All four exhibit distinct but overlapping functions (Rescan, 2001) and are expressed in a hierarchical/sequential fashion during myogenesis (Perry and Rudnicki, 2000). Myf5 and MyoD are initially expressed in proliferating myoblasts and continue to be expressed after muscle determination (Sabourin and Rudnicki, 2000) and promote cellular entry into and through the cell cycle. Myogenin and MRF4 are subsequently expressed following myoblast fusion (Olson, 1992) and act to promote differentiation and exit from the cell cycle (Hinterberger et al., 1991).

Although all four MRFs are important in myogenesis, MyoD and myogenin have been studied more extensively in the literature. Null mutations of an individual or combination of MyoD and myogenin have been implicated in impaired muscular development (Table 1) and have been referred to as markers of skeletal muscle growth

due to their effects on muscle precursor cells and nuclear incorporation (Hyatt et al., 2003). These two MRFs are regulated by electrical activity (Eftimie et al., 1991) and are elevated in human skeletal muscle by 100-400% within 24 hours of a bout of high-intensity resistance exercise (Psilander et al., 2003). Like other smRFs discussed in this review, the response of these MRFs is dependent upon a number of factors, including but not limited to the stimulus (i.e. type, intensity/dose, and duration) as well as initial muscle mass status.

Table 1: Effects of MRF (MyoD and myogenin) null mutations on skeletal muscle characteristics

MRF	Skeletal muscle-specific alterations
MyoD	- near normal muscle without obvious defects; increased expression of Myf-5 (Rudnicki et al., 1992) - increased occurrence of branched myofibres; impaired regenerative capacity (Cornelison et al., 2000) - normal expression of myogenin (Musaro and Rosenthal, 1999)
Myogenin	- marked reduction in skeletal muscle tissue (Rescan, 2001) - die prematurely (Hasty et al., 1993) - severe disorganization of the muscular system (disappearance of most cells in ventrolateral body wall, mononucleation of cells with myoblast properties, absence of Z-lines in most myofibrils) (Nabeshima et al., 1993)
MyoD and Myogenin	- die perinatally; reduced muscle, only mononucleated myotubes present (Musaro and Rosenthal, 1999)

MyoD

MyoD, which is primarily expressed in fast-twitch, Type II skeletal muscle fibres (Voytik et al., 1993), primarily influences transcription and cell proliferation, both in terms of skeletal muscle cell division and replication but also incorporation of satellite cells into existing myofibres. The short half-life of MyoD (20-45 min) suggests that it possesses the ability to rapidly regulate cell cycle progression (Rescan, 2001). MyoD is altered with hypertrophic stimuli, including exercise, overload, and injury (Ishido et al., 2004b) often within hours of the initial stimulus (Ishido et al., 2004a). MyoD protein

levels have been found to increase following denervation (Walters et al., 2000; Hyatt et al., 2003), with speculation that denervation-induced up-regulation may be an attempt to stimulate cell proliferation and attenuate muscle atrophy (Walters et al., 2000). However, MyoD has also been shown to decrease following muscle denervation including sciatic nerve transection (Sakuma et al., 1999), brachial plexus injury (Wu et al., 2002), and joint fixation (Delday and Maltin, 1997). The change in MyoD following denervation may ultimately reflect the characteristics (ie. type, severity and duration) of the denervation protocol or the characteristics of the subject pool (including muscle mass status), an area of research that should be explored further.

MyoD has been shown to interact with a variety of signalling factors known to be involved in the regulation of muscle mass. IGF-1 increases in MyoD mRNA and enhances myoblast differentiation (Hsu et al., 1997). Calcineurin indirectly regulates MyoD expression through MEF2 (Friday et al., 2003). Phosphorylation of the MyoD transcript by the cAMP-dependent kinase, PKA, has been shown to inhibit its function (Li et al., 1992). It remains unclear whether MAPK signalling pathways influence MyoD expression/activity, although the protein sequence of MyoD contains a large number of proline-directed serines and threonines (consensus sites for MAPKs) potentially available for phosphorylation (Puri and Sartorelli, 2000).

Myogenin

Myogenin is necessary for myocyte maturation and is expressed consistently throughout muscle development (Bober et al., 1991), although its expression does not significantly increase until later during differentiation (Venuti et al., 1995). Differentiation is accompanied by cell cycle arrest, fusion of individual myoblasts into

multinucleated myotubes, and the transcriptional activation of muscle-specific genes encoding structural and contractile proteins such as desmin, myosin, actin, troponin, and tropomyosin (Ludolph and Konieczny, 1995). Knocking out myogenin results in defects of the differentiation process (Sakuma et al., 1999) and skeletal muscle structure (Hasty et al., 1993; Nabeshima et al., 1993). Administration of wild-type (healthy) myoblasts to myogenin-null mice results in an improved, but not completely restored, skeletal muscle mass and/or function (Myer et al., 1997). Additionally, myogenin mRNA is more abundant in slow-twitch, oxidative skeletal muscle, suggesting its potential role in slow fibre type characterization and/or preferential activation during different stages of muscle growth (Rescan, 2001).

The response of myogenin to changes in muscle mass is unclear. Pharmacologically- and surgically-induced hypertrophy show differential effects on myogenin protein content as drug-induced hypertrophy of rat soleus muscle decreases myogenin levels and functional overload of the same muscle does not alter levels of the protein (Mozdziak et al., 1998). Stretch-overloaded quail anterior latissimus dorsi (ALD) muscle have an increased amount of myogenin mRNA of ~150% (Lowe and Alway, 1999). With skeletal muscle denervation, the responses of myogenin are also unclear. Myogenin protein levels have been shown to increase after acute brachial plexus injury (Wu et al., 2002), sciatic nerve (Carlson et al., 2002) and tibial nerve (Launay et al., 2001) transections. In contrast, Sakuma et al (1999) found no change in myogenin protein content with up to 1 month of sciatic nerve transection-induced muscle denervation. These results indicate that further examination of the association between myogenin and muscle mass status is needed.

Myostatin

Although the aforementioned signalling factors are primarily involved in muscle growth and/or survival, muscle mass is ultimately regulated by an integrated and complex group of muscle-specific factors, some of which negatively act on mass and/or induce muscle atrophy. Bullough (1965) proposed that tissue size, including that of skeletal muscle, is controlled by the timely activation of negative growth regulators that he termed "chalones". According to his theory, each tissue secreted a specific chalone that systemically circulated through the body to inhibit growth of the chalone-specific tissue. Although Bullough's chalone theory was never substantiated, recent research demonstrates an ability of skeletal muscle to negatively regulate its growth, through the function of a key protein myostatin (McPherron et al., 1997).

Myostatin, also known as GDF-8 (Growth Differation Factor-8), represses muscle growth and its levels are inversely related to the amount of skeletal muscle mass (Lee, 2004). Increases in muscle mass due to strength training is associated with lower levels of myostatin (Roth et al., 2003). Treatment of cultured muscle cells with myostatin results in a net loss of protein, lowered rates of protein synthesis (Taylor et al., 2001) and inhibition of satellite cell production (McCroskery et al., 2003). Over-expression of the myostatin gene systemically leads to cachexia, a wasting syndrome that is characterized by significant muscle loss (Zimmers et al., 2002). In contrast, myostatin-null "mighty mice" have double the body weight of wild-type mice and enlarged skeletal muscles, a consequence of both hyperplasia and hypertrophy (McPherron et al., 1997; Amthor et al., 2002). Mutation of the myostatin gene has been used in the production of "double muscled" cattle that have significantly hypertrophied skeletal muscle (Bellinge et al.,

2005). Myostatin's influence on human muscle mass has been outlined in a case study of a young, German boy who displayed significant muscle hypertrophy within days of birth due to a mutation of the myostatin gene (Schuelke et al., 2004).

Myostatin expression has been shown to increase with skeletal muscle atrophy and denervation, and is also decreased during muscle regeneration (Sakuma et al., 2000; Wehling et al., 2000; Carlson et al., 1999). Increased myostatin activity has been shown in muscle of young men during prolonged bed rest and older individuals with disuse-associated sarcopenia (Roth and Walsh, 2004). In the *mdx* mouse, a model of muscular dystrophy, knocking out or blocking the myostatin gene attenuates symptoms of the disease by not only increasing musculature and strength, but also promoting muscle remodelling and regeneration in the knockout mice (Wagner et al., 2002; Bogdanovich et al., 2002).

Interestingly, mechanical induction of muscle hypertrophy has also been shown to increase muscle myostatin protein (Kocamis and Killefer, 2002), although this may be a reflection of an acute breakdown of protein during this hypertrophic protocol. Myostatin-null mice have been shown to lose a greater amount of muscle mass with a hindlimb suspension protocol than wild-type control mice (McMahon et al., 2003), suggesting that the initial status of the muscle (in this case, larger musculature with the null-mutation), influences how it responds to protocols that alter mass.

The β-Adrenergic System

Adrenergic effects are mediated through the binding of ligands to their respective adrenergic receptor (alpha and beta) including their unique subtypes (6 α and 3 β

identified to date). β-adrenergic receptors are the predominant form of adrenergic receptors expressed in cardiac and skeletal muscle and may play a role in regulating muscle mass and hypertrophy in both muscle types (Kim and Sainz, 1992). β-adrenergic agonists act by binding to their β-adrenergic receptors (βARs) and initiate a series of signalling cascades including the activation of specific trimeric G-proteins. βAR activation initiates the dissociation of G-protein subunits (α and βγ) which are capable of modulating downstream pathways. Many β-adrenergic agonists are coupled to the $G_{\alpha s}$ protein, producing stimulatory effects when the $G_{s\alpha}$ subunit activates the membrane-bound kinase, adenylate cyclase (AC) and subsequently 3', 5'-cyclic adenosine monophosphate (cAMP). It has been suggested that cAMP, a key second messenger, exerts its effects through a variety of signalling factors, including protein kinase A (PKA), however the mechanisms of cAMP action in the regulation of skeletal muscle mass are unclear.

The majority of research evidence pertaining to the adrenergic system and the maintenance of muscle mass involves studies of cardiac tissue. Stimulation of the β_1- and β_2-adrenergic pathways leads to cardiac muscle hypertrophy as the heart expresses both β_1ARs and β_2ARs, although this ratio is thought to be 4:1 in favour of β_1ARs (Kiely et al., 1994). Over-expression of β_1ARs in mice causes hypertrophy of the heart (Bisognano et al., 2000; Engelhardt et al., 1999). Although both the β_1AR and β_2AR are coupled to G_s and activate the AC/PKA/cAMP signalling cascade, β_2ARs have also been shown to be coupled to G_i (the inhibitory form of the small trimeric G-protein) in the heart (Kilts et al., 2000; Daaka et al., 1997). Therefore, stimulation of β_2ARs could

actually inhibit the AC/PKA/cAMP pathway but still increase muscle mass. Stimulation of the β_2AR has been shown to enhance contractile function of the heart without elevating intracellular cAMP levels (Sabri et al., 2000). As a result, β_2AR agonists may actually act through a pathway independent of AC/PKA/cAMP to regulate muscle mass. In fact, β_2AR stimulation has been shown to activate the PI3K/Akt survival (Zhu et al., 2001) and MAPK (Daaka et al., 1997) pathways in cardiac muscle, suggesting that the regulation of cardiac muscle mass, particularly cardiac muscle hypertrophy, may be regulated by β_2ARs and their associated signalling pathways.

Several research groups have used β_2-adrenergic agonists to induce skeletal muscle hypertrophy, prevent atrophy caused by disuse, malnutrition, and denervation, as well as produce beneficial effects in the healing of severe burns (Herrera et al., 2001). Oral administration of β_2-adrenergic agonists have resulted in increases in porcine skeletal muscle mass, protein and RNA content, increase RNA/DNA and protein/DNA ratios, increase rates of protein synthesis and decreased degradation (Kim and Sainz, 1992). One of the most widely examined β_2-adrenergic agonists with respect to muscle mass and function is the substituted phenylethanolamine with β_2 sympathomimetic activity, Clenbuterol.

Clenbuterol

Therapies that act to reverse muscle wasting and/or maintain muscle mass are of great interest to researchers and clinicians given the substantial impact neuromuscular diseases and an aging population pose to our health care system. Although Clenbuterol (also commercially known as Spiropent or Novegam) is primarily used in the treatment

of asthma because it acts as a potent, selective bronchodilator, it also has anabolic effects on striated muscle tissue. Chronic administration of Clenbuterol has been shown to induce both cardiac and skeletal muscle hypertrophy (MacLennan and Edwards, 1989). Hypertrophy of both slow and fast-twitch muscle (per kg wet weight) have been found with Clenbuterol treatment in both healthy as well as compromised/abnormal situations (Hinkle et al., 2002; Herrera et al., 2001; Sneddon et al., 2001; Murphy et al., 1996; Carter and Lynch, 1994b; Carter et al., 1991). Increases in muscle mass have been observed in livestock such as lambs (Claeys et al., 1989) and broiler chickens (Dalrymple et al., 1984) fed Clenbuterol, which led to the increased use and abuse of Clenbuterol in livestock production. This practice has subsequently been banned.

The growth-promoting effects of Clenbuterol appear to occur primarily in muscle tissue as increases in other organ weights do not occur following treatment (Carter et al., 1991). However, Clenbuterol elicits a catabolic action on adipose tissue and with its anabolic effects on muscle, it has been commonly referred to as a "repartitioning agent". Clenbuterol triggers an increase in non-shivering thermogenesis (Yang and McElligott, 1989) and a decrease in fat mass (Kearns et al., 2001; Emery et al., 1984), through the direct interaction of the drug on βAR's on adipocytes, downstream activation of hormone sensitive lipase (HSL), and subsequent breakdown of triacylglycerols (Carmen and Victor, 2006). The decrease in fat mass, combined with an increase in muscle mass, is reflected in studies examining overall body weight that typically show no difference between Clenbuterol-treated and non-treated animals (Bricout et al., 2004).

Clenbuterol treatment stimulates a shift to a faster fibre type (Zeman et al., 1988; Dodd et al., 1996; Criswell et al., 1996; Lynch et al., 1996; Ricart-Firinga et al., 2000)

and preferentially hypertrophies faster fibres (Criswell et al., 1996), as seen in the up-regulation of faster muscle MHC isoforms (Bricout et al., 2004). These alterations are also associated with changes in muscle properties such as contractile speed and fatigability (Chen and Alway, 2001), strength (Maltin et al., 1993), and protein isoform content (Mozdziak et al., 1998; Chen and Alway, 2000). However, these effects are disputed in the literature (Polla et al., 2001; Dodd et al., 1996) and have not yet been fully examined within the context of progressive denervation-induced muscle atrophy.

As a Therapeutic Agent

Due to Clenbuterol's anabolic effects on muscle, researchers have examined the drug as a way to reverse muscle atrophy. However, because of Clenbuterol's role in the slow-to-fast fibre type transition, treatment of atrophied muscle with the drug alone may hinder its therapeutic benefits by up-regulating more easily fatigable fast-twitch fibres. Decreases in oxidative capacity have been observed in skeletal muscle of rats treated with Clenbuterol for 4-6 weeks (Castle et al., 2001; Polla et al., 2001). One research group suggests supplementing Clenbuterol administration to animals with atrophied muscles with light endurance exercise such as low-intensity swimming in order to stimulate slower fibres and prevent a substantial fibre shift (Lynch et al., 1996). Previous studies have demonstrated negative effects on the heart with long-term administration of the drug, including extensive cardiac hypertrophy (Duncan et al., 2000), myocardial necrosis (Burniston et al., 2002), apoptosis and ischemia (Burniston et al., 2005). However, many of these studies administered large doses (in the range of 3-5mg/kgBW), an indication of a dose-response effect of the drug with deleterious effects at supra-physiological doses.

With lower doses, Clenbuterol has been shown to attenuate muscle atrophy following hindlimb suspension (Emery et al., 1984; Herrera et al., 2001; von Deutsch et al., 2002; Dodd and Koesterer, 2002), hyperthyroidism (Carter and Lynch, 1994b), surgical stress (Carter et al., 1991), dietary restriction (Choo et al., 1990), muscular dystrophy (Rothwell and Stock, 1985), glucocorticoid therapy (Pellegrino et al., 2004) and acute denervation (Zeman et al., 1987; Babij and Booth, 1988; Agbenyega and Wareham, 1990; Maltin et al., 1993). Improvements in functional performance via enhanced muscle contractile characteristics have also been observed in Clenbuterol-treated animals (Dodd and Koesterer, 2002; Picquet et al., 2004). Clenbuterol treatment has been shown to have a similar effect on muscle mass in young (3-month), adult (12-month), and elderly (23-month) rats, with increases in mass ranging from 19-39% in all age groups (Carter et al., 1991; Carter and Lynch, 1994a). Clenbuterol increases total muscle protein content (Chen and Alway, 2001) and contractile force in older animals (Smith et al., 2002) although increases in function are not observed with all doses of the drug or muscle groups (Chen and Alway, 2001). Muscle weight/body weight ratios of aged Clenbuterol-treated rats have been shown to be greater only in tibialis anterior muscle, with no change observed in other muscles (i.e. diaphragm and soleus) (Polla et al., 2001). These findings suggest a role for Clenbuterol in the maintenance of muscle mass (or attenuation of sarcopenia) and functionality in aged muscle. Clenbuterol is also able to attenuate the loss of muscle mass in older animals that undergo certain atrophy-inducing protocols. For example, increases in muscle mass have been observed in older (24-month) Clenbuterol-fed animals following protein malnutrition (Carter and Lynch, 1994b) and following hindlimb suspension in mature animals (ages 6-30-months)

(Herrera et al., 2001; Wineski et al., 2002). In contrast, Clenbuterol does not improve atrophy following hindlimb suspension in senescent (38-month old) rats (Chen and Alway, 2000).

In some situations of chronic disease, it has been suggested that Clenbuterol could act as a therapeutic agent to prevent and/or delay disease-associated skeletal muscle wasting. Degeneration of dystrophic muscle of aged (22-month-old) *mdx* mice is greatly reduced with Clenbuterol treatment; muscles obtained from aged Clenbuterol-treated *mdx* display significantly lower levels of fibrosis and fibre loss than untreated *mdx* mice (Zeman et al., 2000). Clenbuterol administration leads to an increase in force production of *mdx* diaphragm muscle strips (Dupont-Versteegden et al., 1995). However, Lynch et al. (2001) observed no change in diaphragm muscle force or power output and also found that Clenbuterol did not attenuate muscle degeneration or necrosis in younger (3-month old) *mdx* mice. The discrepancy may be explained by a number of factors, including the muscles examined, duration of the drug and age of the animals examined in these studies.

Early studies of denervated muscle demonstrate an attenuation of muscle atrophy with acute denervation protocols and Clenbuterol treatment (Maltin et al., 1986; Zeman et al., 1987; Cockman et al., 2001), perhaps due to an increased sensitivity to the drug with denervation (Maltin et al., 1993). Improvements in contractile function following acute denervation have also been observed (Agbenyega and Wareham, 1990). Subsequent studies have confirmed the anabolic effects of Clenbuterol in denervation skeletal muscle fibres following peripheral nerve injury (Fitton et al., 2001) and complete sciatic nerve transection (Frerichs et al., 2001). However, few studies have examined the effects of Clenbuterol on progressive skeletal muscle denervation. Motor neuron degeneration

(mnd) mice demonstrate increases in mass ranging from 17-40% in different muscle groups and a significant increase (61%) in grip strength with Clenbuterol (Zeman et al., 2004). Twenty-eight days of Clenbuterol administration to G93A mice, that undergo progressive muscle denervation, has recently suggested a trend towards the preservation of gastrocnemius muscle mass (Teng et al., 2006), although no concrete data was given in the paper to substantiate this claim. In the same study, Clenbuterol did not prevent the loss of body weight that normally occurs in later stages of the disease but was able to improve functional (RotoRod) performance at 115 days of age (~90% of the mouse lifespan). The authors interpreted this increase in function as a slowing of disease progression with the drug treatment. These studies suggest that the drug may have therapeutic benefits for the treatment and/or prevention not only of muscle wasting/atrophy but also disease-related symptoms and functional declines.

Mechanism(s) of Action

The mechanisms by which Clenbuterol stimulates muscle growth/hypertrophy have yet to be fully elucidated, however several theories have been previously suggested (Figure 2). Increased protein synthesis and/or decreases in protein degradation have been proposed as the general mechanism(s) by which Clenbuterol exerts its effects on skeletal muscle to increase mass (Choo et al., 1992; Moore et al., 1994; Mozdziak et al., 1998). Increases in protein synthesis rates and protein content have been observed with Clenbuterol administration ranging from 2 days to 3 weeks (von Deutsch et al., 2003; Sneddon et al., 2001; Carter et al., 1991). Clenbuterol may increase muscle mass in compromised/atrophied tissue via increases in translational efficiency (Maltin et al., 1987; Maltin et al., 1989), satellite cell activation (Maltin et al., 1992; Katoch and

Sharma, 2004), and/or decreases in protein degradation (Fernandez and Sainz, 1997). There is also some evidence to suggest involvement of the smRFs in this process as Clenbuterol has been shown to acutely (within 24 hours) alter RNA levels in skeletal muscle, including IGF-1 and myogenin (Spurlock et al., 2006).

One theory is that Clenbuterol binds directly to its β_2-receptor and stimulates a cAMP/PKA-dependent cascade of phosphorylations that directly contributes to increases in rates of protein synthesis and decreases in degradation rates in skeletal muscle (Zeman et al., 1987). However, to date only one study has investigated the *in vivo* changes in cAMP (MacLennan and Edwards, 1989) and none have investigated PKA activity in skeletal muscle following Clenbuterol administration.

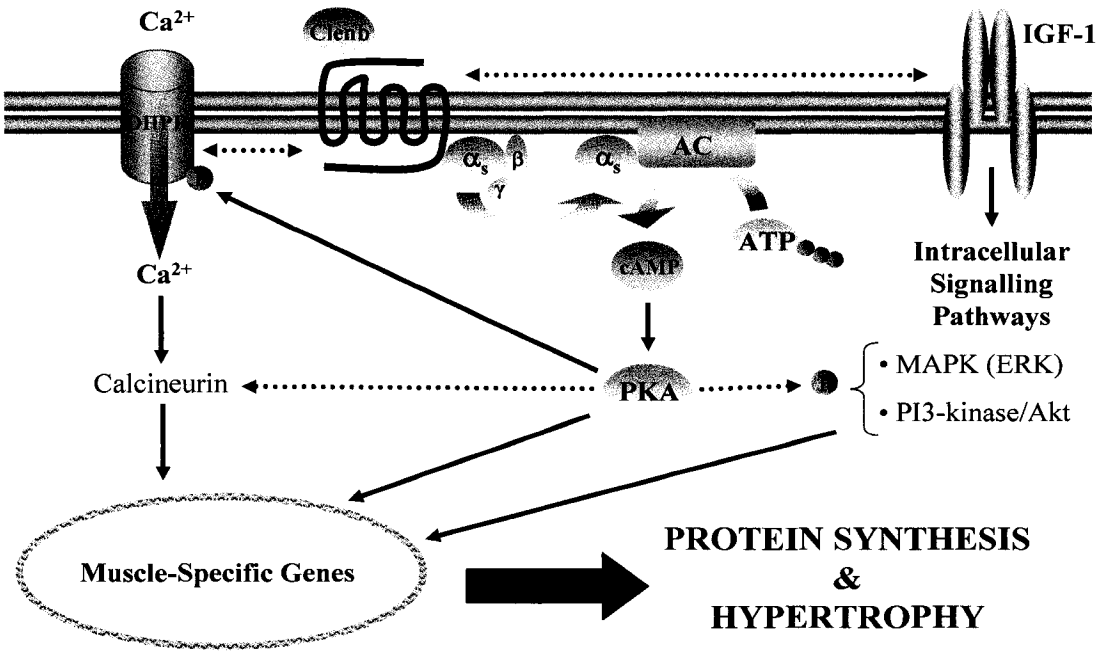

Figure 2: Proposed mechanisms by which Clenbuterol acts to increase muscle mass (hypertrophy) Refer to Abbreviations List for protein nomenclature. Solid lines represent known interactions from previous literature; dotted lines represent hypothesized interactions.

β_1- and β_2-knockout mice have been used to examine the effects of Clenbuterol administration on skeletal muscle mass with hypertrophic and anti-atrophic effects of

Clenbuterol lost upon genetic removal of the β_2AR but not the β_1AR knockout (Hinkle et al., 2002). Propranolol, a non-selective β-adrenergic antagonist, inhibits cAMP and Clenbuterol's anabolic effect on skeletal muscle (MacLennan and Edwards, 1989). However, propranolol and the β_1-antagonist, atenolol, were unable to inhibit a Clenbuterol-induced increase in muscle/carcass protein contents (Reeds et al., 1988; Sillence et al., 1995).

A second line of evidence suggests that Clenbuterol acts indirectly and systemically via increases in the production of hormones or growth factors (Herrera et al., 2001). β-agonists can stimulate an acute release of insulin from the pancreas (Bassett, 1970), but this does not necessarily translate into increases in muscle mass. Longer term studies have shown continued muscle growth with β-adrenergic treatment and no change in insulin levels in both normal and diabetic rats (McElligott et al., 1987). Clenbuterol has little effect on growth hormone levels (Emery et al., 1984; Laakmann et al., 1990). In addition, numerous studies have shown no change in serum IGF-1 levels with Clenbuterol administration (Young et al., 1995; Buyse et al., 1991). Therefore, it has been hypothesized that a local (muscle) production of IGF-1 may be a mechanism by which Clenbuterol exerts its anabolic effect on muscle (Awede et al., 2002). Supporting this theory are studies that have shown increases in skeletal muscle IGF-1 (Awede et al., 2002) and IGF-2 (Sneddon et al., 2001) protein/mRNA content within three days of Clenbuterol treatment.

Thirdly, if Clenbuterol acts to increase muscle mass through increasing rates of protein production, involvement of smRFs that act to increase protein synthesis may be a key to elucidating specific mechanisms of action in Clenbuterol-induced attenuation of

muscle atrophy. Clenbuterol's mechanism may be mediated through the PI3K/Akt pathway as rapamycin blocks Clenbuterol-induced muscle growth, presumably by inhibiting protein synthesis (Bodine, 2006). A six-fold, but transient increase in phospho-p70s6k has been observed within 24 hours of Clenbuterol administration with levels returning to control values after 2 days (Sneddon et al., 2001). However, very few studies have examined smRFs and Clenbuterol in compromised muscle systems. Clenbuterol treatment following acute brachial plexus injury up-regulated MyoD levels in denervated rat muscle, to levels that were similar to those of control (non-denervated) muscle (Wu et al., 2002). Bricout et al (2004) demonstrated a 77% increase in MyoD with Clenbuterol administration in degenerative soleus muscle induced by snake venom, an increase that was comparable to the change observed in non-degenerative, healthy soleus muscle. Clenbuterol treatment also increased myogenin mRNA in atrophied plantaris muscle due to joint fixation (Delday and Maltin, 1997).

Clenbuterol may affect factors that favour the preferential preservation of contractile elements in fast fibres (Chen and Alway, 2000). As a result, one would expect that those factors associated with a fast phenotype to be affected with the drug administration. ERK activity and calcineurin levels have both been shown to be elevated with 2 weeks of Clenbuterol treatment in different types of skeletal muscle, to a greater extent in fast-twitch muscle fibres (Shi et al., 2006; Oishi et al., 2004). Although MyoD, which is preferentially expressed in fast-twitch skeletal muscle fibres, increases with Clenbuterol (Bricout et al., 2004), myogenin (preferentially expressed in slower fibre types) also increases following Clenbuterol treatment (Mozdziak et al., 1998).

Finally, Clenbuterol's hypertrophic effects may be mediated via the nervous system which is closely associated with skeletal muscle. It has been suggested that Clenbuterol mimics normal innervation functions in skeletal muscle in structural and functional reorganization of skeletal muscle following denervation (Katoch et al., 2006). cAMP counteracts denervation-induced destabilization of the neuromuscular junction (Xu and Salpeter, 1995). Clenbuterol, which is able to permeate the blood-brain barrier, enhances neuronal regeneration (Frerichs et al., 2001), reverses the loss of spinal cord tissue following acute injury (Zeman et al., 1999) and protects hippocampal neurons from ischemic degeneration (Semkova et al., 1996). Following complete nerve transection, Clenbuterol stimulates axonal growth (Frerichs et al., 2001). In mnd mice, Clenbuterol treatment not only enhances muscle mass and functional performance, but also reduces the number of eccentric (i.e. defective) motor neuron nuclei (Zeman et al., 2004). The mechanism by which Clenbuterol acts on nervous tissue may involve the production of nerve growth factor (NGF) which promotes survival and outgrowth of neurons (Culmsee et al., 1999a; Semkova and Krieglstein, 1999). Increases in NGF in rat brain and skeletal muscle have been observed with Clenbuterol treatment (Culmsee et al., 1999a; Riaz and Tomlinson, 1999).

In summary, skeletal muscle mass may be regulated by a number of factors, including a variety of models (type, frequency, intensity, duration of stimuli) and status of the muscle itself (including fibre type, age, overall health and functionality). The status of skeletal muscle is reflected in changes/levels of cellular signalling factors (smRFs). However, exactly how these factors respond to situations of Clenbuterol-induced hypertrophy and progressive denervation-induced atrophy are unclear.

Progressive denervation of skeletal muscle leads to extensive muscle atrophy, declines in functionality and overall quality of life. The β_2-adrenergic agonist, Clenbuterol, possesses huge potential to be a therapeutic agent for populations faced with muscle wasting. However, the mechanism by which Clenbuterol acts as well as its effect on progressively denervated skeletal muscle is currently unclear.

Rationale

Maintenance of skeletal muscle mass is essential for overall health, functionality and quality of life. Muscle wasting results in substantial decreases in muscular strength; declines in muscle are associated with increased rates of disability and mortality. However, changes occur within the muscle itself at a cellular level long before observable alterations in mass, rates of protein synthesis and/or levels of circulating growth factors. Previous research has suggested the role of numerous muscle-specific proteins and signalling pathways in the modulation of muscle growth and/or wasting. The cellular mechanisms and factors that act to regulate skeletal muscle mass are currently poorly understood.

Furthermore, it has also been suggested that muscle-specific signalling factors which are a reflection of muscle quality, are critical not only in maintaining mass, but may also function to improve functionality and overall quality of life. As such, identifying key targets could lead to the development of therapeutic strategies in the prevention and rehabilitation of skeletal muscle weakness and disease. The β_2-adrenergic agonist, Clenbuterol, has been shown to attenuate muscle atrophy and improve functionality in some chronic disease models. However, it's mechanism of action as well

as its effects on progressively denervated skeletal muscle are unclear. Given its critical importance to human health and functionality, skeletal muscle and the underlying mechanisms that regulate muscle mass have fascinated researchers for centuries.

CHAPTER 2: ACUTE RESPONSES OF SELECTED SKELETAL MUSCLE REGULATORY FACTORS FOLLOWING A SINGLE INJECTION OF CLENBUTEROL

Abstract

Chronic administration of Clenbuterol, a β_2-adrenergic agonist, has been shown to induce skeletal muscle hypertrophy, but the initial signalling mechanism by which it initiates an increase in muscle mass is currently unclear. The purpose of this study was to examine the initial (24-hour) response of signalling intermediates associated with hypertrophy following a single dose of Clenbuterol in hindlimb muscle. Male Wistar rats were given a dose of either Clenbuterol (1.5mg/kg BW) or saline and subsequently sacrificed at specific time points after injection (10 minutes, 2, 6, 12, and 24 hours). Significant but transient increases in muscle cAMP levels, levels of phospho-proteins p-ERK1/2 and p-Akt were observed without a change in PKA activity. Substantial, acute increases in phospho-kinases PKCα, PAK1/2/3, FAK and Pyk2 were also observed in Clenbuterol-treated skeletal muscle. Direct hypertrophic effects of Clenbuterol treatment were confirmed via the C_2C_{12} skeletal muscle cell line. The results of this study suggest that in the early stages of Clenbuterol-induced muscle hypertrophy, there is PKA-independent stimulation of signalling intermediates known to be involved in the regulation of muscle mass and muscle hypertrophy.

Introduction

Clenbuterol stimulates skeletal muscle hypertrophy via its interaction with the β_2-adrenergic receptor, resulting in increases in both fast- and slow-twitch muscle mass (Hinkle et al., 2002; Herrera et al., 2001; Sneddon et al., 2001; Murphy et al., 1996). Several research groups have used Clenbuterol to induce hypertrophy in both normal and compromised muscle tissue, including atrophied muscle caused by disuse (Herrera et al., 2001; Ricart-Firinga et al., 2000; Maltin et al., 1993), malnutrition (Carter and Lynch, 1994b), denervation (Zeman et al., 1987), and disease (Lynch et al., 2001; Pan et al., 2001). Clenbuterol leads to increased rates of protein synthesis (Carter and Lynch, 1994b) which have been observed within as little as 2 days of treatment (Sneddon et al., 2001). While it is thought that Clenbuterol initially stimulates the β_2-adrenergic cascade, including adenylate cyclase (AC), cAMP, and PKA, the underlying mechanism by which Clenbuterol acts to increase protein synthesis and muscle mass is currently unclear. Information regarding the potential mechanism by which it initiates skeletal muscle hypertrophy warrants investigation as it could identify key signalling targets for early therapeutic treatment and/or prevention of skeletal muscle atrophy.

Recent literature has suggested the acute involvement of IGF-1-dependent signalling factors known to be associated with muscle growth/hypertrophy with this adrenergic agent. Signalling factors known to be associated with IGF-1 include components of the MAPK and/or PI3K pathways. These signalling pathways can be activated acutely in skeletal muscle, within minutes to hours of the following stimuli - acute treadmill exercise, hormone treatment (i.e. insulin, leptin) and growth factor (i.e. IGF-1, HGF) treatment (Williamson et al., 2006; Al-Khalili et al., 2004; Halevy and

Cantley, 2004). Stimulation of one or both of these pathways has been shown to lead to increased rates of protein translation (Williamson et al., 2006), protein synthesis, and decreased rates of protein degradation in muscle tissue (Faridi et al., 2003). Increases in IGF-1 protein and mRNA levels (Awede et al., 2002) and signalling intermediates, p-p70s6k and p-4E-BP1 (Sneddon et al., 2001), have been observed within 1-3 days after a single injection of Clenbuterol. These findings suggest that Clenbuterol-induced muscle hypertrophy could occur via the β_2-adrenergic- and/or IGF-1 signalling pathways, either concurrently or independently of each other. Therefore, the purpose of this study was to examine the initial (24-hour) response of signalling factors associated with hypertrophy, the β-adrenergic-associated factors (cAMP, PKA) and IGF-1 related phospho-kinases (p-ERK1/2 and p-Akt) in hindlimb muscle, following a single dose of Clenbuterol.

Experimental Approach

Animals and Clenbuterol Administration

All procedures followed the guidelines outlined by the Canadian Council on Animal Care and were approved by the Animal Care Committee at Simon Fraser University. Fifty pathogen-free, 3-month old, male, Wistar rats (Charles River, Wilmington, MA) were housed in the SFU Animal Care Facility for 10-14 days prior to experimentation on a 12-h light:dark cycle and free access to animal chow (Purina Rodent Lab Diet 5001, IL) and water. No animals were removed from the study due to illness or disease. Rats were randomly assigned to one of two treatment conditions: saline (S, n=25) or Clenbuterol (CL, n=25). The animals in the CL group were given a single subcutaneous injection of Clenbuterol (1.5 mg/kg body weight) on the day of the study. Saline-treated animals received a single, subcutaneous injection of an equal

volume of saline (150 mM NaCl). Equal numbers of S and CL animals were weighed and sacrificed at the following intervals: 10 minutes, 2, 6, 12, and 24-hours post-injection (n=5/group), with subsequent removal of mixed hindlimb skeletal muscle (including EDL, TA, fibularis muscles and quadriceps) tissue. Tissues were immediately frozen in liquid nitrogen and stored at -80°C until further analysis.

Tissue Preparation

Full details about tissue preparation are outlined in Appendix A. Briefly, whole protein lysate was extracted from mixed hindlimb of 50 rats (n=10 each for time points 10 minutes, 2, 6, 12, and 24 hours). Frozen skeletal muscle tissue was weighed and homogenized in a 10 ml volume of ice-cold modified RIPA buffer. Protease inhibitors [phenylmethysufonyl fluoride (PMSF), leupeptin, pepstatin and aprotinin] as well as phosphatase inhibitors [sodium orthovanadate (Na_3VO_4) and sodium fluoride (NaF)] were added fresh to the buffer solution each day. Samples were then spun at 20,000 g for 15 minutes at 4°C and the resulting supernatant was stored at -80°C until further use.

Protein Determination

Protein content of the resulting supernatant was determined via a Bradford assay (Bio-Rad Laboratories, Hercules, CA) and is fully explained in Appendix A. Samples were prepared via double dilution with distilled water (dH_20). Protein standards were prepared using bovine serum albumin (BSA, Sigma) dissolved in dH_20 resulting in concentrations of 0, 2, 4, 6, 8, 10, and 12 μg/ml. 200 μl of undiluted Bio-Rad Protein Assay Reagent was added to each sample and standard, making a final volume of 1 ml in each tube. The optical density of each solution (normalized to the 0 μg standard) was

measured using a Perkin Elmer UV/VIA Spectrophotometer Lambda 2. Optical density values of the protein standards were recorded and plotted against protein concentration; total protein content of each sample was determined from this plot (using an equation for the slope of the resulting best-fit line).

Determination of cAMP Concentrations

Mixed hindlimb skeletal muscle was homogenized in flat-bottom vials in 9 volumes of 10% TCA using a Janke & Kunkel IKA Labortechnik Ultra-Turrax homogenizer. Supernatant was clarified by centrifugation and extracted twice with 5 volumes of water-saturated ether. Intracellular cAMP concentrations were then determined via I^{125}-radioimmunoassay kit (Biomedical Technologies Inc., Stoughton, MA).

All solutions were prepared from the kit contents. 12x75mm glass borosilicate tubes were numbered for a standard curve (n=18) and muscle homogenates in duplicate. Standards were prepared from a cAMP stock solution and working buffer in the following concentrations: 1, 2, 5, 20, 100, and 200 pmol/ml (0.1, 0.2, 0.5, 2, 10, and 20 pmol/tube). 100 µl of each homogenate sample was added to the appropriately labelled sample tube. Additional tubes used for reference included "total counts" (TC, radioactive tracer solution only), "non-specific binding" (NSB, working buffer + tracer solution + NSB solution), and "Bo" (working buffer + tracer solution + working antibody solution). 100 µl of working buffer was added to all but 2 (TC) tubes. 100 µl of radioactive (working tracer) solution was added to all tubes in the assay in a secure ("hot") area of the laboratory. 100 µl of a working antibody solution was then added to all but the TC

and NSB tubes, including all standards and samples. Tubes were placed in a rack and gently shaken for 1 minute. Tubes were then covered with parafilm and incubated overnight (18-20 hours) at 4°C. The next day, 1 ml of working buffer solution was added to all tubes except the TC tubes, carefully vortexed and centrifuged (3,700 rpm for 20 min at 4°C). Supernatants were decanted and the remaining pellets were analysed for radioactive counts via a Gamma Counter (Scionix). Counts of the cAMP standards were recorded and plotted against cAMP concentration on logarithmic paper; total cAMP concentration of each sample was then determined from this plot.

Determination of PKA Activity

PKA activity was assayed using a Peptag™ Assay Kit from Promega (Madison, WI). Equal amounts of protein (20 µg) were added to buffer solution including 0.4ug/ul of Kemptide (LRRASLG) peptide, to a final sample volume of 20 µl. Samples were incubated at 30°C for 30 minutes and then at 95°C (heating block) for 10 minutes. 1 µl of 80% glycerol was added to each sample to allow sample to settle into wells in a 0.8% agarose gel [50mM Tris-HCl (pH 8.0)]. Samples were then separated for 18 minutes at 100 V with a control peptide for reference. Bands were carefully excised after observation under UV light and quantitative measurements of activated PKA (amount of phosphorylated Kemptide) were determined by spectrophotometry. The assay was repeated and the average PKA activity per sample of two assays was recorded.

Gel Electrophoresis and Immunoblotting

Complete details regarding gel electrophoresis and immunoblotting procedures are outlined in Appendix A. Briefly, equal amounts of protein (70µg/35µl) were

separated on a one-dimensional (8-12%) SDS polyacrylamide gel where the percentage of acrylamide was dependent upon the molecular weight of the protein of interest (the higher the molecular weight, the lower the concentration of acrylamide). A molecular weight marker (Amersham Pharmacia) was run on all gels. Samples were then transferred onto a polyvinylidene difluoride (PVDF) membrane soaked in transfer buffer at 4°C under constant current conditions at maximum voltage and 350 mA for approximately 1-1.5 hours, depending on the size of protein of interest. Following the transfer, membranes were rinsed twice with dH_20, visualized with Ponceau Red (0.2% in 3% TCA, Sigma), and washed with TBST.

Non-specific binding sites on membranes were then blocked with 5% bovine serum albumin (BSA) in TBST for 90 minutes at room temperature, under gentle agitation. Membranes were rinsed in TBST and subsequently incubated overnight at 4°C with appropriate primary antibody [anti-phospho-Akt (Ser^{473}) (*rabbit*) (Cell Signalling), anti-phospho-ERK (Thr^{202}/Tyr^{204}) (*mouse*); 1:1000 dilution (vol/vol) with TBST, 0.5% NaN_3 and 1% BSA]. Membranes were washed 5 x 5 minutes with TBST and incubated with an excess of appropriate IgG-horseradish peroxidase (HRP)-conjugated secondary antibody (1:20,000 with TBST and 1% BSA) for 90 minutes at room temperature with gentle agitation. Membranes were washed three times each in volumes of TBST and TBS, immersed in Enhanced Chemiluminescence (ECL) reagent and exposed to Hyperfilm-ECL (GE Healthcare/Amersham Biosciences, Baie d'Urfé, QC). Relative protein content was evaluated by laser densitometry using an LKB UltroScan XL densitometer and GelScan XL software.

Kinexus™ Protein Kinase Screen

Hindlimb muscle samples from 4 groups (S_{10min}, CL_{10min}, CL_{2h}, CL_{6h}) were analyzed for a wide range of phospho-protein kinases by the Kinetworks™ Phospho-Site Screen (KPSS 11.0 Profile) using validated commercial antibodies (Kinexus Bioinformatics Corporation, Vancouver, Canada) as described previously (Pelech, 2004). Samples from these particular time points in the experiment were chosen based on preliminary cAMP and PKA data. Each sample (500 ug total protein, 1μg/ul protein concentration) was pooled from 3 different rats of the same condition. Appropriate volumes of homogenate were added to 4X Sample buffer (50% glycerol; 125mM Tris-HCl, pH 6.8; 4% SDS; 0.08% Bromophenol Blue; 5% β-mercaptoethanol) and dH_20 for a final volume of 500 μl. Samples were sent to Kinexus Bioinformatics Corporation to be analyzed using the KPSS 11.0 screen. The reproducibility of the Kinetworks™ screens on different days for the same samples is within 15% (Hu et al., 2003).

C_2C_{12} Skeletal Muscle Cell Culture

All cell culture materials were purchased from GIBCO. To verify the direct, hypertrophic effect of Clenbuterol on skeletal muscle cells, C_2C_{12} cells (original stock from ATCC, Manassas, VA) were cultured on 60 mm dishes in proliferation medium consisting of Dulbecco's modified Eagle's medium (DMEM including 4.5 g/L glucose, 4 mM L-glutamine, 1.5 g/L sodium bicarbonate, 110 mg/L sodium pyruvate, and antibiotics) and 10% fetal bovine serum. The medium was changed every 48 hours. When cells reached 80-90% confluence, differentiation was induced by changing to medium composed of DMEM and 5% horse serum. Dishes were randomly selected to be treated with either saline (Hank's Buffered Saline, HBSS) or Clenbuterol (0.1 μM in

HBSS). Cells were treated for 0, 2, and 10 min, rinsed repeatedly with HBSS, and subsequently prepared for cAMP analysis as previously described. Verification of the direct response via β-receptors was performed by incubating cells with propranolol (0.1 μM in HBSS) and analysed for cAMP concentration.

Hematoxylin and Eosin (H&E) Staining

C_2C_{12} cells were grown in culture dishes on cover slips and treated with Clenbuterol [0.1 μM in Hank's Buffered Saline Solution (HBSS)] or saline for 24, 48, or 72 hours. At each time point, cells were rinsed a final time with saline prior to being stained. Cover slips were removed and placed in filtered hematoxylin solution (Sigma) for 1 minute, followed by five rinses in tap water. Cover slips were quickly dipped in acid alcohol (900 ml 70% ethanol, 100 ml concentrated HCl) to differentiate and 'blued' in sodium borate for 20 seconds. Multiple (5-6) washes in tap water and a 1-minute emersion in Eosin (Fisher Scientific) followed. Cover slips were then rinsed quickly with 90% and 100% ethanol and cleared in Xylene for 5 minutes. Slips were mounted onto glass slides with Permount mounting medium (Fisher). Myotube diameter and area measurements were calculated in a blinded fashion from multinucleated cells (at least 10 myotubes in 5 random fields of view) using an inverted light microscope (Leica DM4000B) and corresponding software (Leica Application Suite v.2.3.2 R1).

Statistical Analysis

For hindlimb muscle analyses, extreme data points were determined and examined via boxplot analysis prior to further investigation and were removed from the data set if values were considered questionable (> 3 times the interquartile range, or

boxplot length, measured from the upper or lower quartiles). A two-way, randomized group analysis of variance (ANOVA) (Drug x Time) was used for each signalling molecule examined. Independent t-tests (one-tailed, α-level = 0.05) were used to further compare means between Clenbuterol- and saline-treated animals. C_2C_{12} myotube diameters and areas were compared between the two groups (Clenbuterol vs. saline) using a Student's *t* test with an α-level of 0.05 set as significant. Levene's Test for equality of variance was noted for each variable to ensure the homogeneity of variance and draw conclusions from t-test analyses.

Results – *in vivo*

cAMP Concentration in Mixed Skeletal Muscle

The time course response of cAMP to a single subcutaneous injection of Clenbuterol is shown in Figure 3. cAMP levels in Clenbuterol-treated animals were significantly but transiently elevated from control animals within 10 minutes following injection of the β_2-adrenergic agonist (3.1 ± 0.4 pmol vs. 2.2 ± 0.6 pmol; $p<0.001$). cAMP remained elevated 2 hours (2.6 ± 0.2 pmol vs. 1.1 ± 0.1 pmol; $p<0.001$) but returned to control levels at 6, 12, and 24 hours post- injection (NS; $p>0.05$).

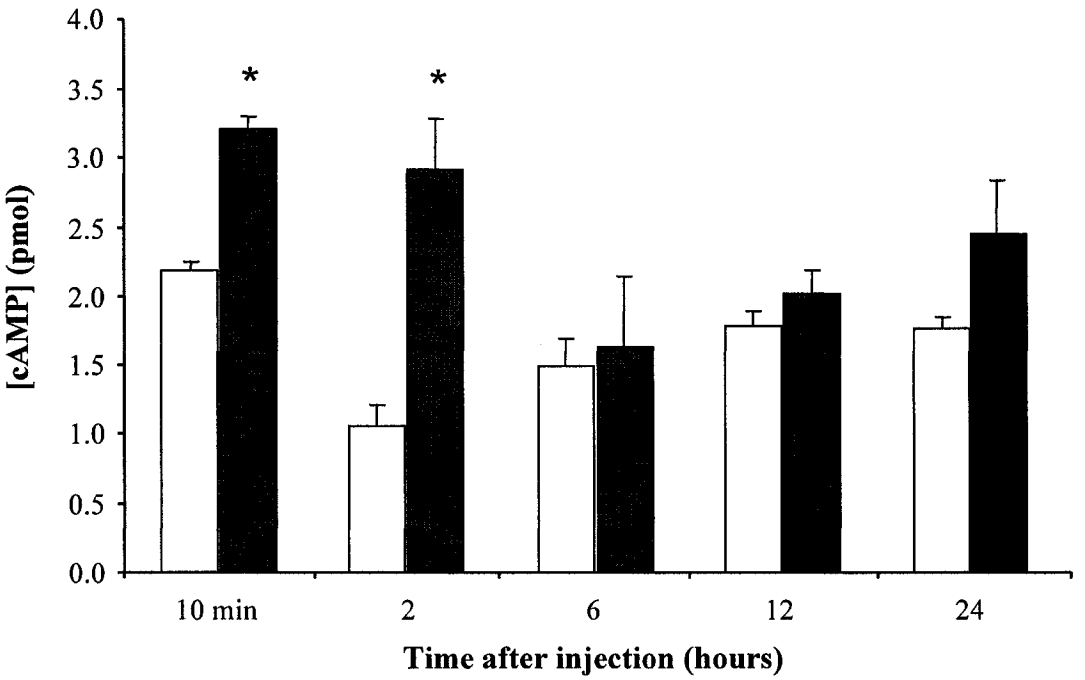

Figure 3: A 24-hour time course comparison of cAMP concentration in rat hindlimb skeletal muscle following a single subcutaneous injection (1.5 mg/kgBW) of Clenbuterol. Saline injection (white bars), Clenbuterol injection (black bars). (n=5-6/group). Data are expressed as a mean ± SE. *Significantly different from saline-treated control muscle of the same time point ($p<0.05$).

PKA Activity

Because of the cAMP trend whereby cAMP was shown to increase significantly at earlier time points (10 minutes and 2 hours post-injection), PKA activity levels were examined in both Clenbuterol- and saline-treated rats at 10 minutes, 2 and 6 hours following Clenbuterol administration. PKA activity (Figure 4) was not altered as a function of the drug treatment at any time point examined ($p=0.15$).

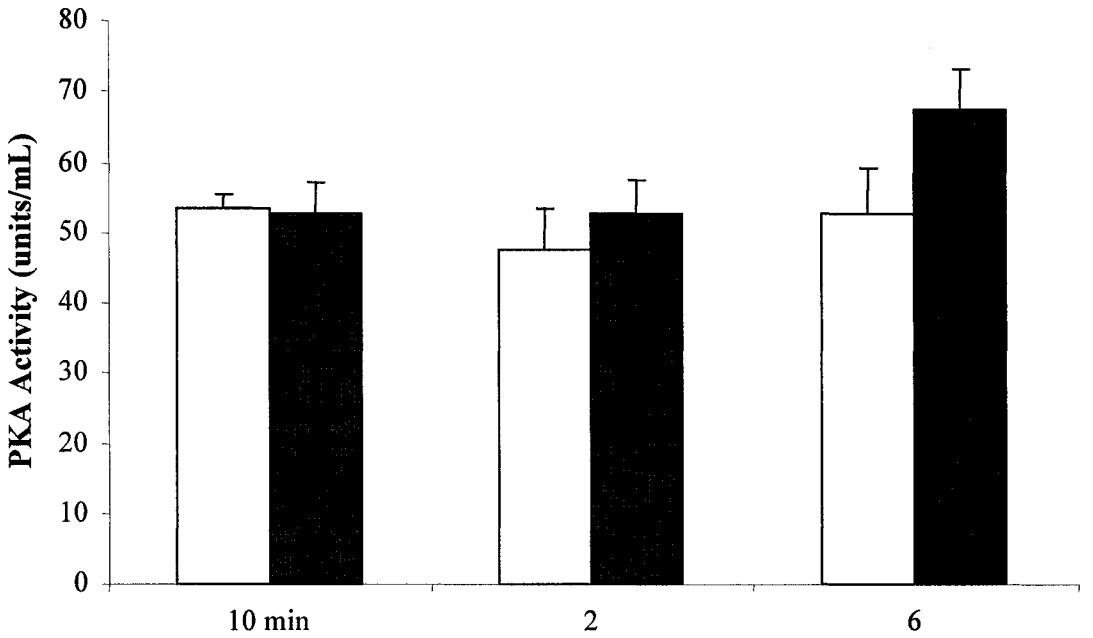

Figure 4: PKA activity in mixed rat hindlimb muscle as determined by PeptagTM PKA Assay Kit (Promega).
Saline injection (white bars), Clenbuterol injection (black bars). (n=4/group). Data are expressed as a mean ± SE.

Immunoblotting of p-ERK and p-Akt

Levels of the phospho-proteins p-ERK and p-Akt were statistically different between Clenbuterol-treated and saline-treated (control) rat hindlimb muscle, both demonstrating immediate but transient increases in levels post-injection (Figure 5). A significant (Drug) main effect increase was observed in levels of p-ERK, 40% greater than saline-treated muscle within 10 minutes and 113% greater at 2 hours. Significant (Time) main and interaction (Drug x Time) effects were also observed in p-ERK levels after Clenbuterol injection. Levels of p-Akt were significantly different in Clenbuterol- vs. saline-treated muscle ($p<0.05$), doubling within 10 minutes of the single injection.

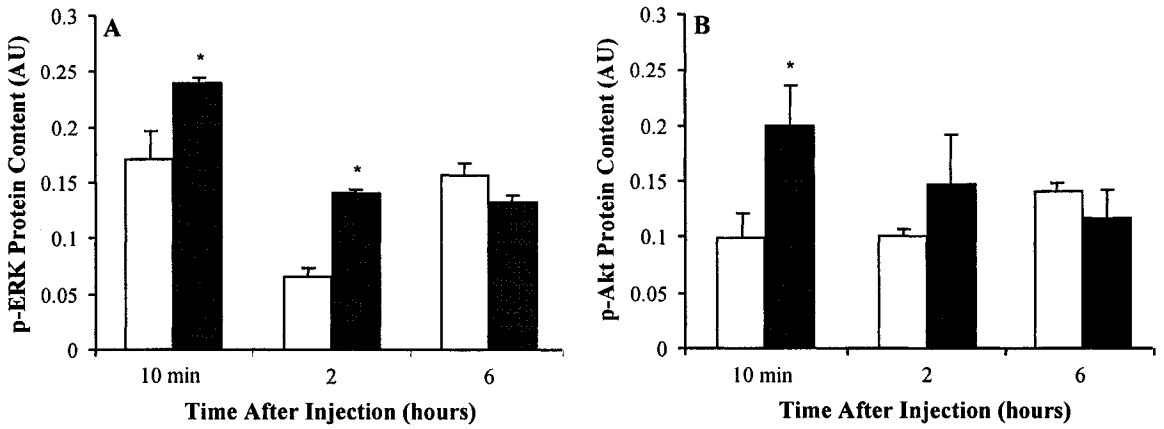

Figure 5: Protein content of p-ERK (A) and p-Akt (B) from mixed rat hindlimb skeletal muscle as determined by Western immunoblotting.
Data are expressed as a mean ± SE (n=5/group). *Significantly different from saline-treated group of the same time point.

Kinexus ™ Protein Kinase Levels

Using the Kinetworks™ Phospho-Site Protein Kinase Screen, changes in additional signalling factors associated with muscle hypertrophy were observed in the initial time points following Clenbuterol injection. The raw screen results (A) and quantification of those phospho-proteins that demonstrated a substantial change from control muscle (B) are shown in Figure 6. Phospho-proteins that were substantially elevated (% change at t=10 min, 2 and 6 hours in parentheses) with Clenbuterol treatment included proline-rich tyrosine kinase 2 (Pyk2, Tyr^{579}; +46%, +132%, +60%), p21-activated protein-serine kinases (PAK1/2/3, $Ser^{144/141/154}$; +79%, +57%, +28%), focal adhesion kinase (FAK, Ser^{722}; +176%, +184%, +200%), protein kinase C alpha (PKC_{α}, Ser^{657}; +291%, +145%, +168%), epidermal growth factor tyrosine kinase (EGFR, Tyr^{1148}; +59%, +44%, +32%). Additional "unspecified" phospho-proteins that appeared to increase with Clenbuterol treatment were also observed in the screens.

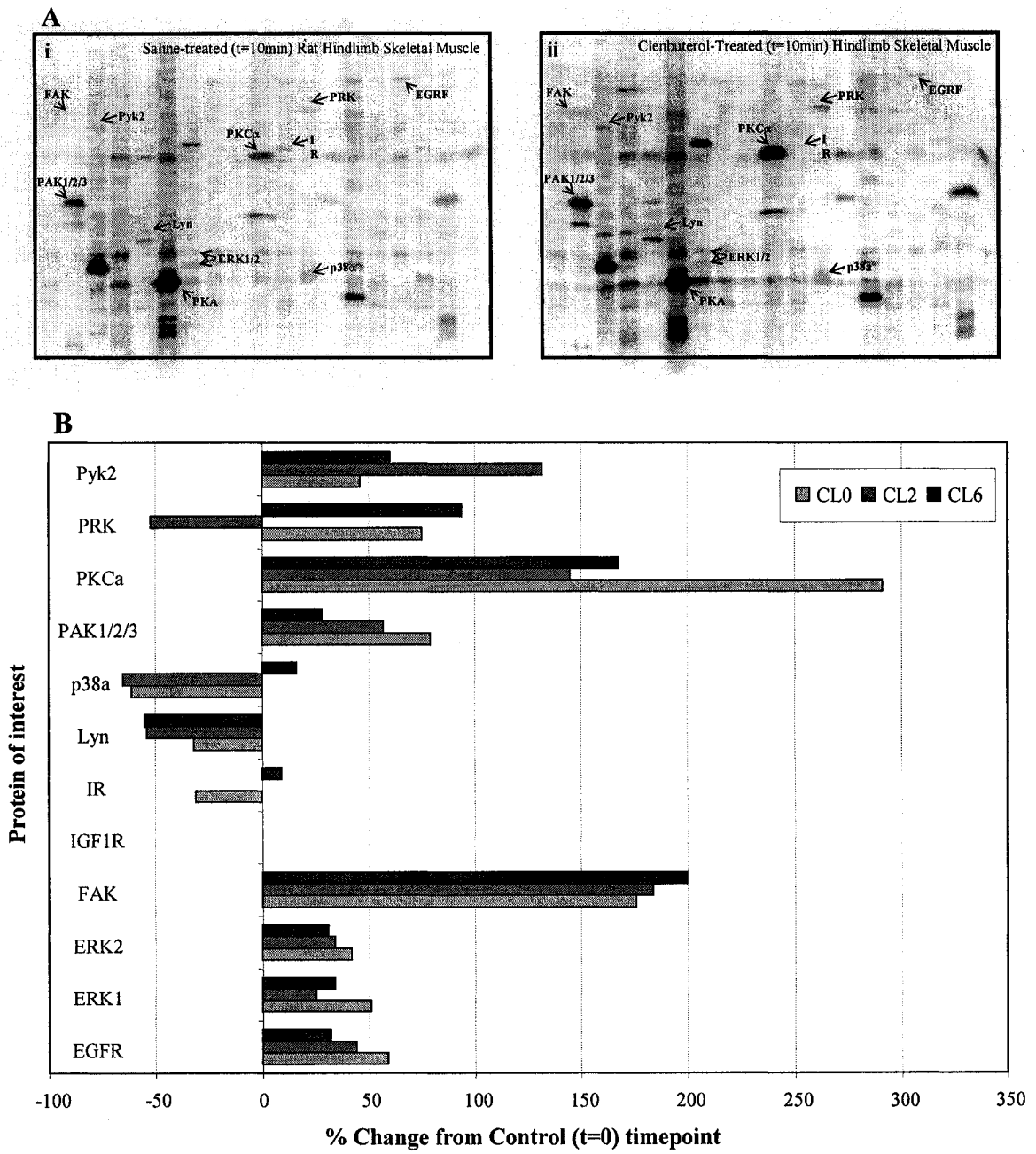

Figure 6: Selected phospho-protein kinase levels as measured by the Kinetworks™ Phopho-Site Screen (KPSS 11.0 Profile).
(A) Representative immunoblots of saline- and Clenbuterol-treated (Panels i and ii respectively) rat hindlimb skeletal muscle (3 animals pooled/sample). Bands corresponding to specific phospho-protein kinases are identified. (B) Percent different in phospho-protein kinase immunoreactivity signal intensity in rat hindlimb skeletal muscle. All values are normalized to saline-treated Control muscle (t=0). Bars: Clenbuterol-treated muscle (t=10 minutes (CL0), 2 (CL2), and 6 (CL6) hours post-injection) indicated as shown.

In contrast, both p38a MAPK (Thr^{180}/Tyr^{182}; -61%, -65%, +16%) and Lyn protein tyrosine kinase (Y^{507}; -32%, -52%, -55%) decreased substantially in skeletal muscle with Clenbuterol treatment. ERK1/2 phosporylation increased slightly, with ERK1 increasing by 51% and ERK2 increasing by 42% within 10 minutes following Clenbuterol injection. These values correspond to increases observed in p-ERK using immunoblotting techniques. PKA (both PKAα/β, Tyr^{197} and PKAβ, Ser^{338}) phosphorylation levels remained unchanged, in agreement with the PKA activity assay results. Insulin receptor phosphorylation did not change with Clenbuterol treatment and phosphor-IGF-1R did not register on the phospho-kinase screen.

cAMP response to Clenbuterol +/- Propranolol

Clenbuterol's action on cAMP was confirmed in C_2C_{12} cells as the drug stimulated immediate increases in intracellular cAMP levels by at least five-fold in myoblasts (Figure 7). Simultaneous administration of the β-adrenergic antagonist, propranolol, at doses of 1 μm and 40 μm attenuated the Clenbuterol-induced cAMP increases, an indication that Clenbuterol stimulates cAMP via the β-adrenergic receptors in the C_2C_{12} cells.

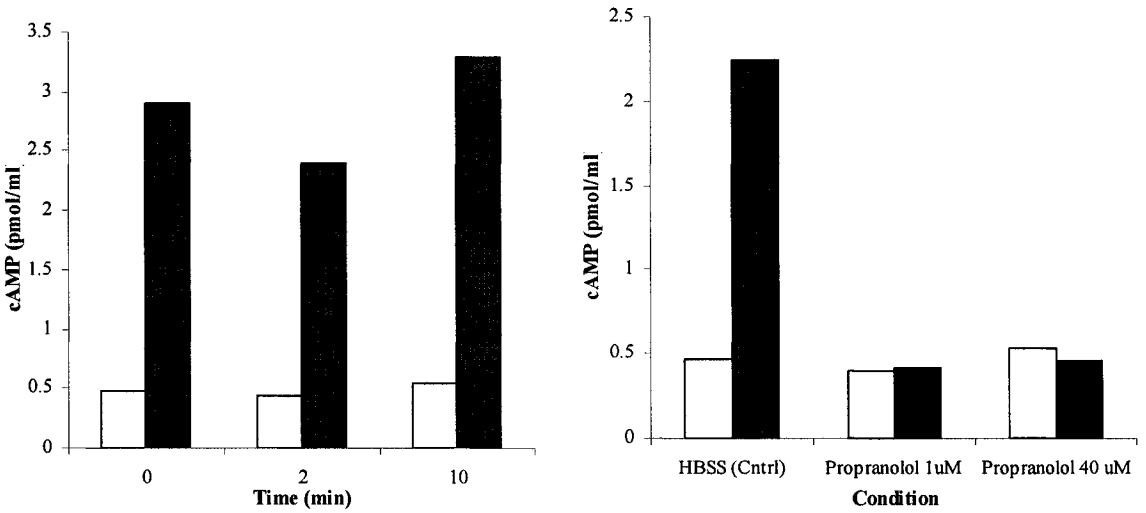

Figure 7: cAMP response in C_2C_{12} cells to 0.1 μM Clenbuterol with and without Propranolol. Left Panel: Time-course response with Clenbuterol. Right Panel: Response with addition of 1μM and 40μM of Propranolol 2 minutes following treatment. n=2/group.

Myotube Diameter with Chronic Administration

C_2C_{12} myotube area and diameter was observed (

Figure 8) and measured (Table 2) following H&E staining of cells treated with and without Clenbuterol for periods of 24-72 hours. No difference in diameter was observed with 24 hours of Clenbuterol administration versus control cells (Panel A vs. D). However, when the drug was administered for 48 hours, cells treated with Clenbuterol demonstrated a significantly larger average myotube area diameter than control cells ($p<0.01$) (48 hours: Panel B vs. E, Table 2; 72 hours: Panel F vs. C). The average myotube diameter and area increased 45% and 34% respectively with Clenbuterol versus HBSS-treated control myotubes.

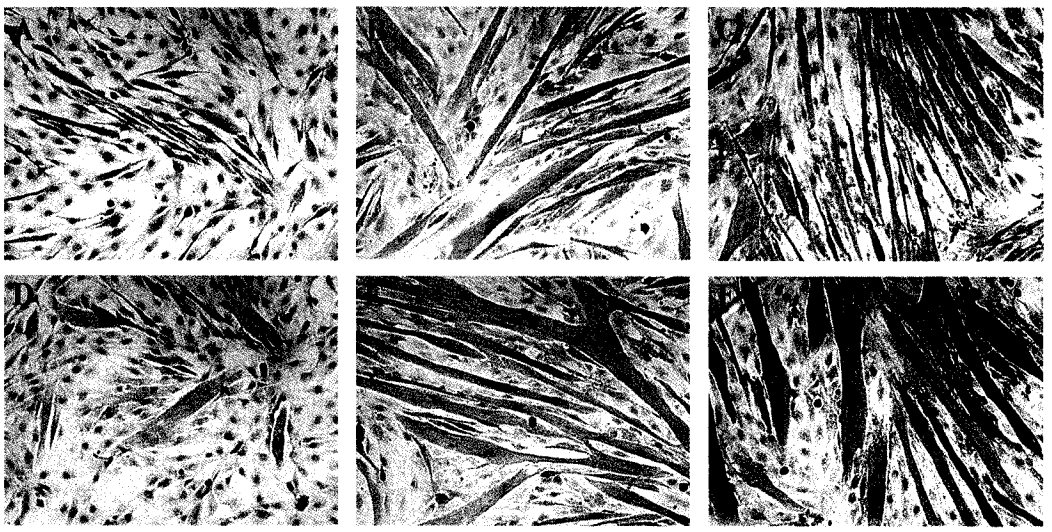

Figure 8: C_2C_{12} myotubes with and without Clenbuterol treatment. Cells were allowed to differentiate for 48 hours prior to drug administration. Control cells treated with HBSS only for 24 hours (A), 48 hours (B), and 72 hours (C) versus Clenbuterol-treated cells for 24 hours (D), 48 hours (E), and 72 hours (F).

Table 2: Area and diameter of C_2C_{12} cells treated with saline and Clenbuterol.

	Number of Myotubes Counted	Myotube Area (um2)	Myotube Diameter (um)
Saline	148	1706 ± 92	9.6 ± 0.3
Clenbuterol	140	2486 ± 154*	12.9 ± 0.5*

Data are expressed as a mean ± SE. Cells were allowed to differentiate for 48 hours prior to treatment with either HBSS or Clenbuterol for 48 hours. *Significantly different from saline-treated group ($p<0.01$).

Discussion

It is generally accepted that alterations in muscle signalling intermediates occur prior to observable change in muscle mass, although few studies have examined this in the context of Clenbuterol-induced hypertrophy. This is the first study to examine specific signalling factors thought to be associated with the regulation of muscle mass within 24 hours of a single injection of the β_2-adrenergic agonist, Clenbuterol. In the

current investigation, there was an acute increase in muscle cAMP levels in Clenbuterol-treated animals, in agreement with previous literature (MacLennan and Edwards, 1989). Interestingly, the increase in cAMP was not accompanied by elevations in PKA protein content or activity, as seen in both the Kinetworks^{TM} screen and PKA activity assay, respectively. This finding indicates that the initial triggers of Clenbuterol-induced muscle hypertrophy may be associated with PKA-independent muscle signalling events.

In the present study, Clenbuterol immediately increased p-ERK and p-Akt levels in skeletal muscle, indicating that Clenbuterol may be acting via these pathways during the initial stages of the hypertrophic process. A downstream signalling intermediate of the MAPK (Ras-Raf-MEK-ERK) pathway, ERK plays a key role in cell proliferation, protein transcription, and cell survival. It has been previously suggested that Clenbuterol may be initially stimulating ERK via the β_2-adrenergic system, via PKA-dependent activation of the MAPK pathway (Pesce et al., 2000). However, given that no change in PKA activity/phosphorylation was observed in this study, this explanation seems unlikely in this model and/or time frame.

Additional signalling factors that were also observed to increase in this study could shed light on a PKA-independent mechanism. It has been well-documented that skeletal muscle growth is dependent upon the PI3K pathway (including PI3K/Akt/mTOR/p70s6k) (Bodine et al., 2001; Rommel et al., 2001). Over-expression of Akt has been shown to increase muscle fibre size in normal and atrophied muscle (Bodine et al., 2001). Elimination of PI3K/Akt via gene knockout mice (Leevers et al., 1996) and/or pharmacological inhibition (Rommel et al., 1999) leads to decreases in cell size, abnormally slow muscle development and significantly smaller muscles versus

control animals. Further evidence also suggests that the MAPK and PI3K pathways interact positively to promote biological responses, through potential cross-talk between signalling intermediates (Wang et al., 2001). In this model, it is possible that activation of Akt is associated with the concurrent ERK activation and initiation of muscle hypertrophy via Clenbuterol (or vice versa). However, this activation appears to occur independently of the insulin and IGF-1 receptors, given that there was relatively no change in phosphorylation status of the insulin receptor with Clenbuterol administration and the IGF-1 receptor did not register on the kinase screen in the time frame examined.

Increases in proline-rich tyrosine kinase 2 (Pyk2), focal-adhesion kinase (FAK), p21-activated protein-serine kinase (PAK), and protein kinase C (PKC_{α}) were also observed within 6 hours of the single injection of Clenbuterol. Pyk2 has been shown to play a role in a variety of cellular processes including calcium-induced and Src-mediated regulation of MAPK activation (Lev et al., 1995; Dikic et al., 1996; Chen et al., 2002). Pyk2 is closely related to focal adhesion kinase (FAK), which also increased acutely in skeletal muscle following the Clenbuterol injection. FAK, a downstream target of Integrin $\beta 1$, is known to be up-regulated in stretch- and mechanical loading-induced muscle hypertrophy, through effects on myocyte proliferation, differentiation, and protein transcription (Carson and Wei, 2000; Barton and Morris, 2003; Fluck et al., 1999). PAK proteins are known to be associated with smooth muscle contraction (Van Eyk et al., 1998) but also have been shown to up-regulate the MAPK pathway through direct activation of signalling intermediates Raf and MEK (Juliano et al., 2004). PKC_{α}, although known primarily for its association with calcium signalling, has also been shown to be involved with both Pyk and ERK signalling in a variety of tissues, including

skeletal and cardiac muscle. Previous research has shown PKC activation in denervated soleus muscle with 3 days of Clenbuterol administration (Sneddon et al., 2000). Further investigation of the relationships between Clenbuterol-induced muscle hypertrophy and these factors, as well as additional "unspecified" phospho-proteins that registered on the kinase screen, is required to fully elucidate Clenbuterol's mechanism.

Taken together, these results suggest that in the acute time following a single injection of Clenbuterol, cAMP, p-Akt and p-ERK increase without concurrent increases in PKA. This suggests a PKA-independent explanation of the early stages of Clenbuterol-induced skeletal muscle hypertrophy, with possible mediation via a variety of protein kinases, including Pyk2, PAK, FAK and PKC_{α}.

CHAPTER 3: CHARACTERIZATION OF SKELETAL MUSCLE REGULATORY FACTORS IN A MURINE MODEL OF PROGRESSIVE SKELETAL MUSCLE DENERVATION

Abstract

Progressive denervation of skeletal muscle leads to significant muscle atrophy, but recent research suggests it may also stimulate myogenic and hypertrophic signalling factors known to be involved in the regulation of muscle mass. The purpose of this study was to characterize protein content of skeletal muscle regulatory factors (smRFs) - signalling intermediates associated with the PI3K/Akt (Akt and p-FOXO) and MAPK (ERK) pathways, as well as calcineurin, MRFs (MyoD and myogenin) and myostatin - in progressively denervated skeletal muscle. Skeletal muscle of G93A mice was examined through various stages of symptom progression with comparison to age-matched, wild-type controls. Increases in Akt, ERK1, ERK2 and calcineurin (CaN), as well as decreases in MyoD were observed in mixed hindlimb muscle of G93A mice versus wild-type controls. Increases in Akt occurred in both slow (red)- and fast (white)-type muscle tissue. This information, combined with previous results from the literature, indicates that although progressive denervation leads to significant muscle atrophy, there is a concurrent up-regulation of specific growth and survival factors potentially acting to prevent and/or delay muscle wasting. The ability of these survival factors to offset the progressive loss of neuronal input and muscle atrophy may ultimately dictate muscle mass status and symptom progression.

Introduction

Skeletal muscle atrophy is associated with changes in muscle-specific proteins known to be involved in the regulation of muscle mass, collectively referred to as skeletal muscle regulatory factors (smRFs). smRFs include signalling intermediates in the PI3K/Akt and MAPK (ERK) pathways, the calcium-dependent phosphatase calcineurin, myogenic regulatory factors (MRFs) and myostatin. Acute denervation-induced atrophy is associated with decreases in protein content and increases in protein degradation (Weinstein et al., 1997), due in part to an up-regulation of apoptotic factors within the muscle (Oliveira et al., 1993; Jejurikar et al., 2002; Schoser et al., 2001). Alterations in muscle-specific signalling factors that occur with progressive denervation associated with chronic neuromuscular diseases such as Amyotrophic Lateral Sclerosis (ALS) have not yet been fully explained. It has been suggested that skeletal muscle attempts to regenerate and repair itself with long-term denervation by initiating myogenesis (Borisov et al., 2001) and/or hypertrophy (Yamaguchi et al., 2004). As such, examination of the effects of progressive denervation on muscle-specific signalling factors involved with the regulation of muscle mass is warranted.

Amyotrophic Lateral Sclerosis (ALS), also known as Lou Gherig's Disease, is a progressive and fatal neurodegenerative disease involving the degeneration of motor neurons (Boillee et al., 2006). This progressive denervation leads to skeletal muscle atrophy (Corbett et al., 1982), functional impairment (Derave et al., 2003) and eventual paralysis (Chiu et al., 1995). The G93A mouse that over-expresses a mutant form of the human superoxide dismutase (mSOD) transgene develops a disorder that resembles ALS in its clinical signs and symptoms (Gurney et al., 1994) and has also proven to be a useful

model to study progressive denervation-induced skeletal muscle atrophy. mSOD-induced skeletal muscle pathology includes a loss of neuromuscular junctions and resulting weakness (Frey et al., 2000; Wooley et al., 2005; Thomas and Zijdewind, 2006). Although the etiology of disease/symptom progression in these animals is currently unknown, previous research has suggested the involvement of protein kinases and phosphatases in both neuronal (Hu et al., 2003; Krieger et al., 2003) and non-neuronal cells such as skeletal muscle (Cunningham, thesis; Leger et al., 2006) in the pathogenesis and progression of symptoms. Evidence also suggests that non-denervated myofibres in progressive neurodegenerative disorders tend to undergo compensatory hypertrophy (Banker and Engel, 1994) possibly via the up-regulation of growth and/or hypertrophic signalling pathways (Yamaguchi et al., 2004; Glass, 2003b).

Progressive denervation-induced skeletal muscle atrophy ultimately involves multiple finely tuned and highly coordinated signalling events. In order to investigate the theory of progressive denervation-induced myogenesis and compensatory hypertrophy, the following study sought to examine levels of muscle-specific signalling factors known to be involved with these processes in progressively denervated skeletal muscle of G93A mice. Specifically, protein levels of signalling intermediates associated with the PI3K/Akt (Akt and p-FOXO) and MAPK (ERK) pathways, as well as calcineurin, MRFs (MyoD and myogenin) and myostatin, were characterized in relation to disease progression in skeletal muscle of the G93A versus age-matched, wild-type control mice.

Experimental Approach

Determination of Animal Genotype

All procedures followed the guidelines outlined by the Canadian Council on Animal Care and were approved by the Animal Care Committee, Simon Fraser University. B6SJL-TgN(SOD1-G93A)1Gur transgenic SOD1 mice (mSOD) and age-matched wild-type (WT) controls were obtained from Jackson Laboratory (Bar Harbor, ME). All animals were kept in a sterile room under a 12-h light:dark cycle with food (Purina Rodent Lab Diet 5001, IL) and water available *ad libitum*. Mice were bred in-house, then weaned and screened for the mSOD transgene by PCR at approximately 30 days of age.

Briefly, ear tissue was digested in a mixture of Chelex (5% w/v, Bio-Rad), Proteinase K (250 μg/150μl, Sigma) and RNase A (125 μg/150μl, Sigma) at 55°C for 2 x 15 minutes and then placed in a heating block (100°C) for 8 minutes. Samples were centrifuged (12,000 rpm for 15 minutes) and supernatant was removed and used for subsequent PCR analysis. Each sample was prepared in 25 μl volumes with 1μl each of forward and reverse primers identifying the mSOD gene (mSOD1: CAT CAG CCC TAA TCC ATC TGA; mSOD2: CGC GAC TAA CAA TCA AAG TGA, both from Invitrogen), as well as 10x buffer (2.5μl), dNTPs (2.5μl), $MgCl_2$ (0.5μl), Taq polymerase (0.3μl) (all from Qiagen) and distilled water (2.5μl). PCR was run with the following setting: 1 cycle at 95°C/5min, 30 cycles at (94°C/30sec, 56°C/30sec, 72°C/30sec), 1 cycle at 94°C/30sec, 1 cycle at 56°C/30sec, 1 cycle at 72°C/10min. Detection of the PCR product and mSOD transgene was achieved via separation of samples on a 1.2% agarose gel containing 0.01% Ethidium Bromide, and visualization with UV light. Mice

expressing the mutant transgene were then referred to as G93A mice whereas mice without the mutant transgene were considered to be wild-type (WT) control animals. Questionable and/or fragmented samples were re-run to confirm the mouse genotype.

Determination of Symptomotology

The staff at the Animal Care Facility (ACF, Simon Fraser University) were informed of the mice genotypes (WT vs. G93A) and monitored mice daily for clinical symptoms via a variety of tests related to disease progression: hindlimb splay (a test of muscle function), mobility, gait and posture, overall behavioural characteristics and body mass. The observation of hindlimb tremor during tail suspension has been shown to be the most simple and sensitive method to detect early symptoms but requires experience and training on the side of the observer (Weydt et al., 2003). Mice were examined at four distinct stages during disease progression: pre-symptomatic (PS), symptom onset (SO), severe symptoms (SS), and end-stage (ES) symptoms (Table 3).

Table 3: Classification of Clinical Symptomotology through disease progression in affected G93A mice (Animal Care Facility, Simon Fraser University).

Stage of Symptom	Clinical Characteristics
Pre-Symptomatic (PS)	▪ animals possess transgene, but do not yet exhibit clinical symptoms ▪ hind legs are extended and splay upon lifting
Symptom Onset (SO)	▪ flexion in one or both of the hind legs ▪ muscle atrophy from hips/hindlimb, progressing into back ▪ rolling gait (whole body moves with each step; progresses from slight to pronounced) or paddling gait- with or without cow-hocked hind feet ▪ hunched posture ▪ behaviour is BAR (Bright, Alert, and Responsive)

Stage of Symptom	Clinical Characteristics
Severe Symptoms (SS)	▪ all mild symptoms, plus: ▪ hindlimb knuckling of one or both feet (dragging of feet) ▪ maximum flexion in the hindlimbs ▪ atrophy in most lower body muscles ▪ decreased mobility ▪ loss of balance due to abnormal gait (occasional hopping gait) ▪ rough coat (in males) ▪ behaviour is QA (Quiet and Alert)
End-Stage Symptoms (ES)	▪ maximum flexion in hindlimbs ▪ severe atrophy in back and hindlimbs ▪ partial or complete paralysis of one or both hindlimbs ▪ lateral recumbency of >10 seconds

When the animals reached the appropriate symptom stage, they were euthanized as per ACF guidelines using blended O_2 and CO_2 with progressive reduction of O_2 until narcosis to minimize animal discomfort. Mixed muscle from the hindlimb (including quadriceps femoris), as well as red and white gastrocnemius and soleus muscles were quickly extracted and snap-frozen in liquid nitrogen. Samples were stored at –80°C for subsequent analyses.

Tissue Preparation

Full details regarding tissue preparation are outlined in Appendix A. Whole protein lysate was extracted from mixed hindlimb or gastrocnemius muscles of 24 G93A mice (n=6 each for PS, SO, SS, and ES) and 24 wild-type (WT) age-matched controls. Lysates from two additional mice (1 WT and 1 G93A) were also prepared to serve as controls during gel electrophoresis. Frozen skeletal muscle tissue was weighed and homogenized in a 10 ml volume of ice-cold modified RIPA buffer. Protease inhibitors [phenylmethysufonyl fluoride (PMSF), leupeptin, pepstatin and aprotinin] and phosphatase inhibitors [sodium orthovanadate (Na_3VO_4) and sodium fluoride (NaF)] were added fresh to the buffer solution each day. Samples were centrifuged (Baxter

Canlab Biofuge A) at 20,000 g for 15 minutes at 4°C and the resulting supernatant was transferred to clean eppendorf tubes and stored at -80°C until further use.

Protein Determination

Protein content of the resulting supernatant was determined via a Bradford assay (Bio-Rad Laboratories, Hercules, CA) and fully explained in Appendix A. Optical density values of the protein standards were recorded and plotted against protein concentration; total protein content of each sample was determined from this plot.

Gel Electrophoresis and Immunoblotting

Complete details regarding gel electrophoresis and immunoblotting procedures are outlined in Appendix A. Briefly, equal amounts of protein (70μg/35μl) were separated on a one-dimensional (8-12%) SDS polyacrylamide gel. A molecular weight marker (Amersham Pharmacia) and two reference samples (lysates from 1 WT mouse and 1 G93A mouse) were run on all gels. Samples were run in two steps (50mA constant current through stacking gel, 100mA constant current through running gel) using an electrophoresis running apparatus (Bio-Rad) immersed in running buffer solution [25mM Tris; 125mM glycine; 0.1% (wt/vol) SDS; pH 8.3].

Gels were removed from the running apparatus and the stacking gel was excised prior to transfer. All transfers were performed at 4°C under constant current conditions with voltage set between 50-70 mV (Bio-Rad Power Pac 3000). Following the transfer, membranes were rinsed twice with dH_20, visualized with Ponceau Red (0.2% in 3% TCA, Sigma), and washed in TBST.

Non-specific binding sites on membranes were blocked with 5% bovine serum albumin (BSA) in TBST for 90 minutes at room temperature, under gentle agitation. Membranes were rinsed 3 x 5 minutes with excess volumes of TBST and subsequently incubated overnight at 4°C with appropriate primary antibody [Akt (*sheep*) (Upstate Biotechnology Inc.), CaN (*rabbit)* (Upstate Biotechnology Inc.), ERK (*rabbit)* (also known as p44/42 MAPK; Cell Signalling), MyoD (*rabbit*) (Santa Cruz), Myogenin (*rabbit*) (Santa Cruz), Myostatin (GDF-8) (*rat*) (R&D Systems), p-FOXO (Ser^{256}) (*rabbit*) (Cell Signalling)]. All antibodies were diluted 1:1000 (vol/vol) with TBST, 0.5% NaN_3 and 1% BSA, the exception being p-FOXO which was diluted 1:400 (vol/vol). Following an overnight incubation, the membranes were washed 5 x 5 minutes with TBST and incubated with an excess volume of appropriate horseradish peroxidase (HRP)-conjugated secondary antibody (all 1:20,000 with TBST and 1% BSA). Secondary antibody incubation occurred under gentle agitation at room temperature for 90 minutes. Membranes were washed three times each with TBST and TBS, immersed in Enhanced Chemiluminescence (ECL) reagent, and exposed to Hyperfilm-ECL (Amersham). Relative protein content was quantified by scanning protein bands using a commercially-available flatbed scanner (Epson) and Scion Image software (NIH).

Statistical Analysis

G93A mice were age and sex-matched to wild-type (WT) controls and grouped according to stage of symptoms: G93A-PS, -SO, -SS, -ES versus WT-PS, -SO, -SS, -ES. For hindlimb muscle analyses, extreme data points were identified via boxplot analysis prior to analysis and were removed from the data set if values were considered questionable (> 3 times the interquartile range/boxplot length, measured from the upper

and/or lower quartile). A 2 x 4 (Disease x Symptom) randomized group analysis of variance (ANOVA) with Tukey's post hoc analysis was used for body and soleus mass, as well as each muscle signalling factor examined. Mean body mass differences (Body Mass $_{WT}$ – Body Mass $_{G93A}$) and soleus mass differences (Sol Mass $_{WT}$ – Sol Mass $_{G93A}$) were compared using a one-way ANOVA. An α-level of 0.05 was set as significant for all tests, and all results are reported as means ± SE. All tests were conducted using SPSS 15.0 statistical software.

Results

Symptomotology, Body and Soleus Mass

Mouse characteristics, including age of mice in each symptom group, as well as body mass and soleus muscle mass of wild-type (WT) control and G93A animals are shown in Table 4. The mean age of pre-symptomatic (PS) G93A mice was 70 ± 5 days. The mean age of G93A mice demonstrated onsets of clinical symptoms (symptom onset, SO) at 84 ± 3 days of age, and G93A mice exhibiting severe (SS) and end-stage (ES) symptoms were 123 ± 5 and 139 ± 5 days of age respectively.

Body mass of G93A mice overall were significantly less than those of the control mice (20.9 ± 1.4 g vs. 25.5 ± 0.9 g) ($p<0.001$). With respect to symptom progression, mean body mass of G93A mice was not significantly different from age-matched WT control mice at pre-symptomatic (PS) and symptom onset (SO) stages of the disease. However, body mass of G93A mice gradually decreased as a function of disease progression, significantly different from WT mice at SS (21.3 ± 1.4g vs. 28.2 ± 1.7 g; $p<0.01$) and ES (18.4 ± 1.1 g vs. 26.6 ± 2.7g; $p<0.005$) symptom stages. In association

with this finding, the difference in mean body mass between G93A and WT mice (Body Mass $_{WT}$ – Body Mass $_{G93A}$) increased over the course of disease progression, significantly greater between mice in SS (7.6 ± 1.9g; $p<0.05$) and ES (7.8 ± 2.4g; $p<0.01$) stages.

Table 4: Mouse characteristics of G93A vs. age-matched wild-type control mice.

Group	Mean Age (days)	Body Mass (g)	Mean Mass Difference (WT-G93A) (g)	Soleus Mass (mg)	Mean Soleus Mass Difference (mg)
WT-PS	70 ± 5	23.4 ± 1.4	1.1 ± 0.8	6.5 ± 1.2	1.6 ± 1.0
G93A-PS	70 ± 5	22.3 ± 1.8		4.9 ± 0.9	
WT-SO	84 ± 3	24.3 ± 1.5	2.9 ± 1.5	6.8 ± 0.5	0.2 ± 1.2
G93A-SO	84 ± 3	21.4 ± 1.2		5.7 ± 0.6	
WT-SS	124 ± 6	28.2 ± 1.7 †	7.6 ± 1.9 ‡	7.6 ± 0.5	3.3 ± 1.2
G93A-SS	123 ± 5	21.3 ± 1.4 *		5.1 ± 1.4	
WT-ES	139 ± 6	26.6 ± 2.7	7.8 ± 2.4 ‡	6.7 ± 0.4	2.3 ± 0.7
G93A-ES	139 ± 5	18.4 ± 1.1 *		4.5 ± 0.3 *	

Values reported as means ± SE. WT = age-matched wild-type control mice (n=5-6/group, matched and identical to G93A mice). PS = Pre-Symptomatic; SO = Symptom Onset; SS = Severe Symptoms; ES = End-Stage symptoms. *Significantly different from age-matched wild-type controls ($p<0.05$). †Significantly different from G93A-PS ($p<0.05$). ‡Significantly different from PS group difference ($p<0.05$).

Soleus muscle mass was 27% less overall in G93A mice versus WT controls (5.0 ± 0.4 mg vs. 6.9 ± 0.4 mg; $p<0.01$). With respect to symptom progression, mean soleus mass was not significantly different between G93A and WT mice at PS, SO, or SS stages, however end-stage G93A mice demonstrated a 33% lower soleus mass than their age-matched, WT controls (4.5 ± 0.3 mg vs. 6.7 ± 0.4 mg; $p<0.05$). The mean soleus mass difference between G93A and matched WT controls (Sol Mass $_{WT}$ – Sol Mass $_{G93A}$) was not observed to be significantly different from PS ($p=0.27$) at any of the three later stages of symptomotology.

Levels of smRFs

Levels of selected skeletal muscle regulatory factors (smRFs) were examined in mixed hindlimb muscle of G93A mice in four stages of disease symptomotology and age-matched WT controls. Overall, significant main effects of disease (i.e. G93A differed significantly from WT protein levels) were observed in the following signalling factors: calcineurin (CaN), ERK1, ERK2, and MyoD. A significant main effect of symptom was observed in p-FOXO, decreasing over time/symptom in both G93A and WT mice. There was no significant difference was observed between G93A vs. WT control skeletal muscle with respect to myogenin and myostatin levels.

CaN ($p<0.001$; Figure 9), ERK 1 ($p<0.05$; Figure 10A) and ERK2 ($p<0.01$; Figure 10B) protein content were significantly elevated in symptomatic G93A mice compared to WT controls. CaN levels in the G93A mixed hindlimb skeletal muscle increased with disease progression, significantly higher than age-matched WT control muscle at SS (1.90 ± 0.33 AU vs. 0.71 ± 0.13 AU) and ES (1.43 ± 0.21 AU vs. 0.90 ± 0.13 AU) symptom stages. Significant differences in CaN between G93A mice in different symptom groups were not observed.

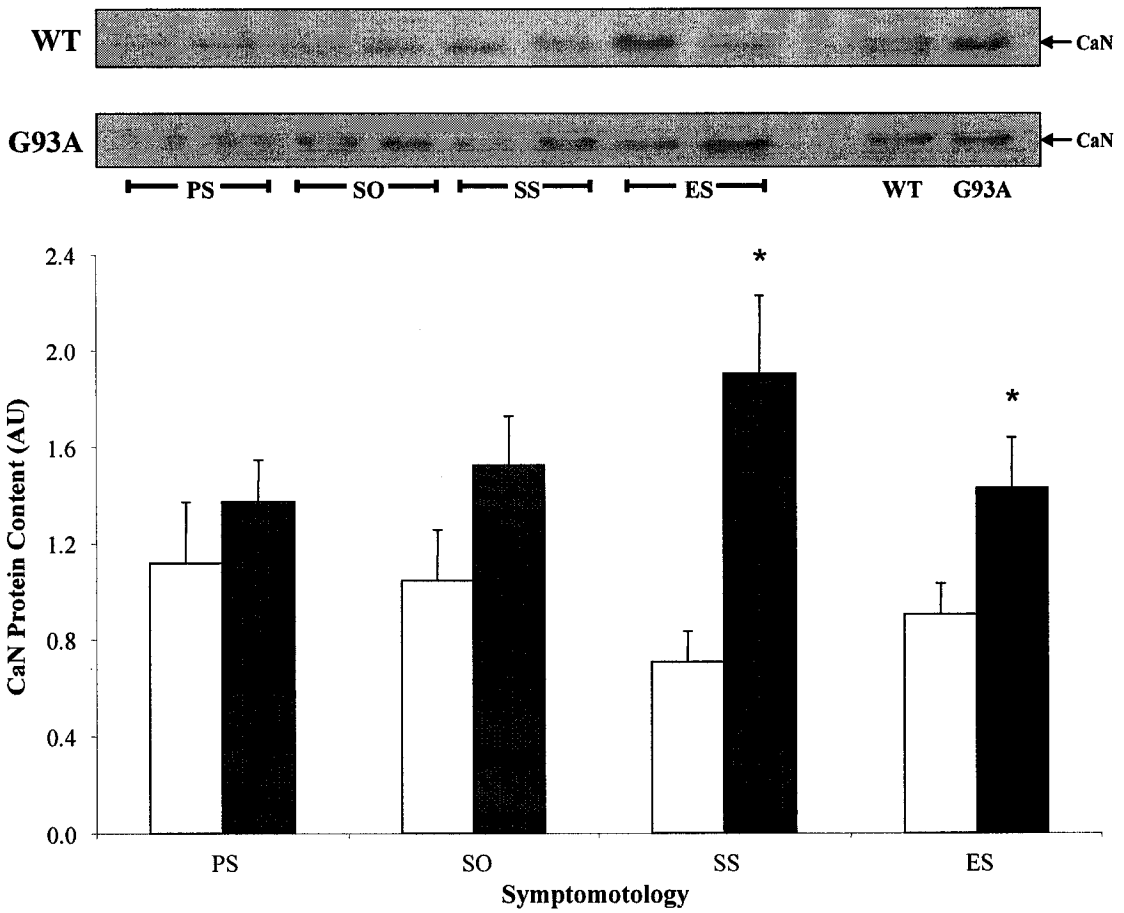

Figure 9: Calcineurin (CaN) protein content (mixed hindlimb skeletal muscle): G93A vs. WT age-matched Controls, as determined by Western immunoblotting.
Top panel shows representative blots. Bottom panel depicts graphed values of WT (white bars) and G93A (black bars) mice. Data are expressed as a mean ± SE (n=5-6/group). PS = G93A, pre-symptomatic; SO = G93A, symptom onset; SS = G93A, severe symptoms; ES = G93A, end-stage. *Significantly different from WT controls of the same age ($p<0.05$).

Although G93A muscle exhibited increased levels of both ERK1 and ERK2 when compared to WT control muscle, their trends differed through disease progression. ERK1 increased progressively with advancing symptom stages, 89% greater in G93A-SS mice versus WT-SS mice (1.34 ± 0.19 AU vs. 0.71=3 ± 0.14 AU; $p<0.05$). In addition, G93A-SS mice were also significantly different from G93A-PS mice (1.34 ± 0.19 AU vs. 0.94 ± 0.10 AU; $p<0.05$), indicating that ERK1 content gradually increased in skeletal muscle of G93A animals through disease progression. ERK2 was elevated in all G93A

mice versus wild-type controls, significantly higher in both G93A-PS ($p<0.05$) and G93A-SS ($p<0.01$) mice. In contrast to ERK1, no significant differences were observed in ERK2 between the different symptom groups of the G93A mice.

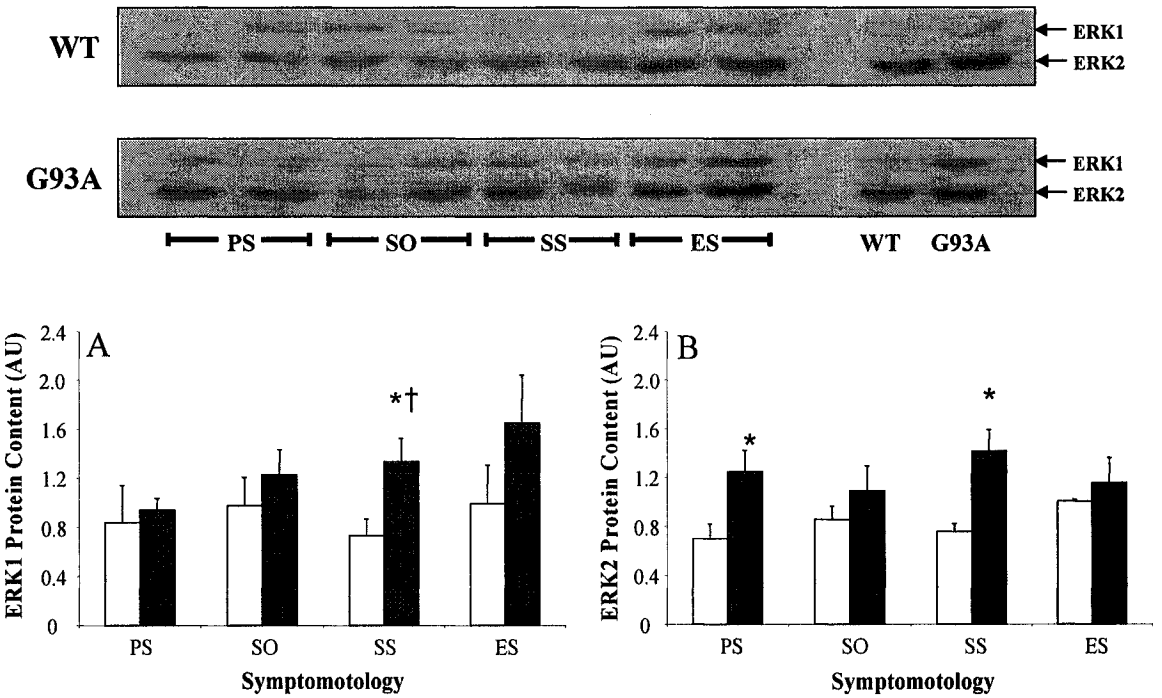

Figure 10: ERK1 (A) and ERK2 (B) protein content (mixed hindlimb skeletal muscle): G93A vs. WT age-matched Controls, as determined by Western immunoblotting.
Top panel shows representative blots. Bottom panel depicts graphed values of WT (white bars) and G93A (black bars) mice. Data are expressed as a mean ± SE (n=5-6/group). PS = G93A, pre-symptomatic; SO = G93A, symptom onset; SS = G93A, severe symptoms; ES = G93A, end-stage. *Significantly different from WT control mice of the same age ($p<0.05$). †Significantly different from G93A, PS ($p<0.05$).

In contrast to CaN and ERK1/2, significantly lower levels of MyoD were observed in G93A mixed skeletal muscle when compared to WT muscle ($p<0.05$; Figure 11). Levels of MyoD in G93A-PS, -SO, and -SS mice were not significantly different from their age-matched controls (WT-PS, WT-SO, and WT-SS respectively). However, G93A-ES mice were found to have 65% less MyoD protein content than WT-ES mice (1.03 ± 0.13 AU vs. 1.70 ± 0.25 AU; $p<0.05$).

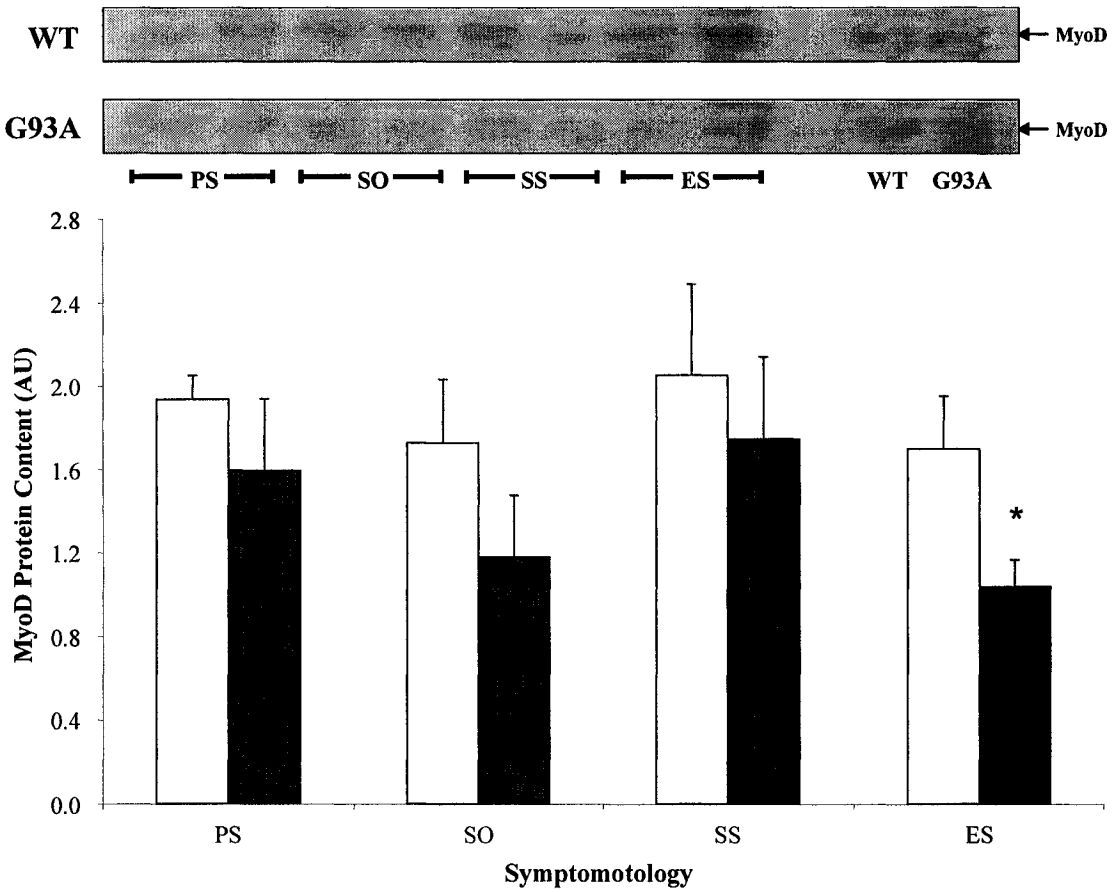

Figure 11: MyoD protein content (mixed hindlimb skeletal muscle): G93A vs. WT age-matched Controls, as determined by Western immunoblotting.
Top panel shows representative blots. Bottom panel depicts graphed values of WT (white bars) and G93A (black bars) mice. Data are expressed as a mean ± SE (n=5-6/group). PS = G93A, pre-symptomatic; SO = G93A, symptom onset; SS = G93A, severe symptoms; ES = G93A, end-stage. *Significantly different from WT control mice of the same age ($p<0.05$).

A significant (Symptom) main effect was observed as p-FOXO content decreased ~2-fold over time/symptom in mixed skeletal muscle of both G93A and WT mice ($p<0.05$; Figure 12). In contrast, neither myogenin (Figure 13) or myostatin (Figure 14) protein content differed significantly between WT and G93A mice or as a function of symptom progression ($p>0.05$). Although it appears as though there is a trend to increase myostatin levels, particularly later in disease progression (SS: +105%; ES: +95%), the

differences between G93A and WT levels were not statistically significant (p=0.12), presumably due to a large variability in myostatin content in G93A muscle.

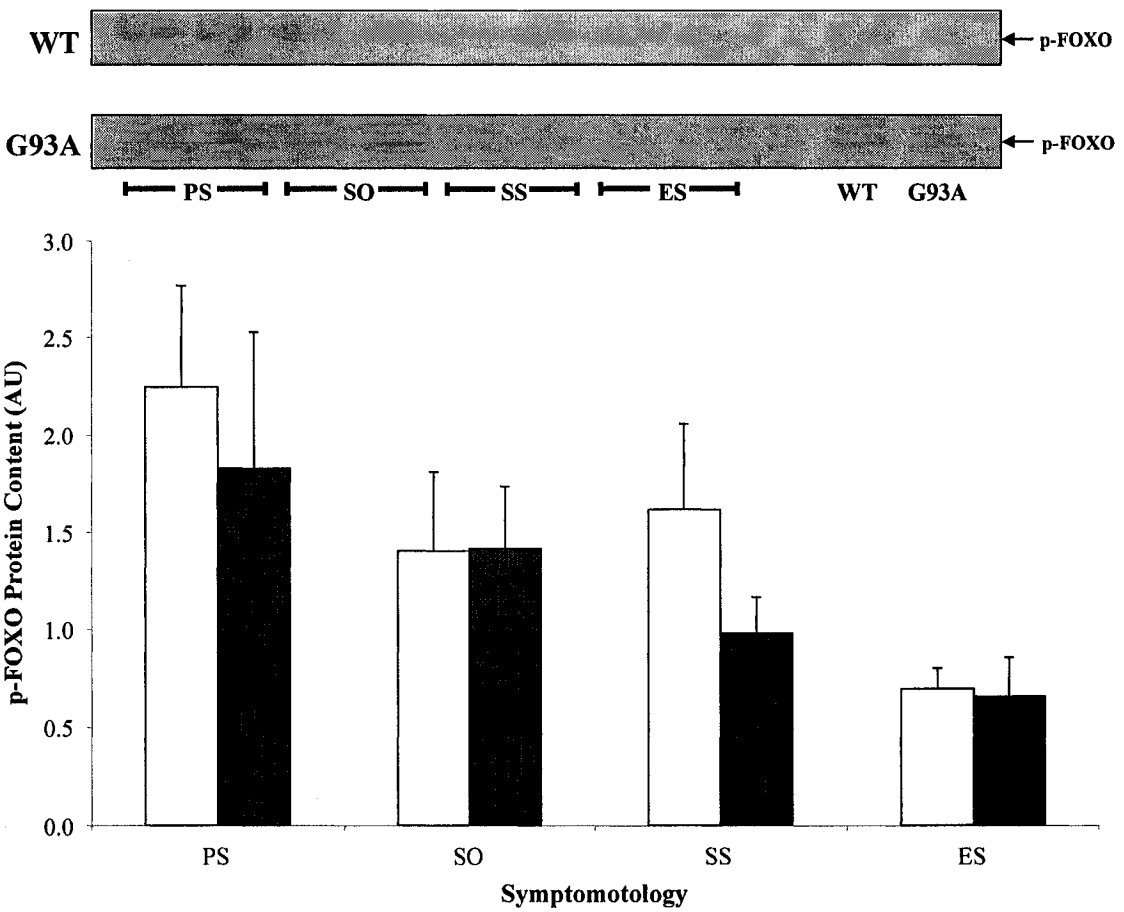

Figure 12: phospho-FOXO protein content (mixed hindlimb skeletal muscle): G93A vs. WT age-matched Controls, as determined by Western immunoblotting.
Top panel shows representative blots. Bottom panel depicts graphed values of WT (white bars) and G93A (black bars) mice. Data are expressed as a mean ± SE (n=6/group). PS = G93A, pre-symptomatic; SO = G93A, symptom onset; SS = G93A, severe symptoms; ES = G93A, end-stage.

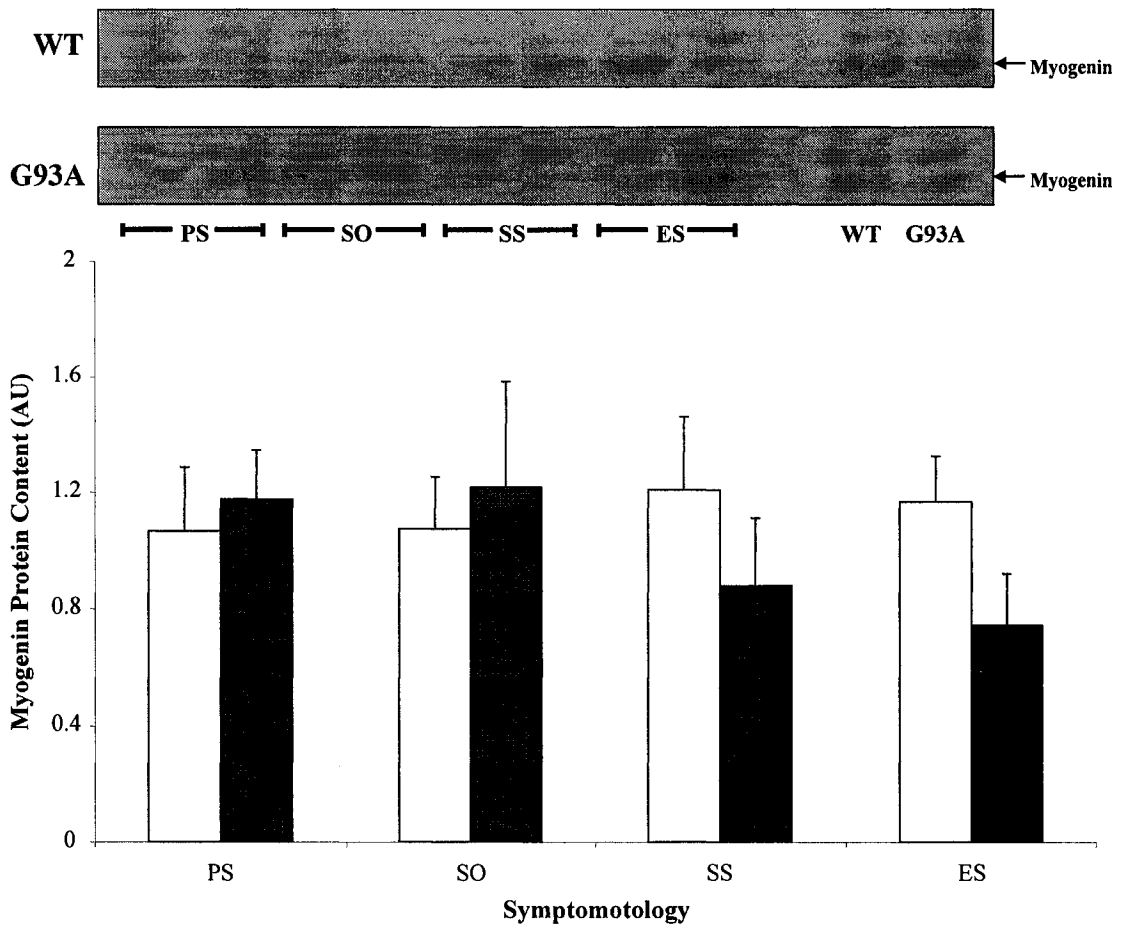

Figure 13: Myogenin protein content (mixed hindlimb skeletal muscle): G93A vs. WT age-matched Controls, as determined by Western immunoblotting.
Top panel shows representative blots. Bottom panel depicts graphed values of WT (white bars) and G93A (black bars) mice. Data are expressed as a mean ± SE (n=6/group). PS = G93A, pre-symptomatic; SO = G93A, symptom onset; SS = G93A, severe symptoms; ES = G93A, end-stage.

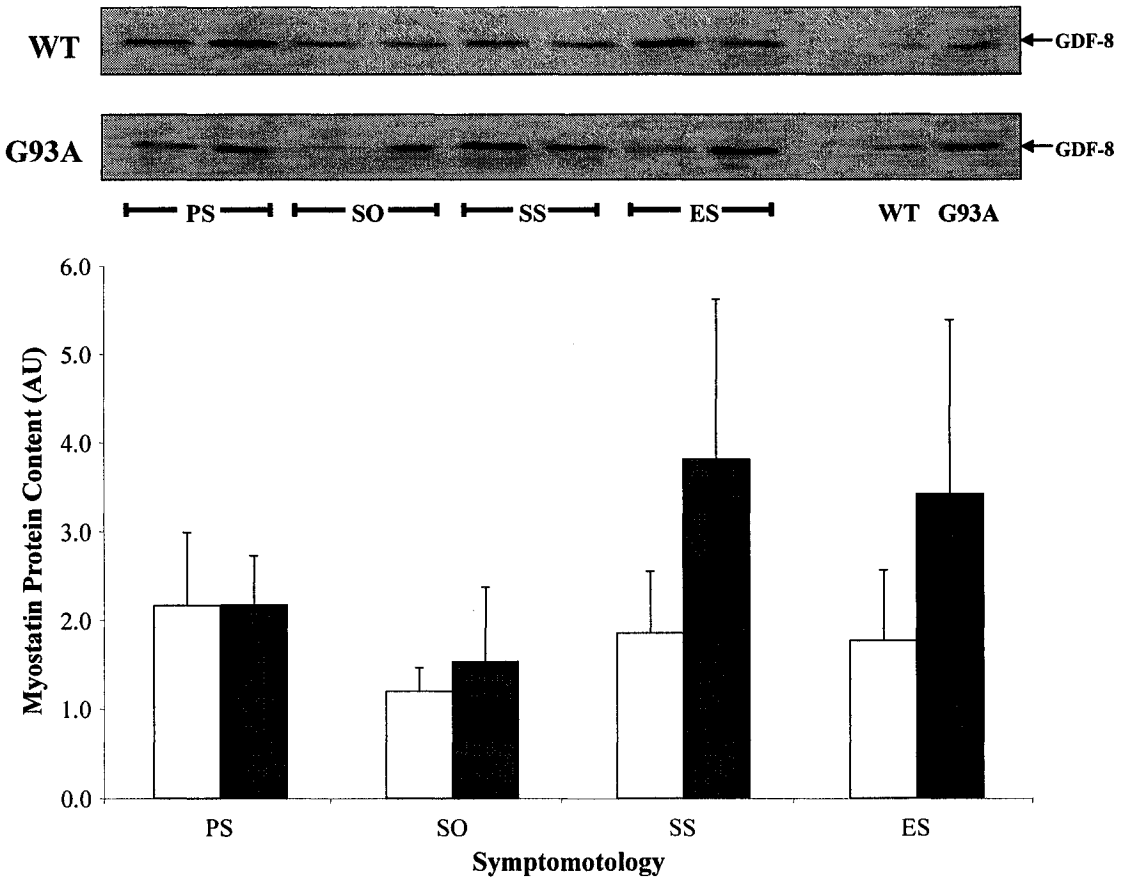

Figure 14: Myostatin (GDF-8) protein content (mixed hindlimb skeletal muscle): G93A vs. WT age-matched Controls, as determined by Western immunoblotting.
Top panel shows representative blots. Bottom panel depicts graphed values of WT (white bars) and G93A (black bars) mice. Data are expressed as a mean ± SE (n=5-6/group). PS = G93A, pre-symptomatic; SO = G93A, symptom onset; SS = G93A, severe symptoms; ES = G93A, end-stage. *Significantly different from controls ($p<0.05$).

In a related experiment ongoing within the laboratory, examination of levels of the survival protein Akt was compared between G93A and age-matched WT control skeletal muscle tissue (Cunningham, thesis). Figure 15 depicts the previously published differences in Akt content.

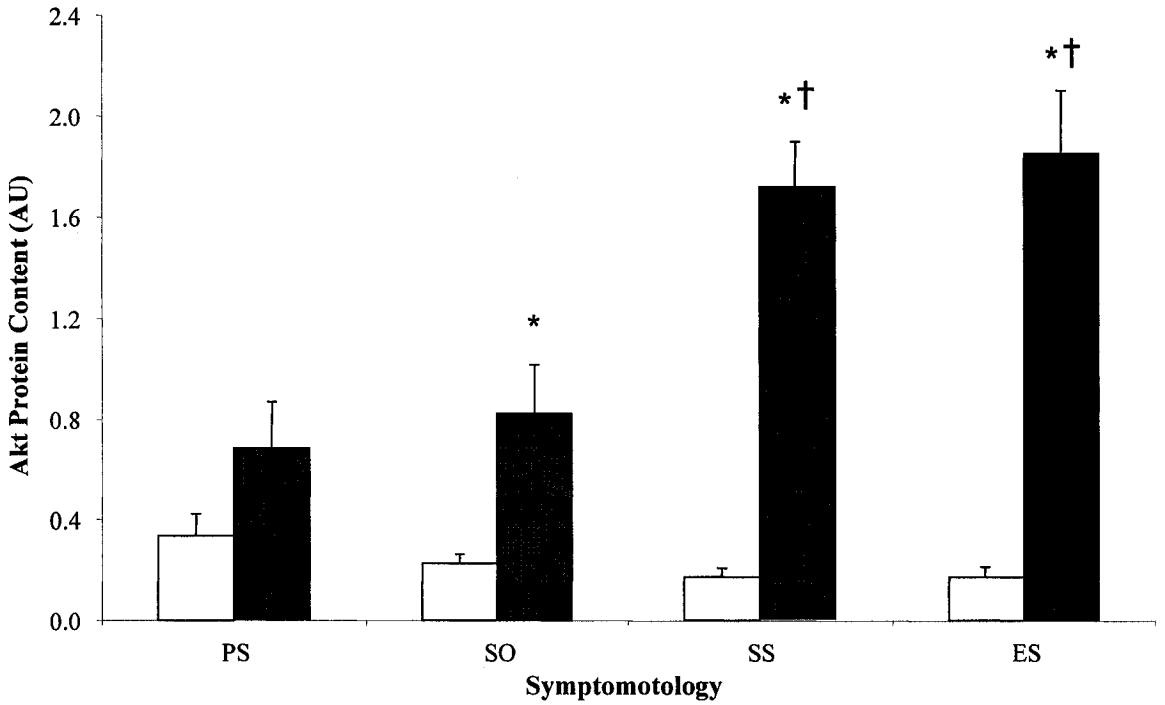

Figure 15: Akt protein content (mixed hindlimb skeletal muscle): G93A vs. WT age-matched Controls, as determined by Western immunoblotting.
Graph, previously published by Cunningham, L (M.Sc. Thesis), depicts values of WT (white bars) and G93A (black bars) mice. Data are expressed as a mean ± SE (n=5-6/group). PS = G93A, pre-symptomatic; SO = G93A, symptom onset; SS = G93A, severe symptoms; ES = G93A, end-stage. *Significantly different from controls ($p<0.05$). †Significantly different from G93A, PS ($p<0.05$).

This trend was further examined in additional muscles, red gastrocnemius (RG) and white gastrocnemius (WG) tissues (Figure 16A and B respectively). Significant main (Disease and Symptom) and interaction effects were found for Akt levels in RG muscle. Akt content increased in red gastrocnemius (RG) mice with severe symptoms (SS) significantly greater than levels measured in wild-type control mice (1.46 ± 0.07 vs. 0.05 ± 0.01) ($p<0.01$). Akt content also increased in white gastrocnemius (WG) muscle throughout symptom progression, significantly different between G93A-ES and WT-ES muscle (4.86 ± 2.46 vs. 0.11 ± 0.02) ($p<0.05$).

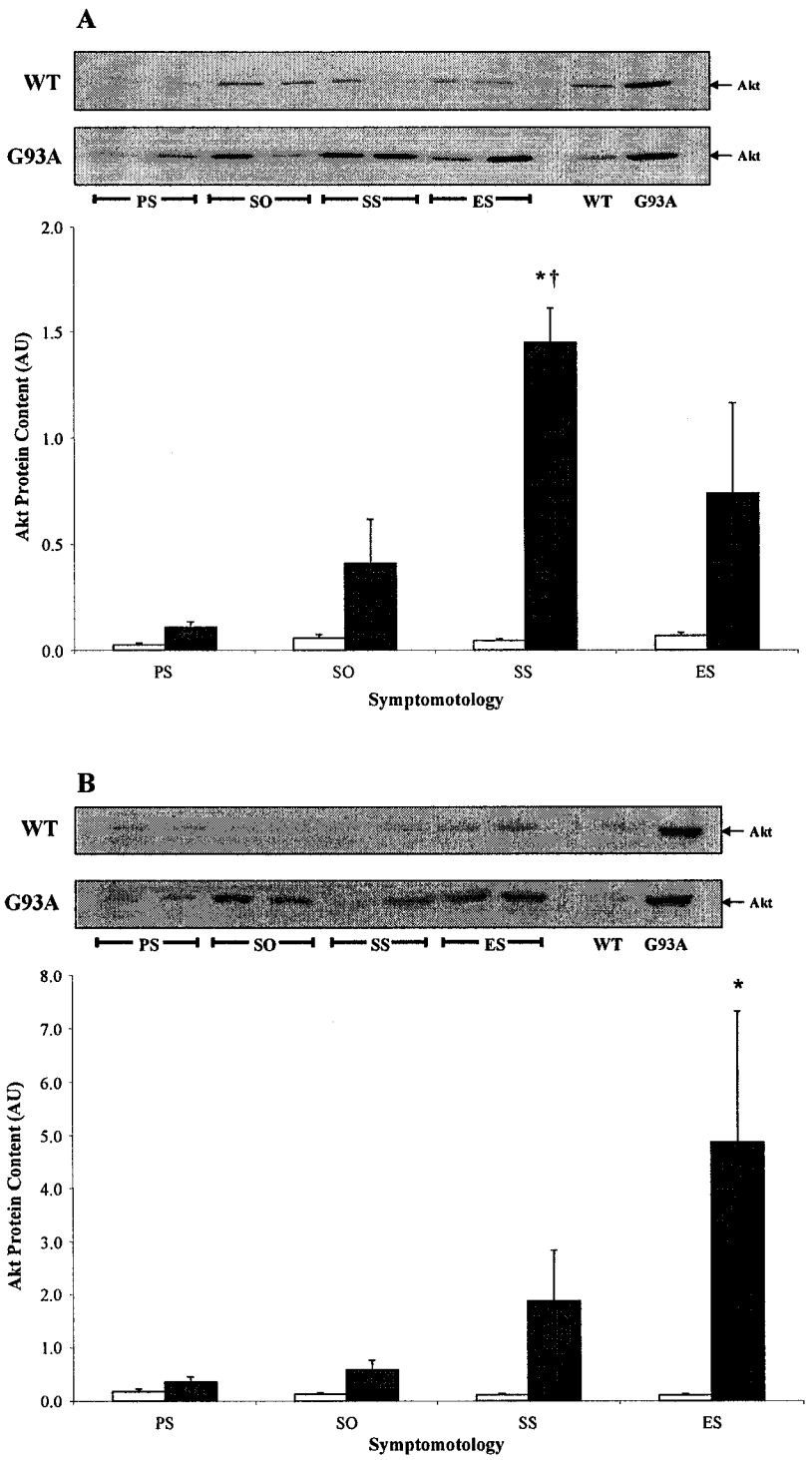

Figure 16: Akt protein content in red (A) and white gastrocnemius (B) skeletal muscle: G93A vs. WT age-matched Controls, as determined by Western immunoblotting.
Top panels show representative blots. Bottom panels depict graphed values of WT (white bars) and G93A (black bars) mice. Data are expressed as a mean ± SE (n=5-6/group). PS = G93A, pre-symptomatic; SO = G93A, symptom onset; SS = G93A, severe symptoms; ES = G93A, end-stage. *Significantly different from controls ($p<0.01$). +Significantly different from G93A, PS ($p<0.05$).

Discussion

Skeletal muscle atrophy has been shown to be associated with changes in protein kinases involved in the regulation of muscle mass (Kandarian and Jackman, 2006), with alterations highly dependent upon the model of atrophy examined. To date, few studies have examined the effects of progressive denervation on muscle-specific signals in the G93A murine model of ALS. Recent research suggests that long-term, progressive denervation may up-regulate myogenic and/or hypertrophic signalling factors in an attempt to combat the denervation process (Yamaguchi et al., 2004; Borisov et al., 2001; Cunningham, thesis). In this study, increases in factors associated with hypertrophy (calcineurin, Akt and ERK1/2), as well as decreases in the myogenic regulatory factor MyoD were found in skeletal muscle of G93A mice when compared to wild-type controls. These results indicate that the protein content of myogenic and hypertrophic signalling factors is altered in G93A skeletal muscle, often prior to the onset of muscle wasting as significant muscle atrophy (-33% of WT soleus mass) was not observed until end-stage of disease progression.

The protein phosphatase, calcineurin (CaN) increased progressively with symptom severity in G93A mice, suggesting that increases in this protein may occur in response to disease development. Given its previously documented role in muscle hypertrophy, cell survival and the prevention of apoptosis (Bodine et al., 2001; Schiaffino and Serrano, 2002; Dunn et al., 2000), the increase in CaN may be an attempt to preserve muscle mass and prevent/delay disease progression. CaN functions to regenerate atrophying muscle fibres and has been found to be essential for muscle regeneration in normal (Sakuma et al., 2003) and *mdx* mice (Stupka et al., 2004). CaN may also

influence neural reinnervation of the muscle. It has been speculated that CaN plays a role in motor neuron degeneration, although whether this role is protective or damaging is unclear. CaN has demonstrated anti-apoptotic (Yakel, 1997) as well as apoptotic (Ankarcrona et al., 1996; Wang et al., 1999) functions in neurons. In G93A mice, increases in brain (Hu et al., 2003) and decreases in spinal cord (Knirsch et al., 2001) CaN levels have been observed. Further clarification of CaN's role in the model of progressive denervation is warranted.

The MAPKs, ERK1 and ERK2, play primary roles in cell proliferation or mitogenesis, and have been shown to regulate skeletal muscle differentiation and hypertrophy (Chuderland and Seger, 2005). The response of ERK to progressive denervation is currently unclear. In this study, significant increases in both ERK1 and ERK2 were observed in progressively denervated G93A muscle. In addition to contributing to the myogenic and hypertrophic response at the muscle level, the function of increasing ERK may be to stimulate a neuroprotective mechanism and reinnervation during this process. Increases in Raf1 and ERK1 phosphorylation have been previously observed in the spinal cords of G93A mice (Hu et al., 2003). Molecules that promote regeneration, including nerve growth factor (NGF), glial-derived neurotrophic factor (GDNF) and FK506 (Wiklund et al., 2002; Price et al., 2003), have been shown to mediate their effects via the MAPK(ERK) pathway (Agthong et al., 2006). Therefore, ERK's role in progressive denervation-induced atrophy may be one of protection at either the level of the muscle and/or nerve.

Levels of Akt and p-Akt have previously been shown to increase significantly in mixed skeletal muscle with disease progression in G93A mice (Cunningham, thesis). In

contrast, Leger et al. (2006) suggests Akt levels decrease in tibialis anterior (TA) muscle of G93A mice. This discrepancy may be due to the muscle fibre type examined in each of these two studies. In this study, levels of Akt were further examined in skeletal muscle based on fibre type (type I, RG vs. type II, WG). Regardless of fibre type, Akt protein content was significantly greater in skeletal muscle of G93A mice compared to wild-type controls. However, the pattern of alterations in, and relative amount of, Akt differed between RG and WG muscle. In the primarily type I, slow-twitch RG muscle, significant increases in Akt were observed in G93A mice with severe symptoms (SS) but not until end-stage (ES) in primarily type II, fast-twitch WG muscle. Leger et al. (2006) examined fast-twitch TA muscle at 120 days of age. Further examination of this study reveals that although the authors suggest a decrease in p-Akt in G93A muscle versus WT controls, empirical data is not reported. To my knowledge, this is the first study to examine the difference in Akt protein content between fibre types of G93A skeletal muscle. Akt increases in progressively denervated skeletal muscle of G93A mice; however the pattern of expression and alteration of Akt is slightly delayed (~15 days) in fast-twitch, type I fibres. Furthermore, levels of Akt in end-stage G93A WG muscle was 43 times that of WT levels (vs. 31x and 10x greater in RG at SS and ES respectively), indicative of a greater up-regulation of the survival factor Akt in fast fibres which are preferentially denervation and atrophied earlier in the disease process (Frey et al., 2000).

In association with alterations in Akt, levels of phosphorylated FOXO were also examined in mixed skeletal muscle. Phosphorylation by Akt inhibits FOXO's function (activation of pro-apoptotic factors) (Brunet et al., 1999). p-FOXO was the only signalling factor to demonstrate a significant symptom main effect, as p-FOXO content

decreased gradually in both G93A and wild-type mice. Decreases in p-FOXO observed in G93A skeletal muscle over symptom progression could reflect a reduction in FOXO protein level and/or enhanced levels of dephosphorylated (apoptosis-inducing) FOXO. It also suggests that although Akt increases at later stages of disease progression and during more extensive denervation of muscle tissue, Akt may not be able to phosphorylate FOXO and is unable to prevent it from inducing cellular apoptosis. However, given that p-FOXO levels also decreased simultaneously in wild-type skeletal muscle, no difference was observed between G93A and WT mice. This result was similar to previous literature (Leger et al., 2006) that demonstrated no difference in FHRKL1 protein levels between 120-day-old G93A and wild-type skeletal muscle. Why levels of p-FOXO decrease in control mice in the present study is unclear, as none of the other proteins examined differed significantly between control mice. Further examination into this finding is warranted.

In contrast to calcineurin, ERK1/2, and Akt, decreased levels of MyoD protein were observed in mixed muscle of G93A mice. The effect of denervation on MyoD levels is controversial as previous studies have shown no change (Ishido et al., 2004a; Delday and Maltin, 1997), increases (Hyatt et al., 2003) and decreases (Sakuma et al., 1999) in MyoD content following 7-28 days of denervation. However, these studies examined acute denervation protocols, which do not necessarily correspond to models of progressive denervation. Skeletal muscle of *dy* mice, a model of muscular dystrophy, demonstrates gradual decreases in MyoD protein expression through disease progression (Jin et al., 2000). Although the etiology of *dy* mice (deficiency of merosin, laminin $\alpha 2$ chain) differs from G93A mice, both animals exhibit a limited lifespan (*dy*: 5-6 months;

G93A: 3.5 months) and similar clinical symptoms (atrophy, weakness and eventual death). MyoD is expressed in small, regenerating muscle cells surrounding necrotic skeletal muscle fibres during progressive denervation (Bhagwati et al., 1996), particularly in fast-twitch fibres (Sakuma et al., 1999). Fast-twitch, glycolytic skeletal muscle fibres are preferentially atrophied during progressive denervation, due to degeneration of fast motor neurons and vulnerability of fast-type synapses (Theys et al., 1999; Frey et al., 2000). It therefore appears that the decrease in MyoD expression is associated with changes in muscle morphology, for example a loss and/or atrophy of fast-twitch muscle fibres. This may also explain why mixed skeletal muscle of G93A mice with severe symptoms (SS) has slightly higher levels of MyoD than other symptom groups. At this stage of symptom progression, approximately 50% of muscle fibres are denervated (Frey et al., 2000; Cunningham, thesis) and differ significantly from WT control muscle. Therefore, the small but relative increase in MyoD at SS occurs in accordance with the initiation of muscle morphological alterations and just prior to the onset of observable muscle atrophy.

Levels of myogenin protein in G93A skeletal muscle were not different from wild-type control muscle. This finding agrees with many studies who have shown no change in myogenin following denervation (Delday and Maltin, 1997; Sakuma et al., 1999) but conflicts with Hyatt et al. (2003) who demonstrated a consistent increase in myogenin protein levels in both tibialis anterior and medial gastrocnemius muscles between 3 and 28 days after sciatic nerve transection. In chronic models of skeletal muscle wasting, such as *dy* muscle, myogenin is most extensively expressed early in disease progression, in conjunction with muscle necrosis but subsides gradually during

disease progression and muscle regeneration (Jin et al., 2000). Myogenin has been shown to be significantly greater in *dy* muscle than wild-type control muscle (Hsu et al., 1997), suggesting differential expression in the two (*dy* vs. G93A) models. The results from the current study suggest that skeletal muscle is unable to up-regulate the entry of cells through the cell cycle (via decreases in MyoD) but maintains differentiation and specification of muscle fibres, potentially within existing, non-denervated myofibres in an attempt to maintain health and survival.

Myostatin gene expression has been shown to increase with skeletal muscle atrophy and denervation, and is also decreased during the muscle regenerative process (Sakuma et al., 2000; Wehling et al., 2000; Carlson et al., 1999; McCroskery et al., 2005). This is the first study to characterize levels of myostatin in skeletal muscle of G93A mice. No significant differences in myostatin were observed between progressively denervation and wild-type muscle. This finding may be explained by the fact that although muscle undergoing denervation (known to be associated with increases in myostatin), it is also attempting to regenerate and survive (associated with decreases in myostatin). These conflicting processes may ultimately lead to no difference in myostatin levels throughout disease progression, although it is apparent that myostatin shows a trend to increase at later symptom stages. A recent study that inhibited myostatin in G93A mice demonstrated increases in muscle mass (Holzbaur et al., 2006), indicating that blocking the protein's apoptotic function still improves mass and function in these animals.

The results of this study suggest that progressive denervation-induced atrophy is associated with alterations in muscle-specific signalling proteins, prior to observable loss

of muscle mass. In this study, all but one (RG Akt) of the proteins were not significantly different prior to the onset of symptoms (PS). Given that research has shown a significant loss of motor neurons prior to the onset of symptoms (McFee, thesis), it is hypothesized that the alterations in muscle-specific signalling factors observed in this study are not responsible for inducing disease progression but rather the muscle's response to progressive denervation. However, further investigation via genetic manipulation should be conducted to support this claim. It appears as though hypertrophic factors (calcineurin, Akt, ERK1/2) may be attempting to compensate for the denervation process, whereas others (MyoD and p-FOXO) are unable to adapt to (or keep up with) the muscle wasting process. However, a significant loss of soleus muscle mass at end-stage of the disease indicates that the up-regulation of compensatory mechanisms is unable to counter-balance the wasting effects of progressive denervation. Identification of the alterations in muscle-specific factors across symptom progression and gradual muscle denervation provides greater insight into key therapeutic targets and potential interventions aimed at maintaining muscle mass and function in this model. The delicate balance between hypertrophic and atrophic factors in this model of progressive muscle denervation ultimately dictates the status of the muscle during the disease process.

CHAPTER 4: THERAPEUTIC EFFECTS OF CLENBUTEROL IN A MURINE MODEL OF PROGRESSIVE DENERVATION-INDUCED SKELETAL MUSCLE ATROPHY

Abstract

The β_2-adrenergic agonist, Clenbuterol, has been shown to attenuate muscle loss and functional impairment following acute denervation; however, information regarding its effects on progressive denervation-induced skeletal muscle atrophy is currently incomplete. This study examined the effects of 6 weeks of Clenbuterol treatment on body and muscle (soleus) mass, symptom progression, functionality, and levels of muscle-specific signalling factors known to be involved in the regulation of muscle mass. Clenbuterol significantly attenuated the progression of symptoms in G93A mice, which was reflected in increased body mass and improved motor coordination (RotoRod) at 120 days of age, as well as levels of the smRFs Akt and MyoD that were similar to wild-type mice. Statistically significant improvements in Paw Grip Endurance (PaGE) performance were observed in female Clenbuterol-treated mice. Increased soleus muscle weights were only observed in Clenbuterol-treated wild-type mice. Results from this study suggest that Clenbuterol is a beneficial therapeutic agent in the prevention of clinical signs and symptoms associated with progressive denervation.

Introduction

Skeletal muscle atrophy is triggered by progressive denervation and is often associated with aberrant reinnervation, aging and neuromuscular disorders (Solomon and Bouloux, 2006). A decrease in mean cross-sectional area and increase in the proportion of angulated fibres have been observed with denervation-induced atrophy (Pachter and Eberstein, 1992). Atrophy is also associated with ultrastructural changes within the muscle including disorganization of sarcomeres via actin and myosin filament disruption and progressive loss of mitochondria (Lu et al., 1997; Borisov et al., 2001). Muscle atrophy leads to functional deficits such as decreases in strength and/or motor co-ordination (Aoyagi and Shephard, 1992). Unfortunately, information on muscle-specific changes that occur with progressive denervation-induced skeletal muscle atrophy and quality treatment options is lacking.

The β_2-adrenergic agonist, Clenbuterol, has been shown to attenuate muscle atrophy following hindlimb suspension (Herrera et al., 2001; von Deutsch et al., 2002; Dodd and Koesterer, 2002), hyperthyroidism (Carter and Lynch, 1994b), surgical stress (Carter et al., 1991), dietary restriction (Choo et al., 1990), glucocorticoid therapy (Pellegrino et al., 2004) and acute denervation (Zeman et al., 1987; Maltin et al., 1993). It has also been shown to maintain muscle mass and/or strength in chronic models of atrophy, such as aging (Smith et al., 2002), muscular dystrophy (Zeman et al., 2000) and motor neuron degeneration (Zeman et al., 2004). Clenbuterol may act via a variety of muscle-specific signalling factors known to be involved in the regulation of muscle mass including MAPK(ERK) (Shi et al., 2006; Litt Miller, thesis Chapter 2), calcineurin (Oishi et al., 2004), Akt/p70s6k (Kline et al., 2007; Litt Miller, thesis Chapter 2; Sneddon et al.,

2001) and the myogenic regulatory factors (Bricout et al., 2004; Mozdziak et al., 1998). However, these findings have primarily been shown in healthy and/or acutely denervated tissue.

The G93A mouse that over-expresses a mutant form of the human superoxide dismutase (mSOD) transgene has proven to be a useful model to study progressive denervation-induced skeletal muscle atrophy. mSOD-induced skeletal muscle atrophy is associated with a loss of neuromuscular junctions and resulting muscle weakness/dysfunction (Frey et al., 2000; Wooley et al., 2005; Thomas and Zijdewind, 2006). Although atrophy has not been shown to occur in these animals until end-stage of disease progression, alterations in muscle-specific signalling factors have been shown prior to this observable decrease in mass (Cunningham, thesis; Litt Miller, thesis Chapter 3). Interestingly, some proteins that are altered in progressively denervated skeletal muscle of this model (i.e. Akt, ERK, MyoD and calcineurin) are also thought to be involved with Clenbuterol-induced muscle growth and therefore further examination of these factors is warranted.

To date, only one study has examined the effects of Clenbuterol treatment on G93A mice. Teng and colleagues (2006) found that Clenbuterol administration delayed the onset of motor coordination dysfunction (via RotoRod performance) when compared to non-treated G93A animals, improved early stage body mass and prolonged lifespan (in female mice only). However, very often G93A mice demonstrate clinical symptoms, including hindlimb tremor, weeks before observable decreases in RotoRod performance. In addition, previous studies have demonstrated sexual differences in symptom onset and responses to various attempts/treatments to prevent disease progression (Veldink et al.,

2003; Teng et al., 2006). The effects of Clenbuterol on the initial symptom stages of G93A mice, as well as gender, muscular strength and muscle-specific signalling factors are currently unclear.

Because of its effect on skeletal muscle and its proposed neuroprotective (Culmsee et al., 1999b) and/or regenerative (Frerichs et al., 2001) properties, Clenbuterol is an attractive therapeutic agent for the treatment of progressive-denervation induced muscle atrophy associated with G93A disease progression. As such, the purpose of this study was to examine the effects of 6 weeks of Clenbuterol treatment on body and skeletal muscle mass, symptomotology, functionality (motor co-ordination, balance and strength), and levels of muscle-specific proteins known to be involved with the regulation of muscle mass in G93A mice undergoing progressive denervation-induced atrophy. More specifically, symptomotology, body mass and functional (RotoRod and PaGE) performance were measured in G93A and wild-type control mice treated with or without Clenbuterol from a pre-symptomatic age of 70 days until 120 days of age. At sacrifice, body and soleus mass, as well as stage of symptomotology and levels of Akt, ERK, calcineurin, and MyoD were compared between groups.

Experimental Approach

Animals

All procedures followed the guidelines outlined by the Canadian Council on Animal Care and were approved by the Animal Care Committee, Simon Fraser University. B6SJL-TgN(SOD1-G93A)1Gur transgenic SOD1 mice (mSOD) and age-matched wild-type (WT) controls were obtained from Jackson Laboratory, (Bar Harbor,

ME, USA). Mice were bred in-house, then weaned and screened for the mSOD transgene by PCR at 30 days of age (refer to Chapter 3).

Clenbuterol Administration

Beginning at 70 days (10 weeks) of age, mice were assigned to one of four groups (n=10-11/group), based on their genotype (WT control vs. G93A affected) and randomly assigned to a treatment condition (saline vs. Clenbuterol). This allocation resulted in four groups, including: 1) wild-type mice + saline (WT_S), 2) G93A mice + saline ($G93A_S$), 3) wild-type mice + Clenbuterol (WT_{CL}), and 4) G93A mice + Clenbuterol ($G93A_{CL}$). Mice administered Clenbuterol (WT_{CL} and $G93A_{CL}$) were given daily subcutaneous injections of the drug (1.5 mg/kgBW/day dissolved in saline, Sigma) beginning at 77 days (11 weeks). This dose of Clenbuterol has been shown *in vivo* to stimulate muscle hypertrophy (Zeman et al., 1988; Carter et al., 1991) and prevent muscle atrophy (Herrera et al., 2001). Mice that were administered saline were given a daily, equal volume, subcutaneous dose of saline (150 mM NaCl, Sigma). Mice received injections for 6 weeks using a 5-day on/2-day off cycle in order to reduce attenuation of the Clenbuterol response (Hayes and Williams, 1994; Lynch et al., 2001). Clenbuterol solution was replenished once per week to avoid evaporation, oxidation, and possible degradation of the drug. Given that G93A (i.e. affected) mice have been found to show clinical symptoms at approximately 85 days of age (Weydt et al., 2003; confirmed by our lab), injections began just prior to symptom onset.

Two days following the final Clenbuterol injection, or approximately 120 days, mice were euthanized using a CO_2-O_2 blend (refer to Chapter 3). This age is a key time point in G93A disease progression as 120-day old mice transition to later stage (i.e.

severe) symptoms that are characterized by a significant loss and apoptosis of motor neurons (Fischer et al., 2004; Fidzianska et al., 2006), neuromuscular denervation (Frey et al., 2000; Cunningham, thesis) and alterations in muscle-specific signalling factors, without a significant degree of skeletal muscle atrophy (Litt Miller, thesis Chapter 3; Cunningham, thesis).

Body Mass and Soleus Weight

Animal body mass was recorded beginning at 70 days of age, every 5 days, until sacrifice. Body mass has been proven to be a parameter that is directly related to the degree of disease progression in G93A animals (Miana-Mena et al., 2005). In addition, a loss of body mass is highly related to, and has been shown to detect, early symptoms in G93A mice with statistical significance (Weydt et al., 2003). At the time of sacrifice, soleus muscle was extracted from the hindlimb, quickly removed, and snap frozen in liquid nitrogen and stored at -80°C for further analysis. Frozen soleus muscle weights from both legs were averaged and subsequently compared between groups.

Symptomotology

The staff at the Animal Care Facility (ACF, Simon Fraser University) were informed of the mice genotypes (WT vs. G93A) and monitored mice daily for clinical symptoms via a variety of tests related to disease progression: hindlimb splay, mobility, gait and posture, overall behavioural characteristics and body mass, further verified by me. The observation of hindlimb tremor during tail suspension has been shown to be the most simple and sensitive method to detect early symptoms but requires experience and training on the side of the observer (Weydt et al., 2003). Mice were examined at five

distinct stages during disease progression: pre-symptomatic (PS), symptom onset (SO), severe symptoms (SS), and end-stage (ES) symptoms (Table 3) as well as an additional level of symptomotology (between SO and SS) defined as Moderate Symptoms (MS). Mice exhibiting moderate symptoms had progressed from symptom onset (SO, displaying mild clinical symptoms) and exhibit hindfoot knuckling, lower levels of physical activity, and a QAR (Quiet, Alert, Responsive) behaviour. Age of onset for each stage of symptomotology (Mild, Moderate, Severe, and End-Stage), if applicable, and the final stage of symptomotology at time of sacrifice, was recorded.

Functional Assessment

One week prior to the start of Clenbuterol injections, or at 70 days of age, mice were introduced to two functional tests designed to primarily assess motor coordination (RotoRod) and muscular strength (Paw Grip Endurance, PaGE). Mice were tested once per week with the two tests performed on separate days, with at least one rest day between the tests to minimize stress. Mice ran on a RotoRod apparatus, modified from Weydt et al. (2003) which consisted of a 5 cm diameter rubber rod rotating at 20 rpm. A calibration of rod velocity was performed at the beginning of each testing day. Mice were required to move (i.e. walk/run/hop) on top of the rotating rod and were monitored until one of three situations occurred: 1) the mouse completed the 180-second test without difficulties, 2) the mouse was unable to maintain consistent locomotion (i.e. clung to the rod while it rotated around), or 3) the mouse fell from the rod onto a padded cage located ~ 30 cm below the rod. Each animal was given three attempts (trials) to complete the 180-second protocol and the time on the rod was recorded for each attempt. The RotoRod test has been used successfully in the literature with this mouse breed and

monitoring of disease/symptom progression (Weydt et al., 2003; Miana-Mena et al., 2005). The percentage of mice able to complete the 180-second task within the 3 trials as well as the average time on the rod (RRavg) was recorded for each group throughout the testing period (weeks 10 through 17) and compared just prior to sacrifice.

Mice also performed a Paw Grip Endurance (PaGE) task that is primarily associated with muscular strength and balance (Weydt et al., 2003) on a weekly basis. Mice were placed on a wire cage lid which was gently shaken to allow mice to gasp tightly to the wire lid. The lid was gently inverted, approximately 30 cm above a padded, woodchip surface. Mice hung upside down from the cage lid and the latency to fall was recorded. Each mouse was allowed up to 3 trials to hang onto the lid for a maximum cut-off time of 90 seconds. It is hypothesized that this task is comes quite naturally to the mice as they are frequently observed climbing the rungs of their cage lids during their active periods. It has also been shown to be a sensitive method for detecting early motor signs in the G93A mice (Weydt et al., 2003). The percentage of mice able to complete the 90-second task within the 3 trials as well as the average time of the hang (PaGEavg) was recorded for each group throughout the testing period (weeks 10 through 17) and compared at sacrifice.

Tissue Preparation and Protein Determination

In addition to soleus muscle tissue, mixed hindlimb muscle was removed at the time of sacrifice. Whole protein lysate was extracted from mixed muscle from 21 G93A mice (n=11 treated with saline, n=10 treated with Clenbuterol) and 18 wild-type (WT) age-matched controls. Muscle tissue was prepared and protein content determined

according to the protocols cited in Appendix A. Samples were stored at -80°C for further analysis.

Gel Electrophoresis and Immunoblotting

Equal amounts of protein (70μg/35μl) were prepared (refer to Chapter 3) and separated on a one-dimensional (8-12%) SDS polyacrylamide gel. A molecular weight marker (Amersham Pharmacia) was run as a reference on all gels. Samples were run in two steps (50mA constant current through stacking gel, 100mA constant current through running gel) using an electrophoresis running apparatus (Bio-Rad) immersed in running buffer solution [25mM Tris; 125mM glycine; 0.1% (wt/vol) SDS; pH8.3].

Protein bands of interest were transferred to PVDF membranes at 4°C under constant current conditions with voltage set between 50-70 mV (Bio-Rad Power Pac 3000). Following the transfer, protein bands were visualized with Ponceau Red (0.2% in 3% TCA, Sigma), and washed in TBST. Non-specific binding sites were blocked with 5% bovine serum albumin (BSA in TBST) for 90 minutes at room temperature, under gentle agitation. Membranes were rinsed 3 x 5 minutes with excess volumes of TBST and subsequently incubated overnight at 4°C with appropriate primary antibody [Akt (*sheep*) (Upstate Biotechnology Inc.), CaN (*rabbit)* (Upstate Biotechnology Inc.), ERK (*rabbit)* (Cell Signalling), MyoD (*rabbit*) (Santa Cruz)]. All antibodies were diluted 1:1000 (vol/vol) with TBST, 0.5% NaN_3 and 1% BSA. Following the overnight incubation, the membranes were washed 5 x 5 minutes with TBST and incubated with an excess volume of appropriate horseradish peroxidase (HRP)-conjugated secondary antibody (all 1:20,000 with TBST and 1% BSA). Secondary antibody incubation occurred under gentle agitation at room temperature for 90 minutes. Membranes were washed three times

each with TBST and TBS (50mM Tris Base, 150mM NaCl, pH 7.4) and then immersed in Enhanced Chemiluminescence (ECL) reagent and exposed to Hyperfilm-ECL (Amersham). Protein content was quantified by scanning protein bands using a commercially-available flatbed scanner (Epson) and Scion Image software (NIH).

Statistical Analyses

Mice were classified into four groups according to genotype and treatment condition: WT_S, WT_{CL}, $G93A_S$, and $G93A_{CL}$. Comparisons of body mass over time, both absolute BM and BM_Δ ($BM_{t=x} - BM_{t=75d}$) were analyzed using a four-way, 2x2x2x10 mixed (Disease x Drug x Gender x Time in 5-day increments) analysis of variance (ANOVA) with Time as a repeated measure. The RotoRod and PaGE functional tests were compared over time using a four-way, 2x2x2x8 (Disease x Drug x Gender x Time in weeks) ANOVA. Groups were examined for differences at the final time point (120 days) using a 2x2 (Drug x Disease) ANOVA. An α-level of 0.05 was set as significant for all tests, and all results are reported as means ± SE.

A 2x2x2 randomized group (Disease x Drug x Gender) ANOVA was used to compare G93A and WT mice on all measures at sacrifice (i.e. body mass, change in body mass, soleus mass, RR_{avg}, $PaGE_{avg}$). An independent t-test was used to examine differences between age of symptom onset for the G93A mice ($G93A_S$ and $G93A_{CL}$). Non-parametric statistics were used to compare the percentage of G93A mice completing functional tests and the number of G93A mice in each symptom stage at 120 days. All tests were conducted using SPSS 15.0 statistical software.

Results

Body Mass

Body mass trends for all four groups are shown in Figure 17. Body mass was similar for all mice at the start of the study (75 days), prior to injections ($p>0.05$), although female mice were 21% lighter overall in mass than males (21.4 ± 0.4g vs. 25.9 ± 0.6g; $p<0.01$) (Figure 18). Significant main effects were observed between mice as a function of gender (male > female; $p<0.01$) and due to the drug treatment (Clenbuterol > saline; $p<0.01$) but not as a function of the disease itself (WT ~ G93A; $p=0.06$).

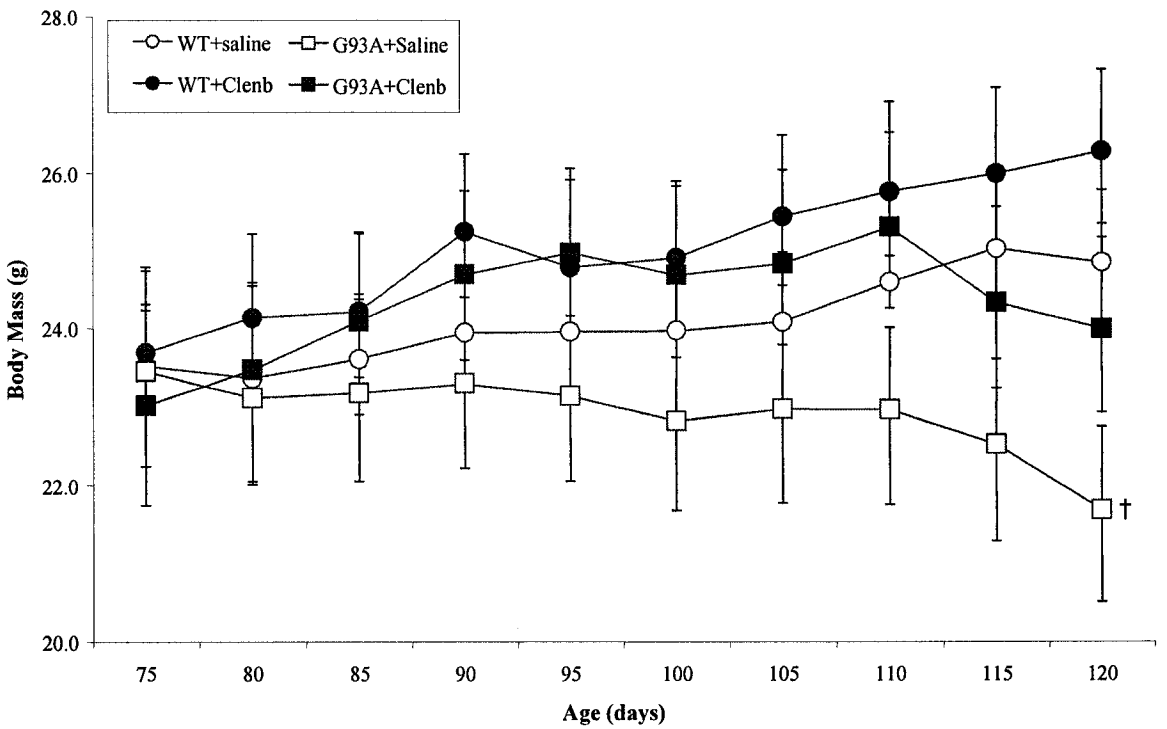

Figure 17: Body Mass of WT and G93A mice treated with saline or Clenbuterol.
Data are expressed as a mean ± SE (n=9-11/group). Circles (○●) represent WT mice, squares (■□) represent G93A mice, both with saline (open symbols) or Clenbuterol (closed symbols). *Significantly different from saline-treated mice of the same genotype. †Significantly different from WTs mice ($p<0.05$).

Mice treated with saline differed in body mass over time from the Clenbuterol-treated animals, as evident by a significant Drug x Time interaction effect ($p<0.01$). Clenbuterol-treated mice (WT_{CL} and $G93A_{CL}$) were significantly heavier than saline-treated animals of the same genotype (WT_S and $G93A_S$), as both Clenbuterol-treated groups demonstrated parallel increases (~9%) in body mass until 110 days, whereas saline-treated animals demonstrated opposite body mass trends (WT_S mice increased and $G93A_S$ mice decreased in mass) over time. Clenbuterol-treated G93A mice showed declines in body mass after the 110-day time point.

When stratified by gender, male Clenbuterol-treated mice (Figure 18A) demonstrated increases in body mass regardless of genotype, statistically different from saline-treated mice of the same genotype at 100 ($G93A_{CL}$) and 105 (WT_{CL}) days of age. Following this age, $G93A_{CL}$ mice declined in body mass until the end of the study period, reaching similar mass to that of WT_S mice at 120 days. Male mice in all experimental groups (WT_{CL}, $G93A_S$ and $G93A_{CL}$) did not differ significantly from WT_S mice throughout the study. In contrast, both female $G93A_S$ and $G93A_{CL}$ mice (Figure 18B) weighed significantly less than their WT_S counterparts beginning at 110 and 115 days of age respectively ($p<0.05$). Furthermore, the two female G93A groups ($G93A_S$ vs. $G93A_{CL}$) differed significantly in body mass during the last three weigh-ins (110-120 days) ($p<0.05$), something that was not observed in male G93A mice.

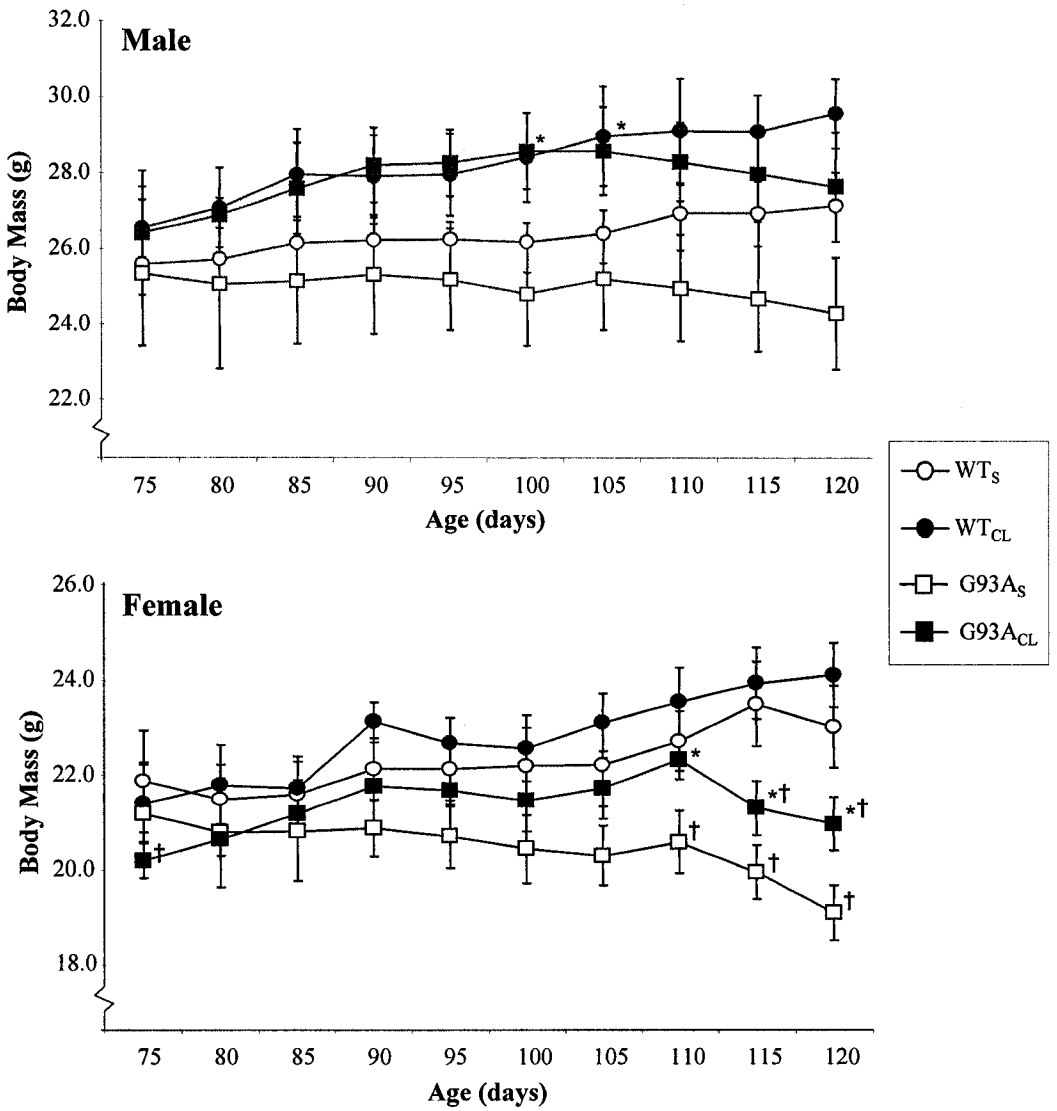

Figure 18: Body Mass of male (top panel) and female (bottom panel) WT and G93A mice treated with saline or Clenbuterol.

Data are expressed as a mean ± SE (n=4-6/group). Circles (○●) represent WT mice, squares (■□) represent G93A mice, both with saline (open symbols) or Clenbuterol (closed symbols). *Significantly different from saline-treated mice of the same genotype ($p<0.05$). †Significantly different from WTs mice ($p<0.05$).

A significant within-subjects interaction effect (Disease x Time) was also observed for mouse body mass, that is, G93A mice demonstrated different body mass trends than WT mice over the time of observations ($p<0.01$). Whereas both WT groups increased steadily over time until the final weigh-in, G93A animals demonstrated

different trends depending on Clenbuterol treatment. Body mass was normalized for comparison between genders and the change in body mass ($BM_{\Delta} = BM_{t=x} - BM_{t=75d}$) was calculated for each mouse and time point relative to body mass just prior to injection (at 75 days) (Figure 19).

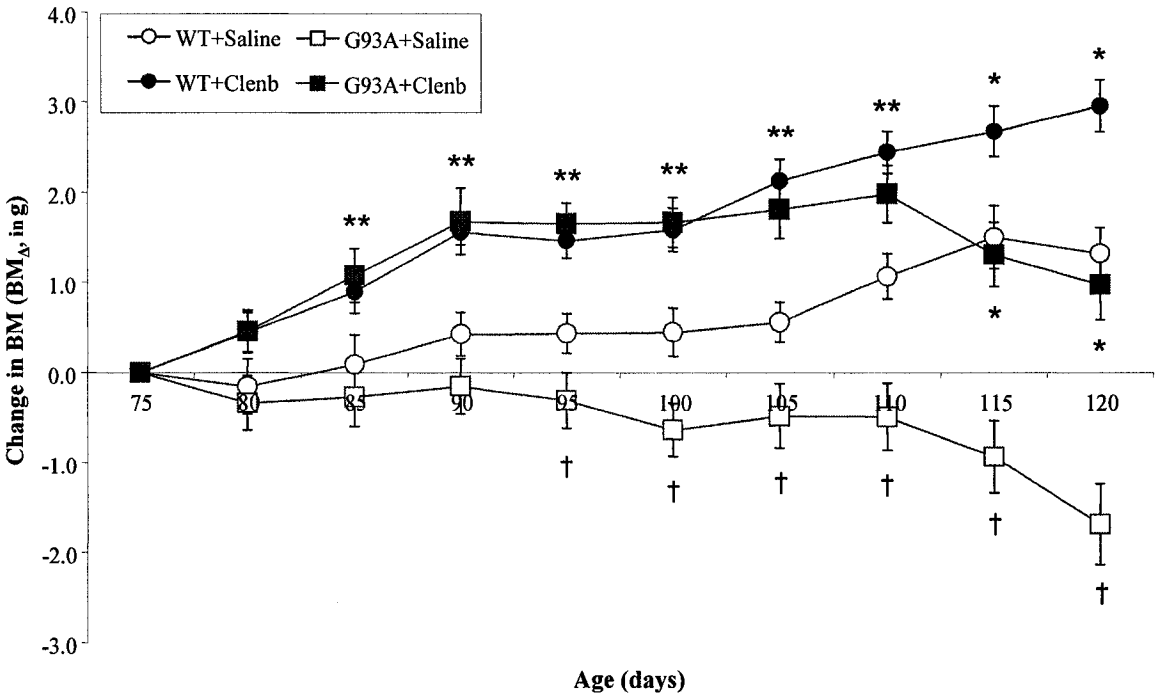

Figure 19: Change in body mass over time of WT and G93A mice treated with saline or Clenbuterol. Data are expressed as a mean ± SE (n=9-11/group). Circles (○●) represent WT mice, squares (■□) represent G93A mice, both with saline (open symbols) or Clenbuterol (closed symbols). *Significantly different from saline-treated mice of the same genotype ($p<0.05$). †Significantly different from WTs mice ($p<0.05$).

Significant main effect differences in BM_{Δ} between groups, as a function of disease, treatment (between-subjects) and over time (within-subjects) ($p<0.05$). Overall, Clenbuterol-treated mice weighed significantly greater than saline-treated counterparts for the majority of the study, beginning at 85 days of age ($p<0.05$) regardless of mouse genotype. In addition, only $G93A_S$ mice differed in body mass from WT_S mice, significantly lower in mass from 95 days of age onwards ($p<0.05$). No other differences

between WT_S mice were observed in the study. Both Disease x Time and Drug x Time interaction effects were significant ($p<0.01$), as was the case with absolute values. As expected, normalizing body mass to 75 days old did not result in significant differences between genders (data not shown, $p>0.05$).

Significant differences in body mass and normalized body mass (BM_Δ) were found between groups at the final time point (120 days). At this time, absolute body mass measures of G93A mice were significantly lower than WT mice ($p<0.01$) (Figure 20). This difference was particularly evident between WT_S and $G93A_S$ mice (24.7 ± 1.0g vs. 21.4 ± 1.3 g). Significant differences in body mass between groups at sacrifice were also observed overall as a function of treatment condition (saline < Clenbuterol; $p<0.01$) and gender (Female < Male; $p<0.05$) regardless of genotype.

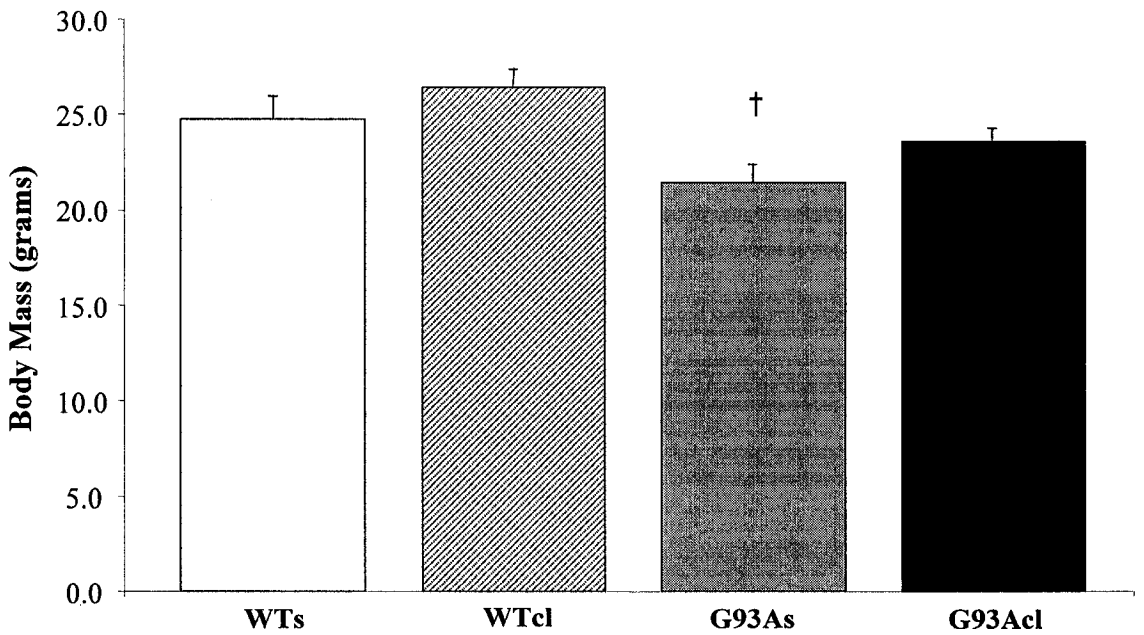

Figure 20: Body mass at sacrifice of WT and G93A mice treated with saline or Clenbuterol. Data are expressed as a mean ± SE (n=9-11/group). †Significantly different from WTs mice ($p<0.05$).

BM_{Δ} was also significantly different between groups at sacrifice as a function of both disease and treatment condition ($p<0.01$) (Figure 21). WT_{CL} mice showed a greater increase in body mass at sacrifice (when normalized to 75 days) than WT_S mice (+2.7 ± 0.2g vs. +1.3 ± 0.4g) ($p<0.01$). G93A mice exhibited significantly different BM_{Δ} ($p<0.001$) with the two treatment conditions, as mice administered Clenbuterol slightly increased in body mass at 120 days ($G93A_{CL}$: +0.5 ± 0.4g), versus the saline-treated G93A mice that ultimately lost mass ($G93A_S$: -2.0 ± 0.4g) throughout the study. There was no significant difference observed in BM_{Δ} between male and female mice as BM_{Δ} trends at sacrifice were similar to overall group means (data not shown).

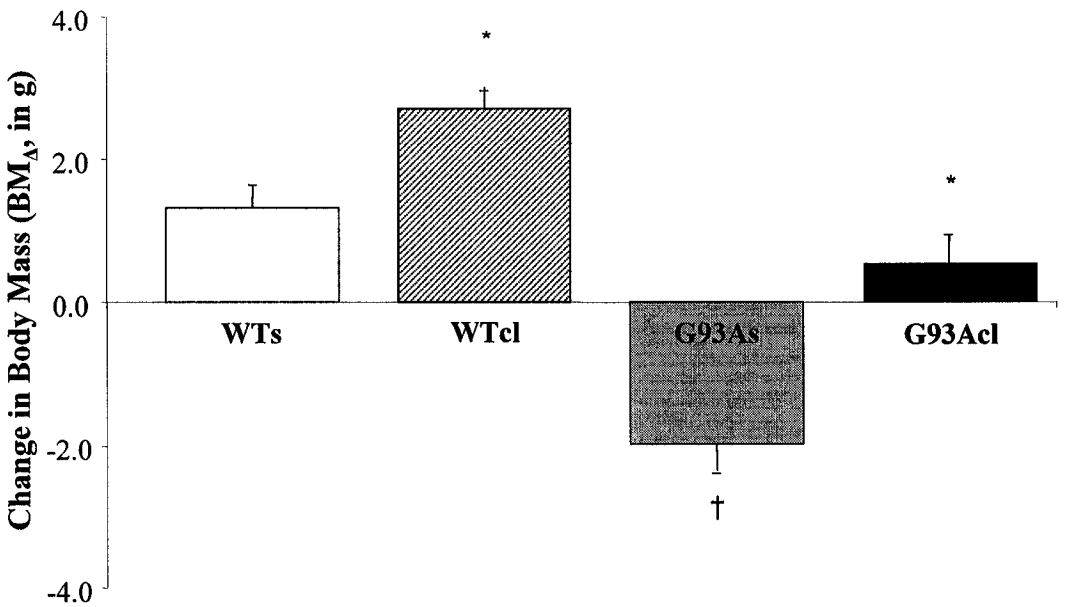

Figure 21: Change in body mass from 75 days to sacrifice (~120 days) for WT and G93A mice treated with saline or Clenbuterol.
Data are expressed as means ± SE (n=9-11/group). *Significantly different from saline-treated mice of the same genotype ($p<0.05$). †Significantly different from WTs mice ($p<0.05$).

Soleus Weight

Soleus weight was significantly different between groups at sacrifice as a function of gender (male > female, $p<0.01$) and drug treatment (Clenbuterol > saline, $p<0.05$) (Table 5). Further examination of these trends revealed that soleus weight increased significantly with Clenbuterol treatment only in WT mice ($p<0.05$). Although male G93A mice demonstrated a trend to increase soleus weight with Clenbuterol administration, this difference did not reach statistical significance ($p=0.09$). In addition, differences between gender were greatest between those mice treated with Clenbuterol, that is, male mice had significantly greater muscle weight than females similarly treated with Clenbuterol ($p<0.05$). No significant differences were determined between soleus weights of male and female mice treated with saline, regardless of whether they possessed the transgene (G93A) or not (WT) ($p>0.05$). When soleus weight was normalized to individual body mass measures at sacrifice, no significant differences were observed between groups; values of normalized soleus muscle weight ranged from 0.25 mg/g (WT_S) to 0.31 mg/g (WT_{CL}).

Table 5: Soleus muscle weight of WT and G93A mice treated with saline or Clenbuterol in absolute (mg) and relative (normalized to BM, mg/g) terms.

Group		Sol weight (mg)	Sol wt/BM (mg/g)
WT + Saline	**Male**	6.8 ± 0.4	0.25 ± 0.01
	Female	5.5 ± 1.0	0.25 ± 0.03
	All	**6.2 ± 0.6**	**0.25 ± 0.01**
WT + Clenbuterol	**Male**	8.8 ± 0.5 *	0.30 ± 0.03
	Female	7.4 ± 0.3 * ‡	0.31 ± 0.01
	All	**7.9 ± 0.3 ***	**0.31 ± 0.01**
G93A + Saline	**Male**	6.9 ± 0.6	0.28 ± 0.02
	Female	5.6 ± 0.8	0.29 ± 0.01
	All	**6.4 ± 0.5**	**0.29 ± 0.01**
G93A + Clenbuterol	**Male**	8.3 ± 0.7	0.28 ± 0.03
	Female	5.9 ± 0.6 ‡	0.29 ± 0.03
	All	**6.7 ± 0.5**	**0.28 ± 0.02**

Data are expressed as a mean ± SE (n=4-6/gender, n=9-11/all). * Significantly different from saline-treated animals of the same genotype and gender ($p<0.05$). ‡Significantly different from male mice of the same genotype and treatment condition ($p<0.05$).

G93A Mouse Symptomotology

The symptom characteristics of all G93A mice, including the age of onset for each stage of symptoms, as well as the percentage of mice that progressed to each symptom stage is outlined in Table 6. Not surprisingly, all (100%) of the G93A mice demonstrated clinical symptoms (Symptom Onset, SO); the mean age of SO was not significantly different between treatment groups, 84 ± 2 days for $G93A_S$ and 88 ± 3 days for $G93A_{CL}$ mice ($p>0.05$). All but 1 out of 11 (92%) of the $G93A_S$ mice progressed to moderate symptoms (MS), compared to only 6/10 (60%) of $G93A_{CL}$ mice. Interestingly, 4/10 Clenbuterol-treated mice remained in the SO stage of symptoms for the entire duration of the study. Furthermore, whereas 7/11 (64%) of $G93A_S$ mice progressed to severe symptoms (SS), only 2/10 (20%) of the $G93A_{CL}$ mice reached the SS stage. There were no significant differences in age of symptom onset for any of the symptom stages

either as a function of treatment condition (saline vs. Clenbuterol) or gender (male vs. female) ($p>0.05$).

Table 6: Symptom characteristics for G93A mice treated with saline or Clenbuterol.

Group	Gender	Age of Onset, days (% of Mice in Stage)			
		SO	MS	SS	ES
G93A	Male	84 ± 2 (100%)	107 ± 5 (83%)	119 ± 4 (67%)	115 ± 0 (17%)
+ Saline	Female	84 ± 3 (100%)	113 ± 3 (100%)	117 ± 3 (60%)	
	All	**84 ± 2 (100%)**	**110 ± 3 (92%)**	**119 ± 2 (64%)**	**115 ± 0 (9%)**
G93A	Male	89 ± 4 (100%)	111 ± 6 (80%)	113 ± 0 (20%)	120 ± 0 (20%)
+ Clenbuterol	Female	88 ± 3 (100%)	120 ± 2 (40%)	120 ± 0 (20%)	
	All	**88 ± 3 (100%)**	**114 ± 5 (60%)**	**117 ± 4 (20%)**	**120 ± 0 (10%)**

Age of onset values are reported as means ± SE. SO = Symptom Onset (n=11 G93As, n=10 G93Acl); MS = Moderate Symptoms (n=10 G93As, n=6 G93Acl); SS = Severe Symptoms (n=7 G93As, n=2 G93Acl); ES = End-Stage symptoms (n=1 G93As, n=1 G93Acl).

Throughout the experiment, G93A mice exhibited a different time course of clinical symptoms based on treatment condition (saline vs. Clenbuterol) (Figure 22). All mice were pre-symptomatic (PS) when recorded at 70 days of age. By 90 days of age, all of the $G93A_S$ had begun to show clinical symptoms of the disease (SO). In contrast, only half of the $G93A_{CL}$ mice exhibited clinical symptoms at 90 days. By the time the mice reached 110 days old, the composition of both groups was similar, consisting of a large proportion of SO mice. However, at 120 days, a greater number of $G93A_S$ mice had progressed further along in the symptom stages as only 1 mouse (9% of the $G93A_S$ group) remained with mild (SO) symptoms. In comparison, 6/10 (60%) of the $G93A_{CL}$ mice remained in the SO stage at 120 days.

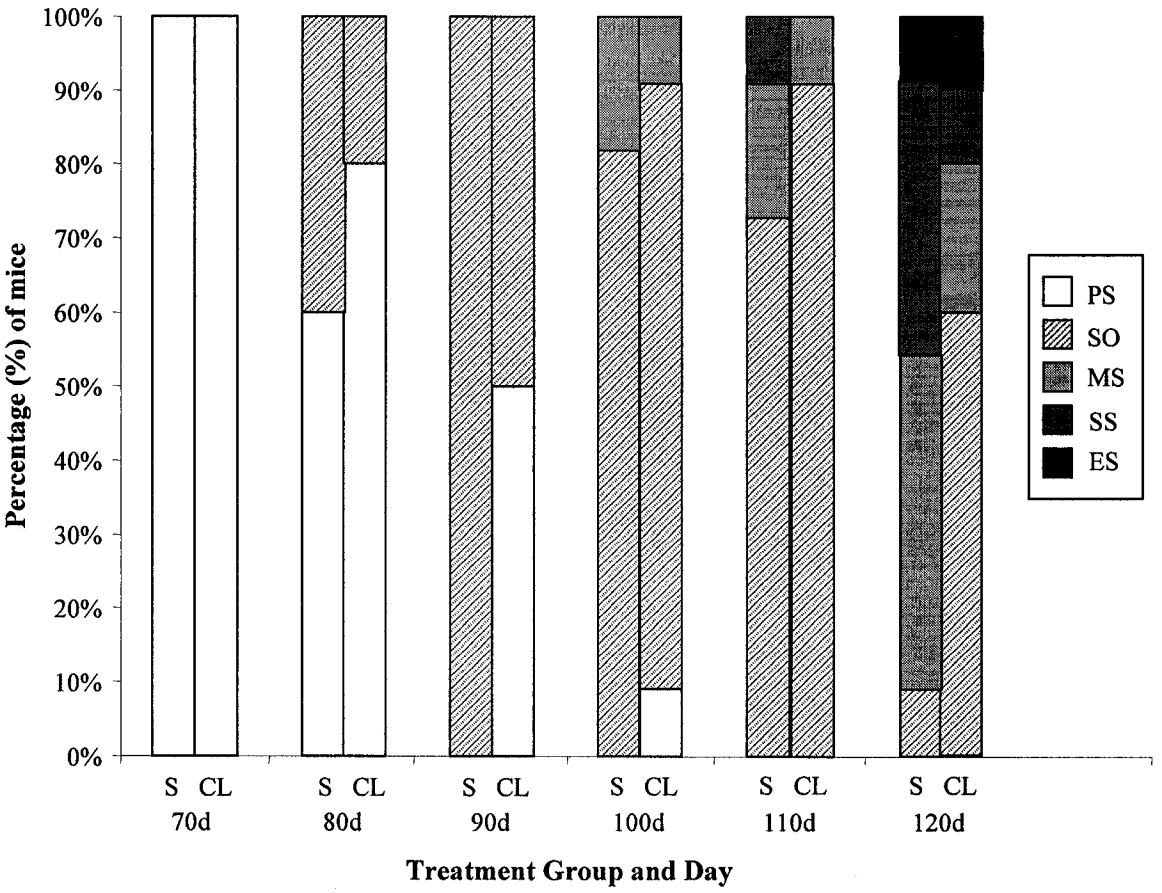

Figure 22: Percentage of G93A mice treated with saline (S) or Clenbuterol (CL) exhibiting symptoms as a function of time (70d: prior to injection, up to 120d).
PS = Pre-Symptomatic; SO = Symptom Onset; MS = Moderate Symptoms; SS = Severe Symptoms; ES = End-Stage symptoms.

At the time of sacrifice, there was a significant difference between the proportion of saline- and Clenbuterol-treated G93A mice that exhibited each level (SO, MS, SS, or ES) of symptoms (Figure 23) ($p<0.05$). The number of mice in each symptom stage at sacrifice slightly differs from the 120 day timpoint in the previous figure as a few mice progressed to a more advance stage between 120 days and the time of individual sacrifice (n=3 $G93A_S$; n=2 $G93A_{CL}$). Overall, the majority (80%) of $G93A_{CL}$ mice exhibited "early stage" (SO and/or MS) symptoms at time of sacrifice, with only 1 mouse

developing ES symptoms. In contrast, the majority (67%) of $G93A_S$ mice demonstrated "later stage" (SS and/or ES) symptoms, mainly exhibiting severe symptoms.

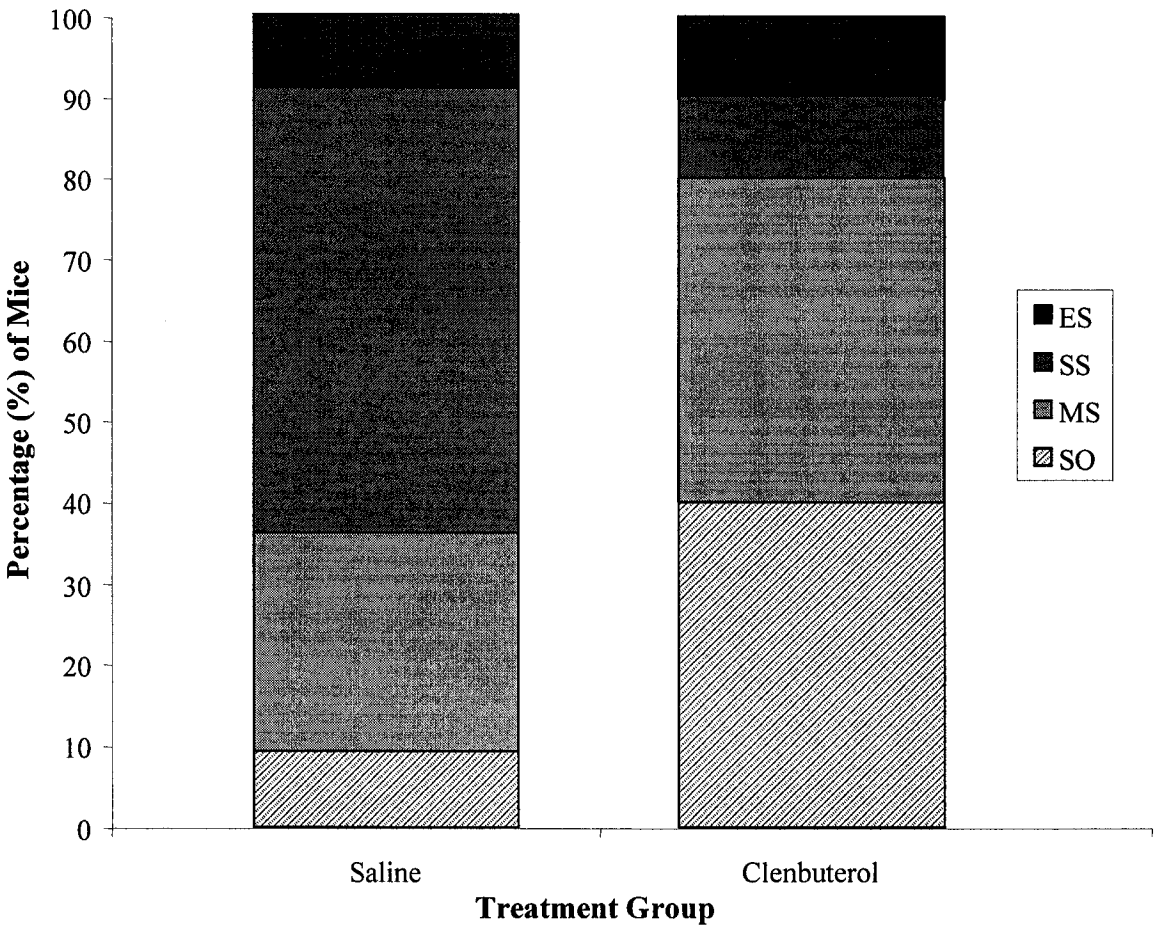

Figure 23: Level/stage of clinical symptoms at sacrifice for saline- and Clenbuterol-treated G93A mice.
SO = Symptom Onset (n=1 G93As, n=4 G93Acl); MS = Moderate Symptoms (n=3 G93As, n=4 G93Acl); SS = Severe Symptoms (n=6 G93As, n=0 G93Acl); ES = End-Stage symptoms (n=1 G93As, n=2 G93Acl). Frequencies of mice in each group differed significantly ($p<0.05$) as per Mann-Whitney U test.

Functional Assessment – RotoRod

The percentage of mice able to complete the 180-second RotoRod (RR) task is shown in Figure 24. Although some G93A mice were unable to complete the task in the first few weeks of the testing (1/11 $G93A_S$; 2/10 $G93A_{CL}$), mice in all groups were able to run for the full 180 seconds by week 13. Essentially all of the WT mice had no

problems completing the RR task, therefore only G93A mice were compared in the analysis. Both G93A groups began to show functional deficits (unable to complete the 180-second test) starting at week 15 with the lowest number of mice able to complete the task during the final testing week (dashed box). At this time point, significantly less $G93A_S$ were able to complete the RR task versus $G93A_{CL}$ mice ($p<0.05$). Whereas 8/10 (80%) of $G93A_{CL}$ mice were able to complete the 180-second RR task, only 4/11 (36%) $G93A_S$ mice completed the task during the final testing session (week 17).

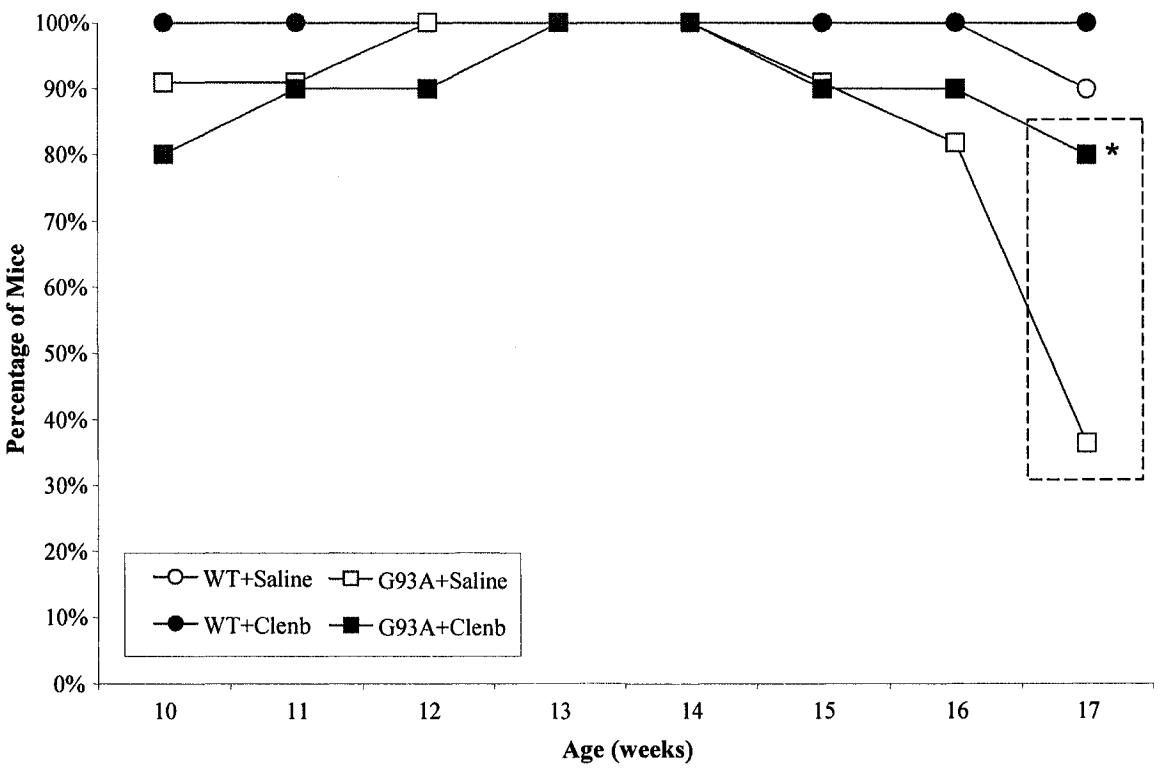

Figure 24: Percentage of WT and G93A mice treated with saline or Clenbuterol able to complete the 180-second RotoRod task within 3 trials.
Circles (○●) represent WT mice, squares (■□) represent G93A mice (n=9-11/group), both with saline (open symbols) or Clenbuterol (closed symbols). Statistical analysis was performed on the final time point (dashed box) using the Mann-Whitney U test between the two G93A groups. *Significantly different from G93As mice ($p<0.05$).

When this data was stratified by gender (Figure 25A/B), all groups of male and female mice were able to complete the task by Week 13.

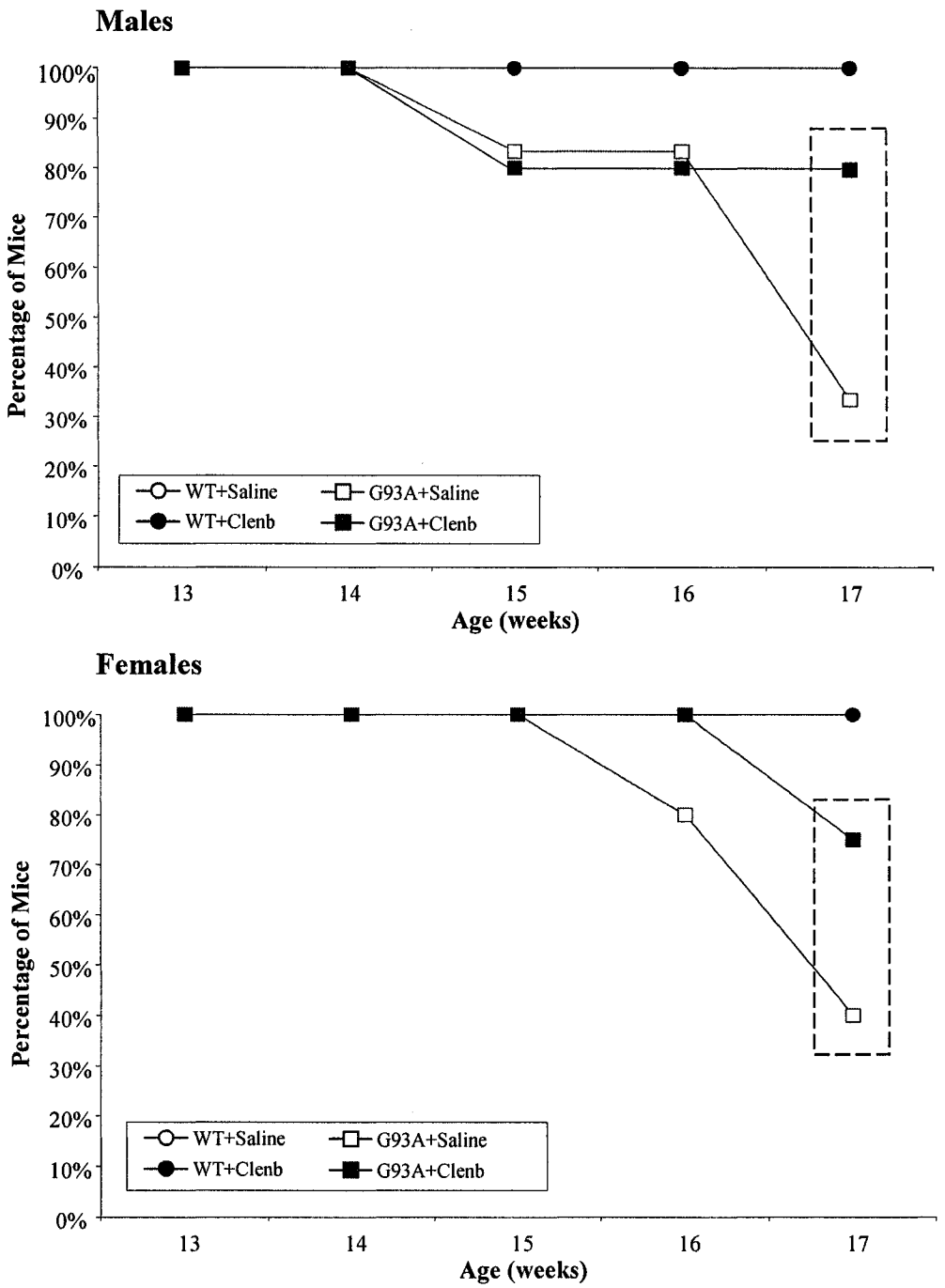

Figure 25: Percentage of male (top panel) and female (bottom panel) WT and G93A mice treated with saline or Clenbuterol able to complete the 180-second RotoRod task in 3 trials. Circles (○●) represent WT mice, squares (■□) represent G93A mice (n=4-6/group) treated with saline (open symbols) or Clenbuterol (closed symbols). Statistical analysis was performed on the final time point (dashed box) using the Mann-Whitney U test between the two G93A groups.

However, whereas both groups of male G93A mice ($G93A_S$ and $G93A_{CL}$) began to fall off the RotoRod at Week 15, female $G93A_S$ mice did not exhibit functional declines until week 16 and female $G93A_{CL}$ mice did not begin to have difficulties with the test until the final week of the study (week 17, dashed boxes). At the final time point (dashed box), significant differences between $G93A_S$ and $G93A_{CL}$ mice were not observed, presumably due to a small sample size when the groups were stratified by gender.

In order to further examine the differences in RotoRod performance between groups, the average time that the mice ran on the RotoRod (RRavg) was calculated throughout the study period (Figure 26). That is, if a mouse was not able to complete the task on the first attempt, the average time of the two (maximum of three) trials was calculated. Mean RRavg of G93A mice was slightly lower than WT mice at the start of the study (10 weeks) but by Week 14 most mice were able to complete the 180-second in one attempt (RRavg ~ 180 seconds). Significant main effect differences in RRavg were observed as a function of disease (G93A < WT) ($p<0.01$). G93A mice decreased RotoRod performance from Week 13 onwards, a significant main effect over time ($p<0.05$). Both groups demonstrated their lowest mean RRavg values during the final testing week ($G93A_S$, 86.1 ± 22.9 sec vs. $G93A_{CL}$, 135.6 ± 24.8 sec). At this final time point, mice differed significantly in RRavg performance as a function of disease (WT > G93A) and drug treatment (Clenbuterol > saline) ($p<0.05$). This difference was particularly evident between saline-treated WT and G93A mice (171.8 ± 5.4 sec vs. 78.2 ± 23.1 sec; $p<0.01$) as well as the two G93A mice groups ($G93A_S$: 78.4 ± 23.1 sec vs.

$G93A_{CL}$: 144.5 ± 22.7 sec; $p<0.05$). RRavg performance was not statistically different between male and female mice ($p>0.05$) (Appendix B).

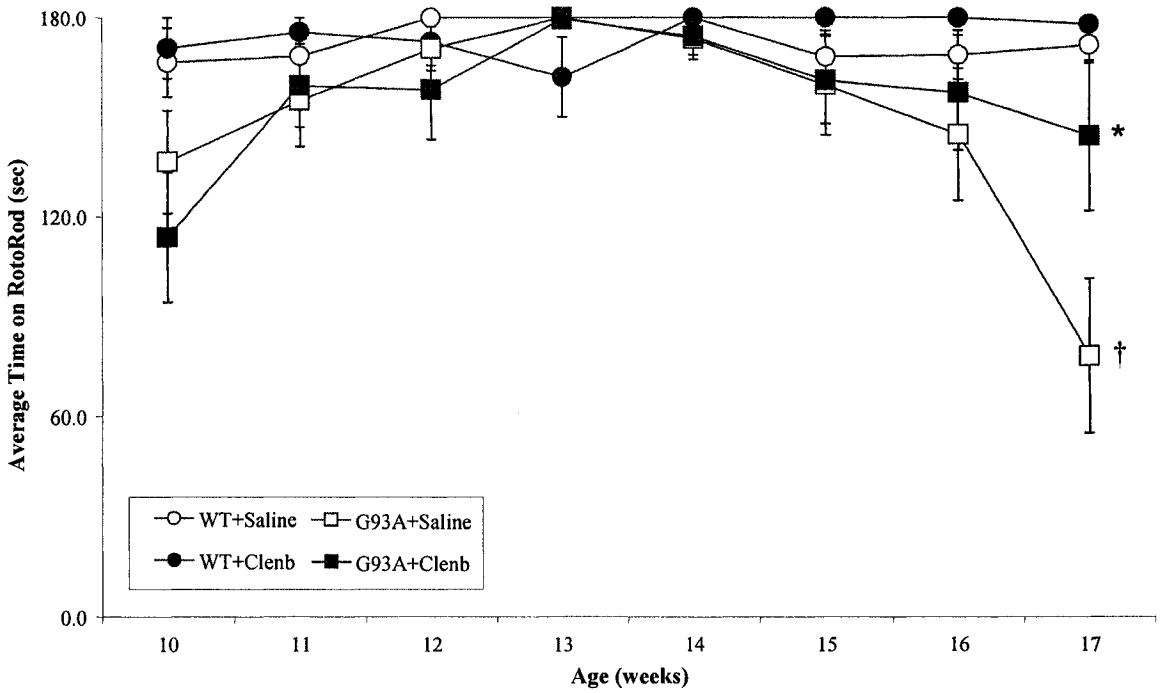

Figure 26: Average time on RotoRod (RRavg) for WT and G93A mice treated with saline or Clenbuterol.

Data are expressed as a mean ± SE (n=9-11/group). Circles (○●) represent WT mice, squares (■□) represent G93A mice, treated with saline (open symbols) or Clenbuterol (closed symbols). *Significantly different from saline-treated mice of the same genotype ($p<0.05$). †Significantly different from WTs mice ($p<0.05$).

Functional Assessment – PaGE

The percentage of mice able to complete the 90-second PaGE task is shown in Figure 27. Interestingly, mice in all four groups found it difficult to complete the test and therefore a trial 'passed' was defined as a hang greater than 70 seconds. At no time point were 100% of mice able to complete the task, with the exception of the WT_{CL} group at Week 15. G93A mice demonstrated consistently poorer performance than their WT controls throughout the study with both groups exhibiting their worst performance during

the final testing session (Week 17, dashed box). No difference was observed between G93A mice treated with Clenbuterol versus saline ($p>0.05$) at this final testing time point.

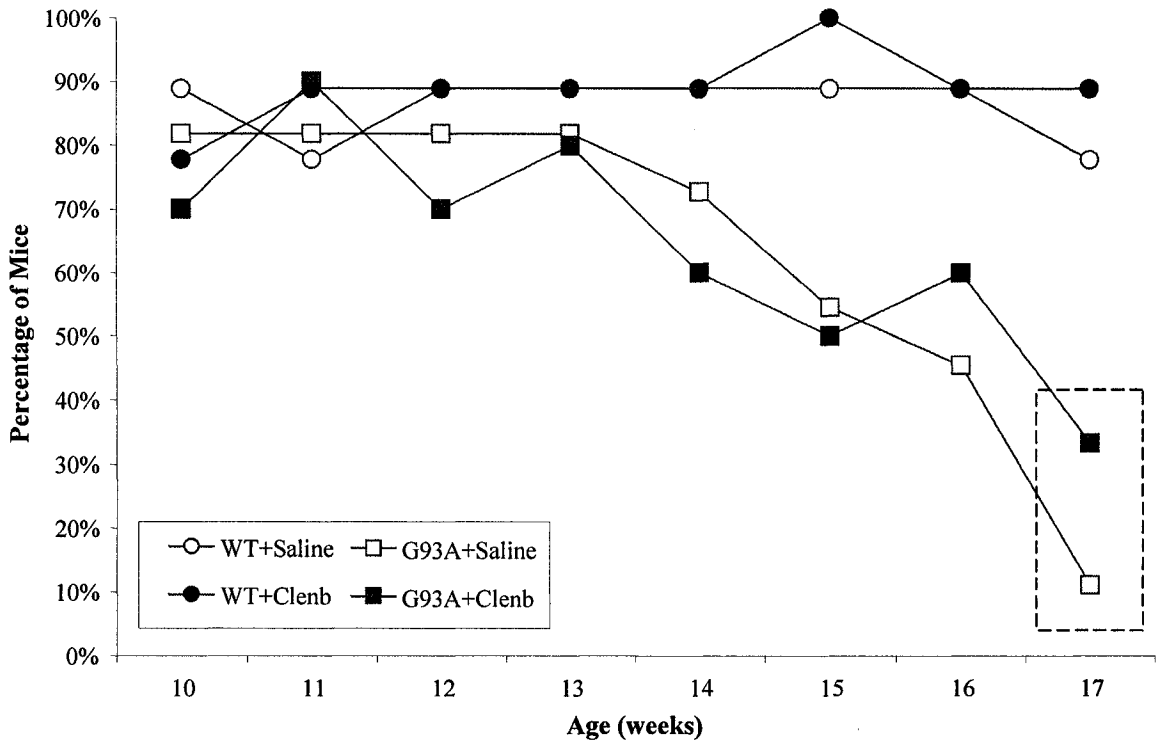

Figure 27: Percentage of WT and G93A mice treated with saline or Clenbuterol able to complete the 90-second PaGE task within 3 trials (attempts).
Circles (○●) represent WT mice, squares (■□) represent G93A mice (n=9-11/group) treated with saline (open symbols) or Clenbuterol (closed symbols). Statistical analysis was performed on the final time point (dashed box) using the Mann-Whitney U test between the two G93A groups.

When this data was stratified by gender (Figure 28A/B), interesting trends appear for the two groups of G93A mice. Clenbuterol appeared to improve PaGE performance of female G93A mice (Figure 28B) when compared to WT mice, as the $G93A_{CL}$ group performed significantly better than the $G93A_S$ group at the final time point (dashed box) ($p<0.05$).

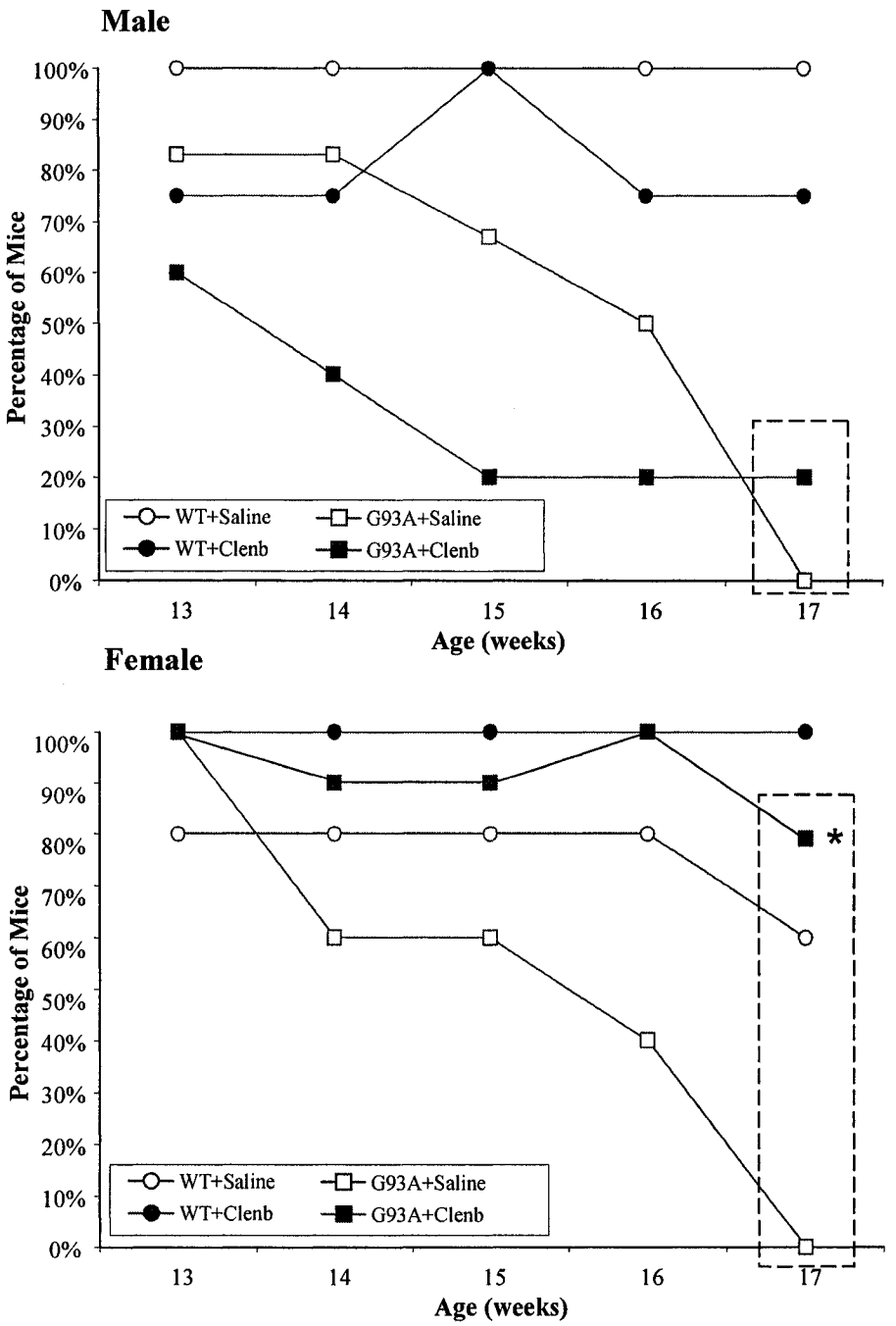

Figure 28: Percentage of male (top panel) and female (bottom panel) WT and G93A mice treated with saline or Clenbuterol able to complete the 90-second PaGE task in 3 trials.

Circles (○●) represent WT mice, squares (■□) represent G93A mice (n=4-6/group) treated with saline (open symbols) or Clenbuterol (closed symbols). Statistical analysis was performed on the final time point (dashed box) using the Mann-Whitney U test between the two G93A groups. *Significantly different from G93As mice ($p<0.05$).

However, male mice showed different trends. Although both groups of male G93A mice ($G93A_S$ and $G93A_{CL}$) were never able to complete the PaGE task, the Clenbuterol-treated G93A mice had poorer performance than the other groups, particularly between weeks 14-16 (Figure 28A). As the male $G93A_S$ group reached its lowest point at week 17, no significant differences were observed between G93A male mice at the final testing session.

In order to further examine the differences in PaGE performance between groups, the average hang time from the cage lid (PaGEavg) for each mouse at each testing session was calculated throughout the study (Figure 29).

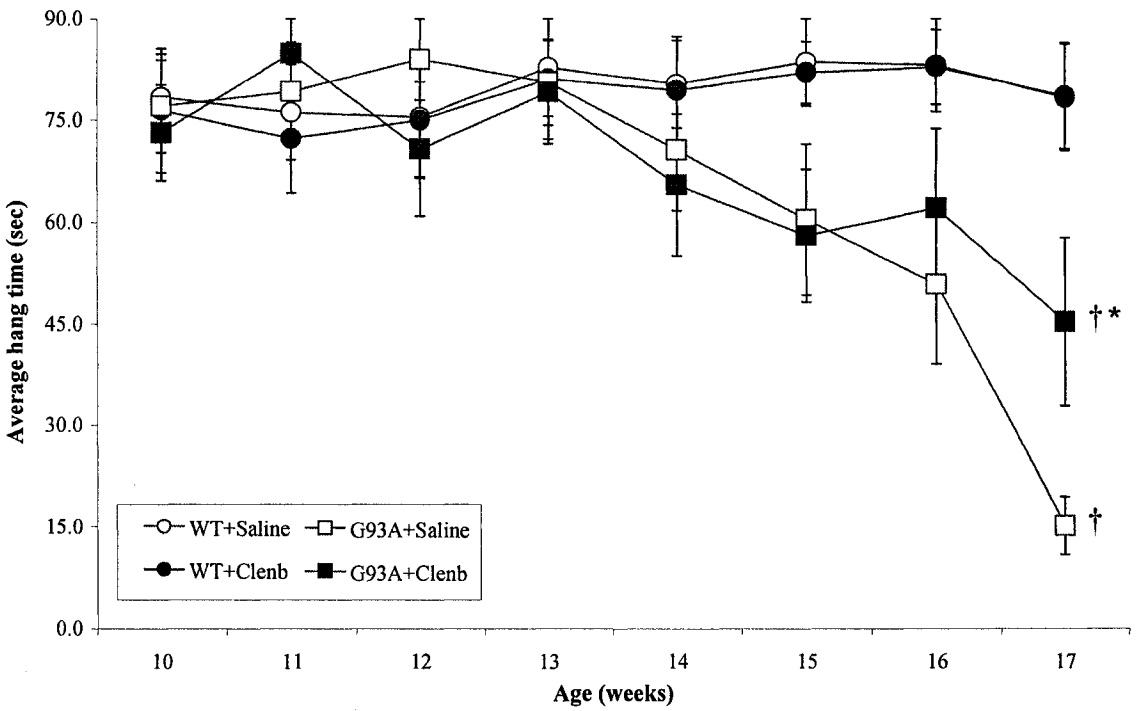

Figure 29: Average time hanging from cage (PaGEavg) for WT and G93A mice treated with saline or Clenbuterol.

Data are expressed as a mean ± SE (n=9-11/group). Circles (○●) represent WT mice, squares (■□) represent G93A mice, treated with saline (open symbols) or Clenbuterol (closed symbols). *Significantly different from saline-treated mice of the same genotype ($p<0.05$). †Significantly different from WTs mice ($p<0.05$).

Mean PaGEavg was not significantly different between groups at the start of the study ($p>0.05$). Significant main effect differences in PaGEavg were observed as a function of disease (G93A < WT) ($p<0.01$). In addition, both groups of G93A mice showed a steady decline in PaGEavg scores beginning at week 13 and demonstrated their lowest mean PaGEavg values during the final testing week ($G93A_S$, 13.3 ± 4.3 sec vs. $G93A_{CL}$, 45.3 ± 12.4 sec). Further examination of this time point revealed that both $G93A_S$ and $G93A_{CL}$ mice were significantly different from WT_S mice ($p<0.05$). Additionally, $G93A_{CL}$ mice had significantly better PaGEavg scores than the $G93A_S$ mice at week 17.

Although no significant differences in PaGEavg were observed over time between genders (i.e. males ~ females), both male and female mice differed in PaGEavg performance as a function of disease, that is, G93A performed significantly worse than WT mice (Figure 30) ($p<0.05$). During the final testing session (week 17), both groups of G93A mice demonstrated their lowest performance as measured by the PaGEavg variable. For male mice (Figure 30A), both G93A groups had significantly lower PaGEavg scores versus WT_S mice ($p<0.05$). In contrast, only the female $G93A_S$ mice were significantly lower than WT_S mice (Figure 30B) ($p<0.05$). No differences were observed between G93A groups as a function of drug treatment or between genders at week 17. However, it appears as though male and female G93A mice show different PaGEavg trends prior to week 17 as a function of drug treatment. Whereas female G93A mice appeared to improve in PaGE performance with the Clenbuterol treatment, male $G93A_{CL}$ mice performed consistently worse when compared to $G93A_S$ mice, the exception being at the final time point.

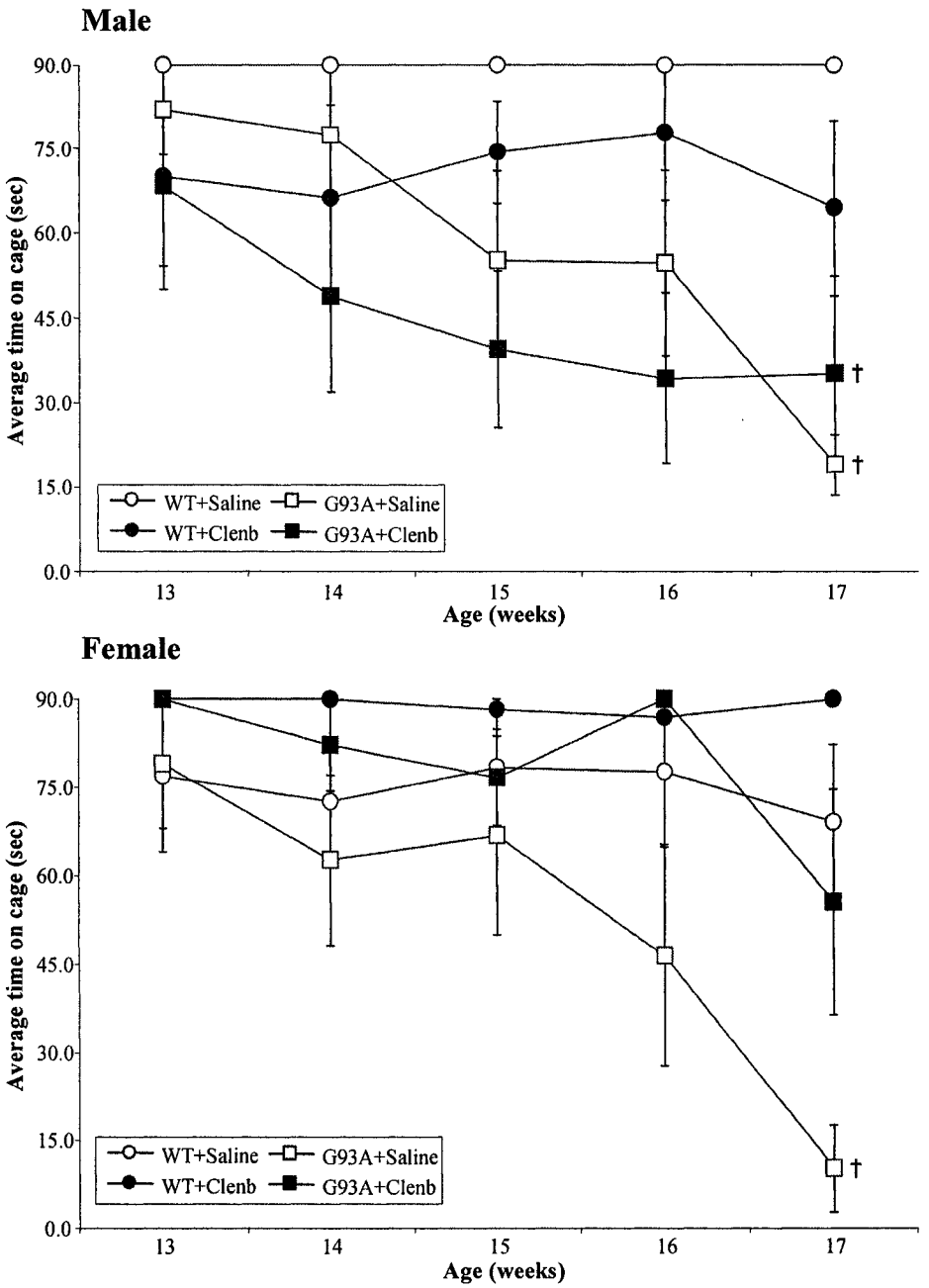

Figure 30: Average PaGE performance of male (top panel) and female (bottom panel) WT and G93A mice treated with saline or Clenbuterol.

Data are expressed as means ± SE (n=4-6/group). Circles (○●) represent WT mice, squares (■□) represent G93A mice, both with saline (open symbols) or Clenbuterol (closed symbols). *Significantly different from saline-treated mice of the same genotype ($p<0.05$). †Significantly different from WTs mice ($p<0.05$).

As Clenbuterol-treated mice gained significantly more weight than saline-treated counterparts, the lower PaGEavg results seen in male G93A mice may be partially

explained by examining PaGEavg performance when normalized to individual mouse body weight (Table 7). Normalized PaGEavg data clearly demonstrates a significant difference between G93A mice and WT mice in PaGEavg performance, but this difference exists only in male mice ($p<0.05$). No differences were found between groups as a function of Clenbuterol treatment, although it appears as though female $G93A_{CL}$ mice were able to maintain performance similar to wild-type levels and $G93A_S$ mice were not (3.1 ± 0.9 vs. 1.9 ± 1.2). This difference was not found to be statistically different ($p=0.21$).

Table 7: Average PaGE performance when normalized to body mass at sacrifice.

	PaGEavg Score Normalized to BM (sec/g)	
	Male	**Female**
WT + Saline	3.3 ± 0.1	3.6 ± 0.4
WT + Clenbuterol	3.1 ± 0.1	3.7 ± 0.1
G93A + Saline	1.6 ± 0.8 †	1.9 ± 1.2
G93A + Clenbuterol	1.3 ± 0.7 †	3.1 ± 0.9

Data are expressed as means ± SE (n=4-6/group). †Significantly different from WTs mice ($p<0.05$).

Levels of smRFs

Protein contents of selected smRFs are depicted in Figure 31 with all values normalized to WT_S protein content. Compared to WT_S muscle, Akt protein levels increased significantly in $G93A_S$ muscle (5.32 ± 1.05 AU times greater) ($p<0.05$). In contrast, levels of Akt in $G93A_{CL}$ mice were not significantly different from WT_S mice ($p>0.05$) but were significantly less than $G93A_S$ mice ($p<0.05$). Protein levels of ERK were increased significantly in both G93A groups, higher than WT_S levels regardless of drug treatment ($p<0.05$). MyoD protein content decreased significantly in $G93A_S$ mice

versus wild-type controls ($p<0.05$) and although levels were slightly increased in G93A mice treated with Clenbuterol, MyoD content was not statistically different from $G93A_S$ mice ($p=0.26$). No significant differences in calcineurin levels were observed between the groups ($p>0.05$).

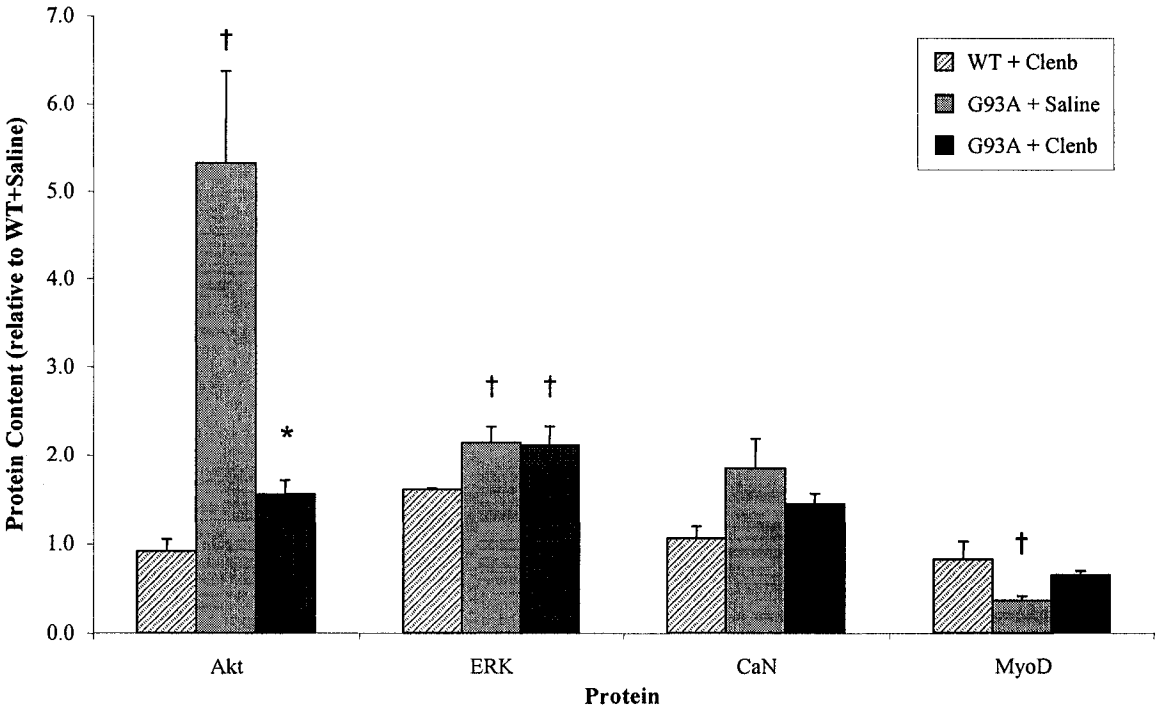

Figure 31: Protein content of selected smRFs (Akt, ERK, Calcineurin and MyoD) in WT and G93A mice treated with saline or Clenbuterol.
Data are normalized to WTs mice and expressed as a mean ± SE. WT+Clenbuterol (n=2), G93A+Saline (n=4), G93A+Clenbuterol (n=5). *Significantly different from saline-treated G93A mice ($p<0.05$). †Significantly different from WTs mice ($p<0.05$).

Discussion

The β_2-adrenergic agonist, Clenbuterol, has been shown to attenuate muscle atrophy following, for example, hindlimb suspension (Herrera et al., 2001) and acute denervation (Zeman et al., 1987; Maltin et al., 1993) protocols. However, information regarding its effect on progressive denervation-induced skeletal muscle atrophy is currently incomplete. Because of its anabolic effects on skeletal muscle and its proposed

neuroprotective (Culmsee et al., 1999b) and/or regenerative (Frerichs et al., 2001) properties, it has been suggested that Clenbuterol could prove to be an attractive therapeutic agent in the treatment of mSOD-induced progressive denervation and muscle atrophy. In the current study, Clenbuterol attenuated the progression of symptoms in G93A mice and this attenuation was further reflected in increases in body mass and improved motor coordination (RotoRod), as well as levels of the smRFs Akt and MyoD that were similar to wild-type mice at 120 days of age. Clenbuterol also led to improvements in Paw Grip Endurance (PaGE) performance in female G93A mice and increases in soleus muscle mass in wild-type mice. Results from this study suggest that Clenbuterol has a potential therapeutic influence on symptom progression and some functional measures of G93A mice but is unable to increase muscle mass at the 120-day time point in the G93A mouse lifespan.

One of the most significant findings of this study was that Clenbuterol attenuated the progression of symptoms in the majority of G93A mice. G93A mice normally begin to show clinical signs and symptoms of disease (i.e. hindlimb tremor) at approximately 85 days of age (Weydt et al., 2003; confirmed by our lab). A lower number of Clenbuterol-treated G93A mice reached later (i.e. moderate and severe) symptom stages when compared to saline-treated G93A mice at 120 days of age. No study has examined the effect of Clenbuterol on G93A mouse symptom progression as measured by the characteristics listed in Table 3. A variety of treatments, including Clenbuterol (Teng et al., 2006), erythropoietin (Grunfeld et al, 2006), and viral delivery/transgenic up-regulation of IGF-1 (Kaspar et al., 2003; Dobrowolny et al., 2005) have been shown to delay symptom onset in G93A mice when treatments begin at ages ranging from 42-60

days old. This, however, is clinically impractical considering therapies are normally not administered until after condition diagnosis. I chose to begin injections around/just prior to the mean age of symptom onset in these mice, knowing that some mice would demonstrate symptoms earlier than 85 days (in fact, 3 mice in the study began to show clinical symptoms at 78 days of age, 1 day after the first injections). The start date of injections did not affect the mean age of onset of mild (SO) symptoms. In addition, there were no significant differences found between $G93A_S$ and $G93A_{CL}$ mice with respect to the age of onest of any stage of symptoms. However, the number of G93A mice in later stages of symptoms was reduced significantly in Clenbuterol-treated G93A mice at 120 days ($G93A_{CL}$: 2/10 vs. $G93A_S$: 7/11). The attenuation of symptoms was subsequently reflected in some of the other variables examined in this work.

Functional performance of G93A mice as measured by the RotoRod task improved with Clenbuterol treatment at 120 days of age, as a greater proportion of both male and female G93A mice completed the 180-second task, similar to previously published findings (Teng et al., 2006). The RotoRod task is a complex task that primarily measures motor coordination and balance (Weydt et al., 2003) and therefore increases in RotoRod performance with Clenbuterol treatment suggest improvements in these characteristics. In the current study, the reasons for the improvement seen in Clenbuterol-treated G93A animals is quite possibly related to the stage of symptomotology in which each mouse was in at 120 days; the less advanced progression of symptoms in Clenbuterol-treated G93A mice was ultimately reflected in an improved (or a less impaired) performance relative to saline-treated mice. Although RotoRod performance was similar in males and females during the final testing session, the

declines in RotoRod performance began 1 week earlier (week 15) in male G93A mice than females (week 16), supported by previous research that suggests that the females do not progress through the disease as quickly as males (Miana-Mena et al., 2005). Interestingly, this decline was further delayed by another week (to week 17) in female mice treated with Clenbuterol, supported by previous research (Teng et al., 2006).

Functional performance as measured by the Paw Grip Endurance (PaGE) task was not different overall between the two G93A groups. To my knowledge, this is the first study to examine the effects of Clenbuterol treatment on PaGE performance of G93A mice. Further examination of this trend found that male G93A mice did not differ in PaGE performance at 120 days of age; female G93A mice treated with Clenbuterol significantly improved their PaGE performance at this time point. The PaGE test, a more basic motor function test, requires balance and strength, and has been shown to be a more sensitive method than the RotoRod for detecting early motor signs in the G93A mice (Weydt et al., 2003). In the current study, all G93A mice had difficulties with the PaGE task throughout the entire duration of the study; however, male $G93A_{CL}$ mice performed substantially worse than any other group. When PaGE performance was normalized to body mass at 120 days, differential trends emerged between the two genders. Male G93A mice, regardless of Clenbuterol treatment had significantly lower performance relative to body weight versus wild-type counterparts, whereas female G93A mice did not differ from their wild-type controls. It was hypothesized that an increase in male body mass explains why male mice in particular fell off the cage lid more often. However, both male and female $G93A_{CL}$ mice gained weight over time and weighed greater than $G93A_S$. Only female mice demonstrated a trend towards maintenance of

PaGE performance (normalized test values were similar to wild-type levels). There is therefore some indication from these results that female mice, regardless of whether they have increased in body mass, are still able to adequately perform the PaGE task, presumably due to an increase in strength at 120 days. Reasons for this differential performance are unclear but could be explained via a possible sexual dimorphic response to Clenbuterol, particularly when examining tests of muscular strength.

Previous literature has shown that female G93A mice have a later onset (Miana-Mena et al., 2005; Teng et al., 2006; Veldink et al., 2003) and longer lifespan (Fischer et al., 2004) than male mice. Many of these findings refer to the decline of functional performance as measured by tests such as the RotoRod task. A trend towards a delay in the onset of more advanced symptoms in female G93A mice treated with Clenbuterol, together with the PaGE data from this study, suggest that it is possible that female G93A mice possess an inherent protective mechanism that prevents the progression of symptoms and/or denervation. This mechanism may involve an estrogen-related neuroprotective effect (Teng et al., 2006), which could be enhanced by Clenbuterol administration. Clenbuterol has also been shown to stimulate the release of neurotrophic factors including nerve growth factor (Culmsee et al., 1999a) and basic fibroblast growth factor (bFGF) (Junker et al., 2002). In addition, Clenbuterol has also been shown to interact with muscle-specific IGF-1-associated signalling pathways (Litt Miller, thesis) and therefore one cannot rule out the possible influence of skeletal muscle growth/hypertrophy in the improved functional performance. Overall, it appears as though Clenbuterol may have a preferential effect in preserving motor function,

particularly balance and strength, in female G93A mice in the early stages of disease progression. The mechanism by which this occurs warrants further investigation.

Another key finding from this study was that although functional performance was enhanced in Clenbuterol-treated G93A mice, particularly in females, there was no observable difference in G93A soleus muscle weight at sacrifice. Clenbuterol induced increases in soleus muscle weight in wild-type animals but no difference was observed in G93A animals. This result contrasts with other chronic models of muscle atrophy that have shown increases in muscle mass with Clenbuterol treatment (Zeman et al., 2000). However, a number of reasons may explain these contradictory findings. First, G93A mice undergo varying levels of dehydration over the course of disease progression that limits the conclusions drawn from measurements of muscle wet weight. In order to minimize this concern, Animal Care staff monitored dehydration daily and administered gels for increased fluid intake if necessary. These measures were not normally taken until end-stage of the disease (in which case only one mouse in each G93A group may have experienced this treatment). Second, previous models of chronic atrophy do not mimic the symptoms observed in the G93A mouse. Zeman et al. (2000) found that Clenbuterol attenuated the loss of muscle mass in *mdx* mice, a model of chronic atrophy, but to date no conclusive evidence exists in the literature regarding the G93A mouse model of progressive denervation. Third, the differential response of the muscle weight of G93A and WT mice may be due to the age of the mice studied in this experiment. It could be argued that wild-type 120-day old mice in this study are still developing, and therefore these mice showed a greater (hypertrophy) response to the 6-week Clenbuterol treatment. In contrast, although significant muscle atrophy is not normally noticed at this

time point, the G93A mice undergo significant denervation and degeneration of muscle tissue prior to 120 days (Cunningham, thesis) and therefore may not respond in the same manner or to an extent of healthy, wild-type muscle. Previous research has found that Clenbuterol is unable to attenuate muscle degeneration or necrosis in young (3-month-old) *mdx* mice following 5 months of treatment (Lynch et al., 2001).

Finally, differential effects of Clenbuterol administration were observed in levels of muscle-specific signalling factors known to be involved in the regulation of muscle mass in skeletal muscle of G93A mice. Of the four proteins examined in this study, Akt, ERK and MyoD exhibited significant differences (increases in Akt and ERK, decreases in MyoD) in $G93A_S$ mice when compared to wild-type controls, in agreement with previous findings in this thesis (refer to Chapter 3). On the other hand, Clenbuterol-treated G93A muscle showed attenuated responses in both levels of Akt and MyoD, as both were found to be at levels similar to the wild-type groups. No significant differences were observed in ERK or calcineurin protein content as a function of Clenbuterol treatment. Given the earlier stage of symptoms of the Clenbuterol-treated G93A mice were in at 120 days, it seems logical that levels of proteins returned to levels that may be seen at earlier symptom stages (or rather, had yet to progress to levels associated with later symptom stages). At these earlier symptom stages, it is hypothesized that proteins such as Akt will not increase, as there has yet to be a sufficient denervation/degeneration stimulus to induce an attempt to protect the muscle from progressive denervation-induced atrophy.

Results from this study suggest that Clenbuterol may prove to be a beneficial therapeutic agent in the prevention of clinical signs and symptoms associated with

progressive denervation but further research is needed to substantiate this claim. Clenbuterol attenuated the progression of symptoms in G93A mice, which was reflected in increases in body mass and improved functionality (preferentially in female mice) at 120 days of age, as well as levels of the smRFs, Akt and MyoD, that were found to be similar to levels in wild-type muscle. Enhanced functional strength in female G93A mice may be explained by an inherent neuroprotective effect, although this should be confirmed in the future. In addition, symptom and functional improvements occurred in the absence of any significant muscle growth in the Clenbuterol-treated G93A mice, suggesting that muscle mass alone is not the only factor involved in Clenbuterol's effect on a model of progressive denervation. Ultimately, the status of the muscle itself, its mass, but also its functionality and overall health (reflected in levels of muscle-specific proteins) may dictate how skeletal muscle responds to anabolic agents such as Clenbuterol.

CHAPTER 5: GENERAL DISCUSSIONS AND CONCLUSIONS

There is strong evidence supporting the involvement of skeletal muscle regulatory factors (smRFs) including the PI3K/Akt and MAPK(ERK) pathways, calcineurin, the myogenic regulatory factors and myostatin in the regulation of myogenesis and the control of skeletal muscle mass. However, the role of these factors in Clenbuterol-induced muscle hypertrophy and progressive denervation-induced muscle atrophy is unclear. The work in this thesis revealed a number of novel findings concerning muscle-specific alterations that occur in these two situations.

smRFs are Involved in Clenbuterol-induced Hypertrophy & Progressive Denervation-induced Atrophy

The work described in Chapter 2 revealed that the β_2-adrenergic agonist, Clenbuterol, stimulates muscle-specific signalling factors such as proteins within the MAPK(ERK) and PI3K/Akt pathways immediately following (within 10 minutes) of Clenbuterol administration. Both of these pathways are well known to stimulate muscle growth and survival but have previously only been linked to Clenbuterol's action with longer-term (days or weeks of) administration and in developing (~4 week-old) animals (Sneddon et al., 2001). The data from this study clearly indicate that these pathways are activated shortly after Clenbuterol administration and remain elevated for 2-6 hours. This study also supports the involvement of IGF-1-dependent signalling factors in

Clenbuterol-induced skeletal muscle hypertrophy, but until now, have not been linked to the initial stages of this process.

Clenbuterol also acutely activated additional phospho-proteins (i.e. PKCα, PAK1/2/3, FAK and Pyk2) that have been previously implicated in the regulation of muscle mass. This is a novel finding and suggests the involvement of some novel signalling pathways in the hypertrophic mechanism, signalling factors that have not yet been associated with Clenbuterol. The immediate (within 10 minutes) phosphorylation of phospho-proteins highlighted in Chapter 2 is interesting, given that Clenbuterol did not activate PKA (confirmed via both the PKA activity assay and protein kinase screen), which is typically cited as a component of the 'classical' β_2-adrenergic pathway. At least initially, Clenbuterol appears to act through PKA-independent means to initiate its hypertrophic action in skeletal muscle, a novel finding from this work.

The work described in Chapter 3 suggests that long-term, progressive denervation alters specific myogenic and hypertrophic signalling factors in an attempt to combat this denervation. Increases in growth/survival factors Akt, ERK and calcineurin as well as decreases in MyoD were observed in later stages of progressively denervated muscle. However, alterations in these smRFs did not occur in G93A skeletal muscle until after the onset of clinical signs of the disease (ie. hindlimb tremor) and most were significantly different from wild-type controls when G93A mice reached severe symptoms. These findings appear to be counter-intuitive as increases in the PI3K/Akt and MAPK(ERK) pathways are also observed in healthy muscle stimulated by the anabolic agent, Clenbuterol. It may be that the smRFs Akt, ERK, calcineurin, and MyoD are altered in an attempt to combat progression of denervation and preserve muscle mass, which is

particularly evident at later symptom stages. In addition, the severe stage of symptoms (SS) and corresponding time point (~120-125 days) appear to be critical in the G93A mouse lifespan and disease-associated muscle-specific alterations. At this time point, there appears to be peak activation of select smRFs, presumably in an attempt to prevent muscle atrophy associated with the progressive denervation.

Alterations in smRFs Occur Prior to Observable Changes in Muscle Mass

In Chapter 2, I found that Clenbuterol induced PKA-independent stimulation of smRFs (cAMP, p-Akt, p-ERK), and additional phospho-kinases (PKCa, PAK1/2/3, FAK and Pyk2), that are thought to be involved in regulating muscle mass. Furthermore, these alterations occurred transiently, within 10 minutes to 6 hours of a single subcutaneous injection of Clenbuterol and long before any observable change in muscle mass. Previous studies have not shown increases in muscle mass with a similar dose of Clenbuterol until at least the third day of treatment (Sneddon et al., 2001). This initial activation raises a question as to whether these proteins are key factors to target in therapeutic interventions designed to increase muscle mass (i.e. in compromised and/or diseased situations).

In the G93A mouse model of progressive denervation, increases in Akt, ERK1/2 and calcineurin (CaN), as well as decreases in MyoD were observed in mixed hindlimb muscle of G93A mice versus wild-type controls. Significant signalling alterations primarily occurred at later stages of disease progression but often prior to any observable decreases in muscle mass. Results from this work indicate that skeletal muscle appears to up-regulate smRFs involved in growth/hypertrophy and survival (i.e. Akt, ERK and

calcineurin), presumably in an attempt to maintain muscle mass and/or function once late-stage symptoms commence. This type of 'compensatory hypertrophy' response with progressive denervation has been suggested previously (Cunningham L, thesis) and is corroborated by additional muscle-specific factors in this thesis.

For the most part, these smRFs remain elevated to a similar extent at end-stage of the disease progression, but do not increase further, potentially because the muscle is unable to further increase levels of these factors to counter-act the disease progression. Alternatively, previous literature has shown that whereas soleus muscle from these mice is 44% denervated when severe symptoms are present, this proportion actually decreases at end-stage of the disease progression to 26% denervated muscle fibres (Cunningham L, thesis). An increased amount of necrotic muscle tissue towards end-stage of the disease may prevent further increases in (and protection via) the smRFs. It would appear that the compensatory up-regulation of growth/survival factors is outweighed by the degenerative effects of the progressive denervation, during the transition between severe and end-stage symptoms. It is not until this stage that significant loss of muscle mass is observed.

Clenbuterol Delays the Progression of Symptoms in a Mouse Model of Progressive Denervation

In Chapter 4, Clenbuterol attenuated the progression of symptoms in G93A mice and this delay was further reflected in levels of the smRFs, Akt and MyoD, which were similar to wild-type mice at 120 days of age. Significantly fewer Clenbuterol-treated G93A mice reached later (i.e. moderate and severe) symptom stages when compared to saline-treated G93A mice at this time point. Protein levels involved in regulating muscle mass remained at levels similar to those observed in wild-type mice and/or the early

stages of disease progression, and reflected this slowing/delay in symptom progression in Clenbuterol-treated G93A mice. For example, at these earlier symptom stages, it is hypothesized that Akt is not significantly greater than wild-type/pre-symptomatic levels as there has yet to be a sufficient denervation/degeneration stimulus to induce the muscle's protective mechanisms.

Interestingly, both the Clenbuterol-induced hypertrophy and the progressive denervation-induced atrophy in the G93A mouse examined in this work were found to up-regulate smRFs such as Akt and ERK. As such, one may have hypothesized that the combination of the two models would further increase Akt and ERK content. This, in fact, was not the case and it appears as though the level of the smRFs (in particular Akt, as well as MyoD) appear to be instead related to the symptoms demonstrated by the G93A mice at this particular time point.

Clenbuterol's influence on delaying symptoms was also reflected in increases in body mass and improved motor coordination (RotoRod). Clenbuterol treatment appeared to have no effect on the onset/rate of RotoRod decline in male mice; however, the decline was further delayed by one week in Clenbuterol-treated female mice. Clenbuterol also led to improvements in Paw Grip Endurance (PaGE) performance in female G93A mice. It is possible that female G93A mice possess an inherent protective mechanism that prevents the progression of symptoms and/or denervation, including an estrogen-related neuroprotective effect that is modulated by Clenbuterol. Further examination of the mechanisms underlying this sexual dimorphism is warranted.

Although Clenbuterol appeared to have beneficial effects on symptom progression, functional performance and some of the smRFs, it did not increase soleus

muscle mass at the time point examined. Increases in muscle mass were observed with Clenbuterol treatment in wild-type mice only. This finding infers that Clenbuterol's anabolic effects are lost or overridden in progressively denervated skeletal muscle in this model. Additionally, an increased variability of the response of skeletal muscle to denervation may also limit Clenbuterol's action in this model. However, the drug is still able to induce changes in the quality/composition (for example, certain smRFs) of skeletal muscle, which may be reflected in improved functional performance. Results from this work suggest that Clenbuterol has a potential therapeutic influence on symptom progression and some functional measures of G93A mice but is unable to increase muscle mass at the 120-day time point in the G93A mouse lifespan.

Future Directions

A number of interesting questions arise from the results of the studies presented in this thesis. As described in Chapter 2, Clenbuterol acutely stimulated the phosphorylation of both Akt and ERK and increased levels of cAMP without altering PKA activity in skeletal muscle. Unfortunately, *in vivo* studies do not demonstrate the direct effect of the drug on these smRFs. As such, complimentary experiments using the C_2C_{12} skeletal muscle cell line would enhance the explanation of the mechanism by which Clenbuterol directly targets muscle cells. Future research should also examine the mechanism by which Clenbuterol initially stimulates the PI3K/Akt and MAPK/ERK pathways independent of PKA. Direct interactions between cell surface receptors or downstream signalling intermediates (such as those identified in the protein kinase screen) could be determined using co-immunoprecipitation and/or inhibitor/blocker experiments in either *in vivo* or *in vitro* situations.

The G93A (mSOD) mouse is a relatively novel model currently used to examine the pathogenesis of ALS as well as progressive denervation-induced atrophy. As a result, there remain many questions to be answered, particularly with respect to determining the cellular muscle-specific alterations that occur during progressive denervation associated with disease progression in this model, and the mechanism(s) by which muscle responds to such a stimulus. Further investigation of different models of progressive denervation-induced atrophy will help to determine the explicit roles of each smRF in muscle atrophy. Examination of specific smRFs and the effect of knocking-out or inhibiting a specific factor in G93A mice would also be useful in examining the smRFs role in progressive denervation-induced atrophy.

Future research should investigate the mechanism by which Clenbuterol attenuates the progression of symptoms in G93A mice. In particular, the effects of the drug on different time points/stages during disease progression as well as its effects on the nervous system are keys to fully explaining this agent's therapeutic properties. Further research is needed to fully evaluate the feasibility of Clenbuterol's use as a therapeutic treatment for diseases associated with progressive denervation-induced skeletal muscle atrophy. Previous research has suggested that superior therapeutic effects may be achieved with higher and/or more frequent dosing (Teng et al., 2006), although this has not been tested. As a number of different treatment options have been explored for the attenuation/delay of clinical symptoms in this model, with varying results/success, identification of those agents that would best prevent/delay the onset of muscle-specific symptoms such as denervation should be determined.

Given a differential response of Clenbuterol in male/female G93A mouse functional parameters, it would be interesting to examine gender effects of smRFs investigated in this work. Although previous research has shown no difference between male and female G93A mixed muscle Akt content (Cunningham L, thesis) without drug treatment, it is unclear if Clenbuterol preferentially alters smRFs in one gender more than the other. The effects of gender on levels of smRFs have primarily been studied in cardiac muscle and none utilizing models of progressive denervation. Further research is needed to not only identify the inherent sexual dimorphism in the G93A mice, but also to determine why Clenbuterol appears to have a beneficial functional effect on female G93A mice.

Finally, in the present study, I did not examine the possible neuroprotective mechanism of Clenbuterol in the G93A mice. Because of its anabolic effects on skeletal muscle and its proposed neuroprotective and/or regenerative properties, the improvements in functionality (particularly in female mice) and levels of Akt and MyoD may be a consequence of enhanced neuronal transmission and/or connectivity with the muscle. Although muscle denervation was not specifically investigated in this work, it is hypothesized that Clenbuterol-treated G93A mice that demonstrate early stage symptoms at 120 days also possess a lesser extent of denervation, given that the degree of denervation is correlated with symptom progression (Cunningham L, thesis). However, as Clenbuterol can permeate the blood-brain barrier, it is highly likely that the benefits to skeletal muscle involve improved neuronal functioning. This concept should be investigated in the future.

APPENDIX A

WESTERN BLOTTING PROTOCOL

1) TISSUE PREPARATION

1.1a Modified RIPA Buffer (Option 1):

Final Concentration in 100 mL:	Stock Taken:	
50 mM Tris-HCl (pH 8.0)	605.7 mg Tris Base to 75 mL in dH_2O	Stir, pH to 8.0 w/ HCl
150 mM NaCl	900 mg NaCl	
1% NP-40	1 mL NP-40	
1 mM EDTA	1 mL of 100 mM EDTA	

* Adjust volume to 100 mL. Can be stored on shelf at RT°.

Protease/Phosphatase Inhibitors – added FRESH:

Final Concentration	*Stock Concentration*	*in 10 mL final*
1 ug/mL Aprotinin	1 mg/mL in H_2O (-20°C)	10 uL
1 ug/mL Leupeptin	1 mg/mL in H_2O (-20°C)	10 uL
1 ug/mL Pepstatin	1 mg/mL in Methanol (-20°C)	10 uL
1 mM PMSF	500 uL of 200 mM stock in Isopropanolol	20 uL
2 mM Na_3VO_4	1 mL activated Na_3VO_4 (200 mM stock)	100 uL
1 mM NaF	500 uL of 1M stock (RT°)	10 uL

* Up to 10 mL w/ dH_2O

1.1b Modified RIPA Buffer (Option 2):

Final Conc:	Stock Sol'n:	Volume in 10mL:	Notes:
50mM Tris (pH 8.0)	2M	250ul	RT°
1% NP-40	100%	100ul	RT°
150mM NaCl	5M	300ul	RT°
1mM EDTA	0.1M	100ul	RT°
1mM PMSF	0.2M	20ul	-20°C, in isopropanolol
1ug/ml Aprotinin	1mg/ml	10ul	-20°C, in water
1ug/ml Leupeptin	1mg/ml	10ul	-20°C, in water
1ug/ml Pepstatin	1mg/ml	10ul	-20°C, in methanol
2mM Na_3VO_4	0.2M	100ul	-20°C, heat activated
1mM NaF	1M	10ul	RT°

1.2 Homogenization

1. Clean homgenizer probe in 0.1N NaOH and rinse in dH_2O.
2. Keep samples frozen in liquid nitrogen (or $-80^{\circ}C$) until use.
3. Make up Eppendorf tubes – one tube holds 50-80 mg tissue homogenized.
4. On ice : flat-bottomed, glass homogenization vials
   : labelled Eppendorfs
   : dH_2O (in 50 mL Falcon tube)
   : 0.1N NaOH (in 50 mL Falcon tube)
   : 10 mL RIPA buffer (enough for ~30 samples)
5. Place tissue into frozen mortar (filled/evaporated liquid N_2) and break apart to smaller pieces
6. Weigh tissue in vial: 50-80 mg
7. Calculate amount of RIPA buffer needed (6x) [ex. 50 mg tissue = 300 uL buffer]
8. Add small volumes of buffer to tissue to homogenize [ex. 100 uL w/ tissue → ½ remaining buffer to homog 2x → ½ rest of buffer to rinse
9. Homogenize sample 10 seconds
10. Add 2nd buffer amount and homogenize 10 seconds
11. Add final buffer amount to rinse off probe
12. Let sample sit on ice to prevent foaming
13. Transfer homogenate to Eppendorf and leave on ice
14. Clean probe after each sample with NaOH and rinse with dH_2O
15. When all samples complete, centrifuge tubes: ~20,000 rpm for 10 min @ $4^{\circ}C$
16. Transfer supernatent to new Eppendorf and store both supernatent and pellet at $-80^{\circ}C$.

1.3 Bradford Protein Determination

1. Dilute 5 uL aliquot of supernatent in 1 mL dH_2O.
2. Take 100 uL of this aliquot and add to 700 uL dH_2O in duplicate.
3. Prepare BSA Standards (0-12 ug BSA in 800 uL) in duplicate.
   * Stock Sol'n: 20 mg BSA in 400 mL dH_2O (1 ug/20ul)

   * 0 ug: 0 uL BSA + 800 uL dH_2O
   * 2 ug: 40 uL BSA + 760 uL dH_2O
   * 4 ug: 80 uL BSA + 720 uL dH_2O
   * 6 ug: 120 uL BSA + 680 uL dH_2O
   * 8 ug: 160 uL BSA + 640 uL dH_2O
   * 10 ug: 200 uL BSA + 600 uL dH_2O
   * 12 ug: 240 uL BSA + 560 uL dH_2O

   Note: for cell lysates, decrease std curve values to 0, 0.5, 1, 1.5, 2, 2.5, 3 ug

4. Add 200 uL of undiluted Bio-Rad Protein Assay Reagent to sample and Standard tubes
5. Cap tubes and invert gently, avoid bubbles (do not vortex).
6. Allow tubes to sit for exactly 10 minutes for colour development – be consistent between assays.
7. Transfer tube contents (1mL) to disposible optical cuvettes.
8. Read @ 595 nm using Spectrophotometer.
9. Back correct spec using 0 ug Standard tube.

2) ELECTROPHORESIS

2.1 Sample Preparation

2.1.1 Laemmli Sample Buffer:

Final Concentration:	*For 25 mL 2x concentrate Laemmli Buffer:*
60 mM Tris	363 mg Trizma Base (electrophoresis grade)
2% (wt/vol) SDS	10 mL 10% SDS solution
10% (vol/vol) Glycerol	5 mL glycerol
5% (vol/vol) b-mercaptoethanol	2.5 mL b-mercaptoethanol (fumehood!)

* Adjust to pH 6.8. Complete up to 25 mL with dH_2O. Store at 4°C.

2.1.2 Sample Preparation for Loading:

1. Prepare samples so that equal amounts of protein are loaded in each lane.
2. Calculated volumes of supernatent are diluted in and equal volume of 2x Laemmli buffer and the final volume is completed by adding 1x Laemmli buffer.
   Ex. Loading 60ug/30 uL: Make up excess Sx (ie. 70ug/35ul)
   Sx = 70/[prot]
   2x Laemmli = same volume of Sx
   1x Laemmli = 35-Sx-2x Laemmli
3. Prepare one lane for Molecular Marker:
   Ex. 1 MM = 15 uL concentrated NEB Violet Molecular Marker (broad range)
4. Any empty lanes should be filled with Empty Lane Buffer:
   Ex. 1 EL = 5 uL 0.1% Bromothymyl Blue
   5 uL 2x Laemmli Buffer
   20 uL 1x Laemmli Buffer
5. Diluted samples are boiled for 4-5 minutes in Eppendorf tubes.
6. Samples are then centrifuged quickly, ~15,000 rpm for 30 seconds to eliminate evaporated liquid on lid.

2.2 SDS-PAGE Stock Solutions

Note: use electrophoresis grade reagents where possible
: work from 10% SDS stock solution
: for improved safety, use Bio-Rad premixed 40% acrylamide solution

Lower Tris Stock Solution	For 250 mL:
1.5 mM Tris	45.41 g Trizma Base
0.4% SDS	10 mL SDS 10% solution
pH 8.8	pH 8.8
	Complete to 250 mL with dH_2O
	Store at 4°C

Upper Tris Stock Solution	For 100 mL:
1 M Tris 0.4% (wt/vol) SDS pH 6.8	12.11 g Trizma Base 4 mL SDS 10% solution pH 6.8 Complete to 100 mL with dH_2O Store at 4°C

Lower Acryl Stock Solution	For 250 mL:
32% (wt/vol) acrylamide 0.43% (wt/vol) bis-acrylamide	200 mL acrylamide 40% solution 1.075 g bis-acrylamide Allow bis to dissolve 15 minutes. Complete to 250 mL with dH_2O Store at 4°C

Upper Acryl Stock Solution	For 100 mL:
20% (wt/vol) acrylamide 0.52% (wt/vol) bis-acrylamide	50 mL acrylamide 40% solution 0.52 g bis-acrylamide Allow bis to dissolve 15 minutes Complete to 100 mL with dH_2O Store at 4°C.

2.3 Gel Recipes (Mini-Gels)

Running Gel (for 2 gels):

	6%	8%	10%	12%	15%	
Lower Tris	4 mL	4 mL	4 mL	4 mL	4 mL	
Lower Acryl	3 mL	4 mL	5 mL	6 mL	7.5 mL	
dH_2O	9 mL	8 mL	7 mL	6 mL	4.5 mL	
10% APS	32 uL	32 uL	32 uL	32 uL	32 uL	} Add
TEMED	9.8 uL	9.8 uL	9.8 uL	9.8 uL	9.8 uL	} last

* Note: 10% APS prepared FRESH each day: ie. 0.025 g APS in 250 uL dH_2O.

Stacking Gel (for 2 gels):

Upper Tris	2.5 mL
Upper Acryl	2.5 mL
dH_2O	5 mL
10% APS	40 uL
TEMED	25 uL

2.4 Casting Procedure

Running Gel:

1. Clean glass plates with ethanol and Kimwipes.
2. Clean appropriate foamies and combs with ethanol and Kimwipes.

3. Assemble glass sandwiches into green holders. Use counter to align bottom edges of glass plates. Close green gates on holders.
4. Inspect the glass-spacer-glass interface to ensure alignment.
5. Attach sandwiches/green holders to apparatus for gel casting.
6. Check for leakage by adding distilled water. If there is leakage, return to step 3.
7. Mark 2 cm down from small plate for line at which running gel is to be poured.
8. Discard any excess water by tipping upside down.
9. Once APS and TEMED have been added to Running Gel, quickly use plastic syringe or P1000 pipette to add liquid running gel between glass plates of sandwich up to marked line.
10. Add a thin layer of distilled water on top of running gel to prevent gels from drying. Slowly adding from one side of gel works best as water diffuses across surface and does not dilute running gel.
11. Ensure gel is approximately level. Allow approximately 60 minutes for polymerization at room temperature.

Stacking Gel:

1. Once a definitive line has formed between the Running Gel and water layers, suck up water with a small piece of filter paper.
2. Make Stacking Gel according to recipe, working *quickly* after APS and TEMED have been added.
3. Using clean syringe or P1000, add Stacking Gel on top of Running Gel, up to top of small plate.
4. Carefully place combs into Stacking Gel on angle to prevent bubble formation (placing into gel on an angle prevents bubbles from getting trapped under comb).
5. Allow to polymerize for approximately 15 minutes at room temperature.

2.5 Loading Procedure

1. Remove combs once Stacking Gel has polymerized.
2. Suck up excess gel and bubbles with pipette and loading tip or add Running Buffer directly to lanes and load samples into buffer (note: I prefer the latter).
3. Use gel loading tips and add samples into each lane (avoid running samples on outside lanes as they will run on an angle, causing gel "smiling").
4. Fill one lane with Molecular Marker and additional empty lanes with Empty Lane Buffer.

2.6 Gel Electrophoresis

2.6.1 Running Buffer:

Final Concentration (1x):	*For 3L of 10x Stock*:
25 mM Tris Base	90.825 g Tris Base
192 mM glycine	432.4 g glycine
0.1% (wt/vol) SDS	30 g SDS
pH 8.3	pH 8.3

* Adjust to 3 L with dH_2O
* Store on shelf at RT°
* *For 1x*: 100 mL 10x + 900 mL dH_2O

2.6.2 Electrophoretic Run:

1. Place the electrophoresis apparatus (glass sandwiches and attachment) inside tank.
2. Carefully fill the inside of apparatus with NEW running buffer.
3. Fill outside of tank with rest of running buffer (can be used up to 3x). Store any leftover Running Buffer in cold room for later use.
4. Place lid (red:red, black:black) over appropriate anode and cathode.
5. Connect to power source and set as follows:
6. Manual setting – constant mA
7. Step 1, through Stacking Gel: 50mA/tank (new RB), 60mA/tank (old RB)
8. Step 2, through Running Gel: 100mA/tank (ne RB), up to 120mA/tank (old RB) Step 1 of run should take 45-60 minutes. Step 2 of run should take ~1 hour (total 1.5-2 hours). Stop power supply when tracer (blue dye) has almost reached bottom of glass plates (do not let it run off into buffer, discard solution if buffer is blue).
9. Always check power supply to ensure running conditions.

2.7 Electrotransfer

2.7.1 Transfer Buffer:

Final Concentration (1x):	*For 4L of 10x Stock:*
25 mM Tris	121.1 g Tris base
192 mM glycine	576.5 g glycine
10% Methanol	*(add FRESH when making up 1x)*
pH 8.3	pH 8.3

* Adjust to 4 L with dH_20. Store on shelf at RT°.
* *For 1x*: 100 mL 10x + 100 mL Methanol + 800 mL dH_2O

2.7.2 Membrane Preparation:

1. Cut PVDF membrane to appropriate size (~7 x 9 cm)
2. Clip top left corner for orientation.
3. With a pencil, carefully mark for identification (protein, date, initials)
4. Activate membrane with Methanol for 5 seconds.
5. Rinse membrane in dH_2O for 5 minutes on shaker.

2.7.3 Gel Extraction:

1. Dump Runing Buffer from center of apparatus. Save remaining buffer from outside of apparatus (up to 3x use). Store in cold room.
2. Remove glass sandwiches from green holders and gently pry glass plates apart using spacers or scalpel.
3. Cut off Stacking Gel using clean scalpel (small cuts).

4. Cut gel above and below molecular weight of interest (if applicable).
5. Moisten gel with Transfer Buffer to prevent drying.

2.7.4 Transfer Procedure:

1. Place sandwich assembly in large Tupperware bin filled with Transfer Buffer, CLEAR SIDE DOWN.
2. Wet fibre pads and 2 filter paper squares (cut to ~ 7x9 cm) per side with Transfer Buffer. Place them onto assembly and roll out bubbles with plastic pipette shaft.
3. Place membrane onto CLEAR side and roll out bubbles.
4. Carefully place gel onto membrane and smooth out any bubble formation.
5. Very gently press two sides together, seal sandwich assembly and position into transfer case with the BLACK side of each sandwich facing the BLACK side of the case.
6. Place case, magnetic stir bar, and ice pack into tank and fill tank with Transfer Buffer. Be sure to cover sandwiches with the buffer.
7. Cover container with lid and connect to power source in Cold Room on stirplate.
8. Set power source as follows: Manual Setting – constant mA
9. Set mA to specific level so that Voltage reads:
   65-70V for 3 hour transfer
   45-50V for overnight transfer
10. Leave in Cold Room for desired time (3 hours or overnight).

2.7.5 After the Transfer:

1. Remove transfer sandwiches from case and save Transfer Buffer (up to 3x use).
2. Rinse membrane with dH_2O for 5 min.
3. Soak in Ponceau Red solution (Sigma) for ~1 min or until the protein bands are visible.
4. Remove from dye solution and rinse excess 2-3 x with small volumes of dH_2O.
5. Place membrane on glass plate, cover with Saran Wrap, and photocopy for reference (indication of protein loading, molecular marker location).
6. Rince membrane with dH_2O for 5 min and then in TBST for 5 min.
7. Let membrane air dry on filter paper or proceed to immunodetection procedure.

3) IMMUNODETECTION

3.1 Solutions:

Tris-Buffered Saline + Triton (TBST):

50 mM Tris
150 mM NaCl
0.5% (vol/vol) Triton X-100
pH 7.4

* *For 1x: 100 mL 10x + 900 mL dH_2O*

For 3L of 10 x Concentrate:

181.65 g Tris Base
263 g NaCl
150 mL Triton X-100 (viscous)
pH 7.4
Complete to 3L with dH_2O
Store on shelf at RT^{o}

Tris-Buffered Saline (TBS):

50 mM Tris
150 mM NaCl
pH 7.4

For 4L of 10 x Concentrate:

242.2 g Tris Base
350.7 NaCl
pH 7.4
Complete to 4L with dH_2O
Store on shelf at RT°

** For 1x: 100 mL 10x + 900 mL dH_2O*

3.2 Blocking

1. If working from a dry blot, membrane must be activated by immersing in methanol for 5 seconds, then rinsed 5 min in dH_2O and TBST for 5 min.
2. Block membrane for **90 min at RT°** or **overnight at 4°C** with a 5% BSA (Fraction V) solution in TBST under gentle agitation. Use ~10mL in a heat-sealed plastic bag on an orbital shaker. Blocker can be used 3-4x before discarding. [Ex. 5g in 100 mL TBST = 5% BSA in TBST for block].
3. Wash 3 x 5 minutes with TBST at RT° with moderate agitation (note: this step can be accelerated if low on time).

3.3 Primary Antibody

1. Incubate membrane **overnight at 4°C** (cold room) or **2.5 hours RT°** in appropriate primary HRP-conjugated antibody (most kept at -20°C) .
2. Use 10 mL in a heat-sealed plastic bag on an orbital shaker.

   For 10 mL 1° Ab: 1 mL 10x TBST
   1 mL 10% BSA in TBST
   1 mL 5% NaN_3 solution (in water, store at 4°C)
   appropriate volume of Ab (ie. 1:1000 = 10ul)
   Complete up to 10 mL with dH_2O

3. Save 1° Antibody for reuse, store at –20°C (can be used up to 3-4x).
4. Wash 5 x 5 minutes with TBST at RT° with moderate agitation.

3.4 Secondary Antibody

1. Incubate membrane for **90 minutes at RT°** in appropriate secondary antibody (most kept at 4°C) .
2. Use 10 mL in a heat-sealed plastic bag on an orbital shaker.

   For 10 mL 2° Ab: 1 mL 10x TBST
   1 mL 10% BSA in TBST
   appropriate volume of Ab (ie. 1:20,000 =0.5 uL)
   Complete up to 10 mL with dH_2O

3. Discard 2° Antibody down sink.
4. Wash 3 x 5 minutes in TBST.
5. Wash 3 x 5 minutes in TBS.
6. Prepare membrane for detection procedure.

*Note: procedure may be stopped at any TBST step and blot dried or stored at 4°C in TBST.

3.5 ECL Detection

1. Make up appropriate volume of Amersham ECL solution (2 mL/membrane = 1 mL Solution 1 + 1 mL Solution 2).
2. Remove membrane for washes (TBS) and dab onto benchcoat to remove excess TBS.
3. Place membrane onto even surface (plastic dish) and coat fully and evenly with ECL mixture for *exactly* 1 minute.
4. Quickly transfer membrane onto glass plate, cover with Saran Wrap and smooth out any bubbles.
5. Place glass plate and membrane into cassette and close firmly.
6. Proceed to dark room development.

3.6 Dark Room Development

3.6.1 Solutions:

Developer (Kodak D-19, from VWR): Dissolve developer powder as directed on package.

Fixer: Dilute in 1:4 ratio as specified on Fixer jug.

3.6.2 Dark Room:

1. Ensure that NO LIGHT is entering the Dark Room at anytime. Turn on Kodak red light.
2. Pour out developer and fixer solutions into appropriate Tupperware containers.
3. Remove film (Amersham Hyperfilm) from light-sealed box and cut piece to cover membrane.
4. Place film on top of membrane in cassette, close and start timer. First exposure attempt should be 1 minute.
5. Remove film from cassette after 1 min and place quickly into developer for 1 min or until dark bands appear on film. Note time in developer if different from 1 min.
6. Place into bin of distilled water to rinse.
7. Place film into fixer (film will turn transparent instead of yellowish).
8. Alter exposure and developing times to get clear band(s). For example, if no bands appear with 1min-1min, expose for longer and develop until bands appear. If dark blobs appear on film, decrease exposure/development time.
9. Before turning lights back on in Dark Room, ensure that all film is back into light-sealed box and that all films have been fixed.
10. Leave films in distilled water for 15 min – overnight
11. Dry films by hanging with clothes pins.
12. Wash membrane for 5 minutes in TBST and air dry on filter paper.

4) REACTIVATING/STRIPPING

4.1 Solutions:

Stripping Buffer (for 1L):

9.85 g Trizma-HCl
7 mL b-mercaptoethanol
200 mL 10% SDS
pH 6.7

Complete up to 1 L with dH_2O
Store at 4°C.

4.2 Stripping Procedure:

1. Immerse dry membrane in methanol for 5 seconds
2. Rinse with dH_2O for 5 minutes.
3. Rinse with TBST for 5 minutes.
4. Preheat oven to 65°C.
5. Immerse activated membrane in Stipping Buffer.
6. Incubate membrane for ~30 minutes with occasional agitation.
7. Wash membrane with TBST for 5 minutes and the proceed onto Blocking Step.

APPENDIX B

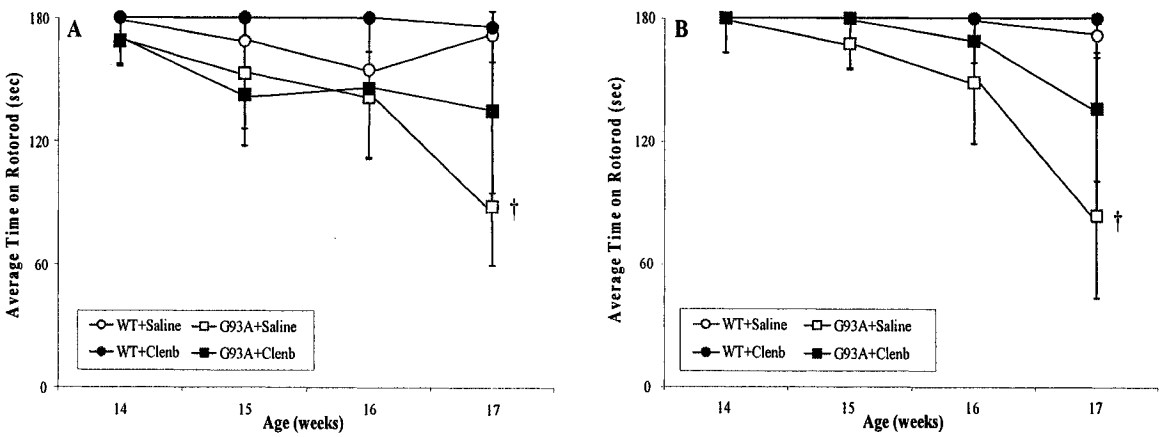

Average RotoRod (RRavg) performance of male (A) and female (B) WT and G93A mice treated with saline or Clenbuterol. Data are expressed as a mean ± SE (n=5-6/group). Circles (○●) represent WT mice; squares (■□) represent G93A mice, treated with saline (open symbols) or Clenbuterol (closed symbols). †Significantly different from WTs mice.

REFERENCES

Adams GR. 1998. Role of insulin-like growth factor-I in the regulation of skeletal muscle adaptation to increased loading. *Exerc Sport Sci Rev* 26: 31-60

Adams GR, Caiozzo VJ, Haddad F, Baldwin KM. 2002. Cellular and molecular responses to increased skeletal muscle loading after irradiation. *Am J Physiol Cell Physiol* 283: C1182-95

Adi S, Bin-Abbas B, Wu NY, Rosenthal SM. 2002. Early stimulation and late inhibition of extracellular signal-regulated kinase 1/2 phosphorylation by IGF-I: a potential mechanism mediating the switch in IGF-I action on skeletal muscle cell differentiation. *Endocrinology* 143: 511-6

Agbenyega ET, Wareham AC. 1990. Effect of clenbuterol on normal and denervated muscle growth and contractility. *Muscle Nerve* 13: 199-203

Agthong S, Kaewsema A, Tanomsridejchai N, Chentanez V. 2006. Activation of MAPK ERK in peripheral nerve after injury. *BMC Neurosci* 7: 45

Alessi DR, Andjelkovic M, Caudwell B, Cron P, Morrice N, Cohen P, Hemmings BA. 1996. Mechanism of activation of protein kinase B by insulin and IGF-1. *Embo J* 15: 6541-51

Alessi DR, Kozlowski MT, Weng QP, Morrice N, Avruch J. 1998. 3-Phosphoinositide-dependent protein kinase 1 (PDK1) phosphorylates and activates the p70 S6 kinase in vivo and in vitro. *Curr Biol* 8: 69-81

Al-Khalili L, Kramer D, Wretenberg P, Krook A. 2004. Human skeletal muscle cell differentiation is associated with changes in myogenic markers and enhanced insulin-mediated MAPK and PKB phosphorylation. *Acta Physiol Scand* 180: 395-403.

Alway SE, Siu PM, Murlasits Z, Butler DC. 2005. Muscle hypertrophy models: applications for research on aging. *Can J Appl Physiol* 30: 591-624

Amthor H, Huang R, McKinnell I, Christ B, Kambadur R, Sharma M, Patel K. 2002. The regulation and action of myostatin as a negative regulator of muscle development during avian embryogenesis. *Dev Biol* 251: 241-57

Ankarcrona M, Dypbukt JM, Orrenius S, Nicotera P. 1996. Calcineurin and mitochondrial function in glutamate-induced neuronal cell death. *FEBS Lett* 394: 321-4

Aoyagi Y, Shephard RJ. 1992. Aging and muscle function. *Sports Med* 14(6): 376-96

Awede BL, Thissen JP, Lebacq J. 2002. Role of IGF-I and IGFBPs in the changes of mass and phenotype induced in rat soleus muscle by clenbuterol. *Am J Physiol Endocrinol Metab* 282: E31-7

Baar K, Esser K. 1999. Phosphorylation of p70(S6k) correlates with increased skeletal muscle mass following resistance exercise. *Am J Physiol* 276: C120-7

Babij P, Booth FW. 1988. Clenbuterol prevents or inhibits loss of specific mRNAs in atrophying rat skeletal muscle. *Am J Physiol* 254: C657-60

Baldwin KM, Haddad F. 2002. Skeletal Muscle Plasticity: Cellular and Molecular Responses to Altered Physical Activity Paradigms. *Am J Phys Med Rehabil* 81(11)Suppl: S40-51

Bamman MM, Shipp JR, Jiang J, Gower BA, Hunter GR, Goodman A, McLafferty CL, Jr., Urban RJ. 2001. Mechanical load increases muscle IGF-I and androgen receptor mRNA concentrations in humans. *Am J Physiol Endocrinol Metab* 280: E383-90

Banker BQ, Engel AG. 1994. Basic reactions of muscle. In: Engel AG, Franzini-Armstrong C (Ed.), Myology: basic and clinical. McGraw-Hill, New York: 832-88

Barton E, Morris C. 2003. Mechanisms and strategies to counter muscle atrophy. *J Gerontol* 58A(10): 923-6

Bassel-Duby R, Olson EN. 2003. Role of calcineurin in striated muscle: development, adaptation, and disease. *Biochem Biophys Res Commun* 311: 1133-41

Bassett JM. 1970. Metabolic effects of catecholamines in sheep. *Aust J Biol Sci* 23: 903-14

Bellinge RH, Liberles DA, Iaschi SP, O'Brien P A, Tay GK. 2005. Myostatin and its implications on animal breeding: a review. *Anim Genet* 36: 1-6

Bhagwati S, Ghatpande A, Shafiq SA, Leung B. 1996. In situ hybridization analysis for expression of myogenic regulatory factors in regenerating muscle of mdx mouse. *J Neuropathol Exp Neurol* 55: 509-14

Bisognano JD, Weinberger HD, Bohlmeyer TJ, Pende A, Raynolds MV, Sastravaha A, Roden R, Asano K, Blaxall BC, Wu SC, Communal C, Singh K, Colucci W, Bristow MR, Port DJ. 2000. Myocardial-directed overexpression of the human beta(1)-adrenergic receptor in transgenic mice. *J Mol Cell Cardiol* 32: 817-30

Bober E, Lyons GE, Braun T, Cossu G, Buckingham M, Arnold HH. 1991. The muscle regulatory gene, Myf-6, has a biphasic pattern of expression during early mouse development. *J Cell Biol* 113: 1255-65

Bodine SC, Stitt TN, Gonzalez M, Kline WO, Stover GL, Bauerlein R, Zlotchenko E, Scrimgeour A, Lawrence JC, Glass DJ, Yancopoulos GD. 2001. Akt/mTOR pathway is a crucial regulator of skeletal muscle hypertrophy and can prevent muscle atrophy in vivo. *Nat Cell Biol* 3: 1014-9

Bodine SC. 2006. mTOR signaling and the molesular adaptation to resistance exercise. *Med Sci Sports Ex* 38(11): 1950-7

Bogdanovich S, Krag TO, Barton ER, Morris LD, Whittemore LA, Ahima RS, Khurana TS. 2002. Functional improvement of dystrophic muscle by myostatin blockade. *Nature* 420: 418-21

Boillee S, Yamanaka K, Lobsiger CS, Copeland NG, Jenkins NA, Kassiotis G, Kollias G, Cleveland DW. 2006. Onset and progression in inherited ALS determined by motor neurons and microglia. *Science* 312: 1389-92

Booth FW, Thomason DB. 1991. Molecular and cellular adaptation of muscle in response to exercise: perspectives of various models. *Physiol Rev* 71: 541-85

Borisov AB, Dedkov EI, Carlson BM. 2001. Interrelations of myogenic response, progressive atrophy of muscle fibers, and cell death in denervated skeletal muscle. *Anat Rec* 264: 203-18

Bricout VA, Serrurier BD, Bigard AX. 2004. Clenbuterol treatment affects myosin heavy chain isoforms and MyoD content similarly in intact and regenerated soleus muscles. *Acta Physiol Scand* 180: 271-80

Brunet A, Bonni A, Zigmond MJ, Lin MZ, Juo P, Hu LS, Anderson MJ, Arden KC, Blenis J, Greenberg ME. 1999. Akt promotes cell survival by phosphorylating and inhibiting a Forkhead transcription factor. *Cell* 96: 857-68

Bullough WS. 1965. Mitotic and functional homeostasis: a speculative review. *Cancer Res* 25: 1683-727

Burniston JG, Ng Y, Clark WA, Colyer J, Tan LB, Goldspink DF. 2002. Myotoxic effects of clenbuterol in the rat heart and soleus muscle. *J Appl Physiol* 93: 1824-32

Burniston JG, Tan LB, Goldspink DF. 2005. beta2-Adrenergic receptor stimulation in vivo induces apoptosis in the rat heart and soleus muscle. *J Appl Physiol* 98: 1379-86

Butler AA, Blakesley VA, Poulaki V, Tsokos M, Wood TL, LeRoith D. 1998. Stimulation of tumor growth by recombinant human insulin-like growth factor-I (IGF-I) is dependent on the dose and the level of IGF-I receptor expression. *Cancer Res* 58: 3021-7

Buyse J, Decuypere E, Huyghebaert G, Herremans M. 1991. The effect of clenbuterol supplementation on growth performance and on plasma hormone and metabolite levels of broilers. *Poult Sci* 70: 993-1002

Campbell M, Allen WE, Sawyer C, Vanhaesebroeck B, Trimble ER. 2004. Glucose-potentiated chemotaxis in human vascular smooth muscle is dependent on cross-talk between the PI3K and MAPK signaling pathways. *Circ Res* 95: 380-8

Carlson CJ, Booth FW, Gordon SE. 1999. Skeletal muscle myostatin mRNA expression is fiber-type specific and increases during hindlimb unloading. *Am J Physiol* 277: R601-6

Carlson BM, Borisov AB, Dedkov EI, Khalyfa A, Kostrominova TY, Macpherson PC, Wang E, Faulkner JA. 2002. Effects of long-term denervation on skeletal muscle in old rats. *J Gerontol A Biol Sci Med Sci* 57: B366-74

Carmen GY, Victor SM. 2006. Signalling mechanisms regulating lipolysis. *Cell Signal* 18(4): 401-8

Carson JA, Wei L. 2000. Integrin signaling's potential for mediating gene expression in hypertrophying skeletal muscle. *J Appl Physiol* 88: 337-43

Carter WJ, Dang AQ, Faas FH, Lynch ME. 1991. Effects of clenbuterol on skeletal muscle mass, body composition, and recovery from surgical stress in senescent rats. *Metabolism* 40: 855-60

Carter WJ, Lynch ME. 1994a. Comparison of the effects of salbutamol and clenbuterol on skeletal muscle mass and carcass composition in senescent rats. *Metabolism* 43: 1119-25

Carter WJ, Lynch ME. 1994b. Effect of clenbuterol on recovery of muscle mass and carcass protein content following dietary protein depletion in young and old rats. *J Gerontol* 49: B162-8

Castle A, Yaspelkis BB, 3rd, Kuo CH, Ivy JL. 2001. Attenuation of insulin resistance by chronic beta2-adrenergic agonist treatment possible muscle specific contributions. *Life Sci* 69: 599-611

Castro C, Diez-Juan A, Cortes MJ, Andres V. 2003. Distinct regulation of mitogen-activated protein kinases and p27Kip1 in smooth muscle cells from different vascular beds. A potential role in establishing regional phenotypic variance. *J Biol Chem* 278: 4482-90

Charge SBP, Rudnicki MA. 2004. Cellular and molecular regulation of muscle regeneration. *Physiol Rev* 84: 209-38

Chen HC, Bandyopadhyay G, Sajan MP, Kanoh Y, Standaert M, Farese RV, Jr., Farese RV. 2002. Activation of the ERK pathway and atypical protein kinase C isoforms in exercise- and aminoimidazole-4-carboxamide-1-beta-D-riboside (AICAR)-stimulated glucose transport. *J Biol Chem* 277: 23554-62

Chen KD, Alway SE. 2000. A physiological level of clenbuterol does not prevent atrophy or loss of force in skeletal muscle of old rats. *J Appl Physiol* 89: 606-12

Chen KD, Alway SE. 2001. Clenbuterol reduces soleus muscle fatigue during disuse in aged rats. *Muscle Nerve* 24: 211-22

Childs TE, Spangenburg EE, Vyas DR, Booth FW. 2003. Temporal alterations in protein signaling cascades during recovery from muscle atrophy. *Am J Physiol Cell Physiol* 285: C391-8

Chiu AY, Zhai P, Dal Canto MC, Peters TM, Kwon YW, Prattis SM, Gurney ME. 1995. Age-dependent penetrance of disease in a transgenic mouse model of familial amyotrophic lateral sclerosis. *Mol Cell Neurosci* 6: 349-62

Cho H, Thorvaldsen JL, Chu Q, Feng F, Birnbaum MJ. 2001. Akt1/PKBalpha is required for normal growth but dispensable for maintenance of glucose homeostasis in mice. *J Biol Chem* 276: 38349-52

Choo JJ, Horan MA, Little RA, Rothwell NJ. 1990. Effects of the beta 2-adrenoceptor agonist, clenbuterol, on muscle atrophy due to food deprivation in the rat. *Metabolism* 39: 647-50

Choo JJ, Horan MA, Little RA, Rothwell NJ. 1992. Anabolic effects of clenbuterol on skeletal muscle are mediated by beta 2-adrenoceptor activation. *Am J Physiol* 263: E50-6

Chuderland D, Seger R. 2005. Protein-protein interactions in the regulation of the extracellular signal-regulated kinase. *Mol Biotechnol* 29: 57-74

Claeys MC, Mulvaney DR, McCarthy FD, Gore MT, Marple DN, Sartin JL. 1989. Skeletal muscle protein synthesis and growth hormone secretion in young lambs treated with clenbuterol. *J Anim Sci* 67: 2245-54

Cockman MD, Jones MB, Prenger MC, Sheldon RJ. 2001. Magnetic resonance imaging of denervation-induced muscle atrophy: effects of Clenbuterol in the rat. *Muscle Nerve* 24: 1647-58

Coleman ME, DeMayo F, Yin KC, Lee HM, Geske R, Montgomery C, Swartz RJ. 1995. Myogenic vector expression of insulin-like growth factor I stimulates muscle cell differentiation and myofiber hypertrophy in transgenic mice. *J Biol Chem* 270(20): 12109-16

Condorelli G, Drusco A, Stassi G, Bellacosa A, Roncarati R, Iaccarino G, Russo MA, Gu Y, Dalton N, Chung C, Latronico MV, Napoli C, Sadoshima J, Croce CM, Ross J, Jr. 2002. Akt induces enhanced myocardial contractility and cell size in vivo in transgenic mice. *Proc Natl Acad Sci U S A* 99: 12333-8

Coolican SA, Samuel DS, Ewton DZ, McWade FJ, Florini JR. 1997. The mitogenic and myogenic actions of insulin-like growth factors utilize distinct signaling pathways. *J Biol Chem* 272: 6653-62

Corbett AJ, Griggs RC, Moxley RT, 3rd. 1982. Skeletal muscle catabolism in amyotrophic lateral sclerosis and chronic spinal muscular atrophy. *Neurology* 32: 550-2

Cornelison DD, Olwin BB, Rudnicki MA, Wold BJ. 2000. MyoD(-/-) satellite cells in single-fiber culture are differentiation defective and MRF4 deficient. *Dev Biol* 224: 122-37

Criswell DS, Powers SK, Herb RA. 1996. Clenbuterol-induced fiber type transition in the soleus of adult rats. *Eur J Appl Physiol Occup Physiol* 74: 391-6

Culmsee C, Semkova I, Krieglstein J. 1999a. NGF mediates the neuroprotective effect of the beta2-adrenoceptor agonist clenbuterol in vitro and in vivo: evidence from an NGF-antisense study. *Neurochem Int* 35: 47-57

Culmsee C, Stumm RK, Schafer MK, Weihe E, Krieglstein J. 1999b. Clenbuterol induces growth factor mRNA, activates astrocytes, and protects rat brain tissue against ischemic damage. *Eur J Pharmacol* 379: 33-45

Cunningham LR. 2005. Increased skeletal muscle Akt content in a murine model of motor neuron disease. M.Sc. (Kinesiology) Thesis, SFU

Daaka Y, Luttrell LM, Lefkowitz RJ. 1997. Switching of the coupling of the beta2-adrenergic receptor to different G proteins by protein kinase A. *Nature* 390: 88-91

Dalrymple RH, Baker PK, Gingher PE, Ingle DL, Pensack JM, Ricks CA. 1984. A repartitioning agent to improve performance and carcass composition of broilers. *Poult Sci* 63: 2376-83

Delday MI, Maltin CA. 1997. Clenbuterol increases the expression of myogenin but not myoD in immobilized rat muscles. *Am J Physiol* 272: E941-4

Derave W, Van Den Bosch L, Lemmens G, Eijnde BO, Robberecht W, Hespel P. 2003. Skeletal muscle properties in a transgenic mouse model for amyotrophic lateral sclerosis: effects of creatine treatment. *Neurobiol Dis* 13: 264-72

DeVol DL, Rotwein P, Sadow JL, Novakofski J, Bechtel PJ. 1990. Activation of insulin-like growth factor gene expression during work-induced skeletal muscle growth. *Am J Physiol* 259: E89-95

Dijkers PF, Medema RH, Pals C, Banerji L, Thomas NS, Lam EW, Burgering BM, Raaijmakers JA, Lammers JW, Koenderman L, Coffer PJ. 2000. Forkhead transcription factor FKHR-L1 modulates cytokine-dependent transcriptional regulation of p27(KIP1). *Mol Cell Biol* 20: 9138-48

Dobrowolny G, Giancinti C, Pelosi L, Nicoletti C, Winn N, Barberi L, Molinaro M, Rosenthal N, Musaro A. 2005. Muscle expression of a local Igf-1 isoform protect motor neurons in an ALS mouse model. *J Cell Biol* 168(2): 193-9

Dodd SL, Powers SK, Vrabas IS, Criswell D, Stetson S, Hussain R. 1996. Effects of clenbuterol on contractile and biochemical properties of skeletal muscle. *Med Sci Sports Exerc* 28: 669-76

Dodd SL, Koesterer TJ. 2002. Clenbuterol attenuates muscle atrophy and dysfunction in hindlimb-suspended rats. *Aviat Space Environ Med* 73: 635-9

Downward J. 1998. Mechanisms and consequences of activation of protein kinase B/Akt. *Curr Opin Cell Biol* 10: 262-7

Dudek H, Datta SR, Franke TF, Birnbaum MJ, Yao R, Cooper GM, Segal RA, Kaplan DR, Greenberg ME. 1997. Regulation of neuronal survival by the serine-threonine protein kinase Akt. *Science* 275: 661-5

Duncan ND, Williams DA, Lynch GS. 2000. Deleterious effects of chronic clenbuterol treatment on endurance and sprint exercise performance in rats. *Clin Sci (Lond)* 98: 339-47

Dunn SE, Burns JL, Michel RN. 1999. Calcineurin is required for skeletal muscle hypertrophy. *J Biol Chem* 274: 21908-12

Dunn SE, Chin ER, Michel RN. 2000. Matching of calcineurin activity to upstream effectors is critical for skeletal muscle fiber growth. *J Cell Biol* 151: 663-72

Dupont-Versteegden EE, Katz MS, McCarter RJ. 1995. Beneficial versus adverse effects of long-term use of clenbuterol in mdx mice. *Muscle Nerve* 18: 1447-59

Dupont-Versteegden EE, Houle JD, Dennis RA, Zhang J, Knox M, Wagoner G, Peterson CA. 2004. Exercise-induced gene expression in soleus muscle is dependent on time after spinal cord injury in rats. *Muscle Nerve* 29: 73-81

Eftimie R, Brenner HR, Buonanno A. 1991. Myogenin and MyoD join a family of skeletal muscle genes regulated by electrical activity. *Proc Natl Acad Sci U S A* 88: 1349-53

Emery PW, Rothwell NJ, Stock MJ, Winter PD. 1984. Chronic effects of beta 2-adrenergic agonists on body composition and protein synthesis in the rat. *Biosci Rep* 4: 83-91

Engelhardt S, Hein L, Wiesmann F, Lohse MJ. 1999. Progressive hypertrophy and heart failure in beta1-adrenergic receptor transgenic mice. *Proc Natl Acad Sci U S A* 96: 7059-64

Fernandez C, Sainz RD. 1997. Pathways of protein degradation in L6 myotubes. *Proc Soc Exp Biol Med* 214: 242-7

Fidzianska A, Gadomski R, Rafalowska J, Chrzanowska H, Grieb P. 2006. Ultrastructural changes in lumbar spinal cord in transgenic SOD1G93A mice. *Folia Neuropathol* 44(3): 175-82

Fischer LR, Culver DG, Tennant P, Davis AA, Wang M, Castellano-Sanchez A, Khan J, Polak MA, Glass JD. 2004. Amyotrophic lateral sclerosis is a distal axonopathy: evidence in mice and man. *Exp Neurol* 185(2): 232-40

Fitton AR, Berry MS, McGregor AD. 2001. Preservation of denervated muscle form and function by clenbuterol in a rat model of peripheral nerve injury. *J Hand Surg [Br]* 26: 335-46

Fluck M, carson JA, Gordon SF, Xiemiecki A, Booth FW. 1999. Focal adhesion proteins FAK and paxillin increase in hypertrophied skeletal muscle. *Am J Physiol* 277: C152-62

Frerichs O, Fansa H, Ziems P, Schneider W, Keilhoff G. 2001. Regeneration of peripheral nerves after clenbuterol treatment in a rat model. *Muscle Nerve* 24: 1687-91

Frey D, Schneider C, Xu L, Borg J, Spooren W, Caroni P. 2000. Early and selective loss of neuromuscular synapse subtypes with low sprouting competence in motoneuron diseases. *J Neurosci* 20: 2534-42

Friday BB, Mitchell PO, Kegley KM, Pavlath GK. 2003. Calcineurin initiates skeletal muscle differentiation by activating MEF2 and MyoD. *Differentiation* 71: 217-27

Furuyama T, Yamashita H, Kitayama K, Higami Y, Shimokawa I, Mori N. 2002. Effects of aging and caloric restriction on the gene expression of Foxo1, 3, and 4 (FKHR, FKHRL1, and AFX) in the rat skeletal muscles. *Microsc Res Tech* 59: 331-4

Glass DJ. 2003a. Molecular mechanisms modulating muscle mass. *Trends Mol Med* 9: 344-50

Glass DJ. 2003b. Signalling pathways that mediate skeletal muscle hypertrophy and atrophy. *Nat Cell Biol* 5: 87-90

Glass DJ. 2005. Skeletal muscle hypertrophy and atrophy signallingn pathways. *Int J Biochem and Cell Biol* 37: 1974-84

Goldberg AL. 1969. Protein turnover in skeletal muscle. II. Effects of denervation and cortisone on protein catabolism in skeletal muscle. *J Biol Chem* 244: 3223-9

Goodpaster BH, Park SW, Harris TB, Kritchevsky SB, Nevitt M, Schwartz AV, Simonsick EM, Tylavsky FA, Visser M, Newman AB. 2006. The loss of skeletal muscle strength, mass, and quality in older adults: the health, aging and body composition study. *J Gerontol A Biol Sci Med Sci* 61: 1059-64

Grunfeld JF, Barhum Y, Blondheim N, Rabey JM, Melamed E, Offen D. 2006. Erythropoietin delays disease onset in an amyotrophic lateral sclerosis model. *Exp Neurol* Dec 14 [Epub ahead of print]

Gurney ME, Pu H, Chiu AY, Dal Canto MC, Polchow CY, Alexander DD, Caliendo J, Hentati A, Kwon YW, Deng HX, et al. 1994. Motor neuron degeneration in mice that express a human Cu,Zn superoxide dismutase mutation. *Science* 264: 1772-5

Haddad F, Adams GR. 2002. Selected contribution: acute cellular and molecular responses to resistance exercise. *J Appl Physiol* 93: 394-403

Halevy O, Cantley LC. 2004. Differential regulation of the phosphoinositide 3-kinase and MAP kinase pathways by hepatocyte growth factor vs. insulin-like growth factor-I in myogenic cells. *Exp Cell Res* 297: 224-34

Hasty P, Bradley A, Morris JH, Edmondson DG, Venuti JM, Olson EN, Klein WH. 1993. Muscle deficiency and neonatal death in mice with a targeted mutation in the myogenin gene. *Nature* 364: 501-6

Hernandez JM, Fedele MJ, Farrell PA. 2000. Time course evaluation of protein synthesis and glucose uptake after acute resistance exercise in rats. *J Appl Physiol* 88: 1142-9

Herrera NM, Jr., Zimmerman AN, Dykstra DD, Thompson LV. 2001. Clenbuterol in the prevention of muscle atrophy: a study of hindlimb-unweighted rats. *Arch Phys Med Rehabil* 82: 930-4

Hinkle RT, Hodge KM, Cody DB, Sheldon RJ, Kobilka BK, Isfort RJ. 2002. Skeletal muscle hypertrophy and anti-atrophy effects of clenbuterol are mediated by the beta2-adrenergic receptor. *Muscle Nerve* 25: 729-34

Hinterberger TJ, Sassoon DA, Rhodes SJ, Konieczny SF. 1991. Expression of the muscle regulatory factor MRF4 during somite and skeletal myofiber development. *Dev Biol* 147: 144-56

Holzbaur EL, Howland DS, Weber N, Wallace K, She Y, Kwak S, Tchistiakova LA, Murphy E, Hinson J, Karim R, Tan XY, Kelley P, McGill KC, Williams G, Hobbs C, Doherty P, Zaleska MM, Pangalos MN, Walsh FS. 2006. Myostatin inhibition slows muscle atrophy in rodent models of amyotrophic lateral sclerosis. *Neurobiol Dis* 23: 697-707

Horne Z, Hesketh J. 1990. Increased association of ribosomes with myofibrils during the skeletal-muscle hypertrophy induced either by the beta-adrenoceptor agonist clenbuterol or by tenotomy. *Biochem J* 272(3): 831-3

Hsu HH, Zdanowicz MM, Agarwal VR, Speiser PW. 1997. Expression of myogenic regulatory factors in normal and dystrophic mice: effects of IGF-1 treatment. *Biochem Mol Med* 60: 142-8

Hu C, Pang S, Kong X, Velleca M, Lawrence JC, Jr. 1994. Molecular cloning and tissue distribution of PHAS-I, an intracellular target for insulin and growth factors. *Proc Natl Acad Sci U S A* 91: 3730-4

Hu JH, Zhang H, Wagey R, Krieger C, Pelech SL. 2003. Protein kinase and protein phosphatase expression in amyotrophic lateral sclerosis spinal cord. *J Neurochem* 85: 432-42

Hutter D, Yo Y, Chen W, Liu P, Holbrook NJ, Roth GS, Liu Y. 2000. Age-related decline in Ras/ERK mitogen-activated protein kinase cascade is linked to a reduced association between Shc and EGF receptor. *J Gerontol A Biol Sci Med Sci* 55: B125-34

Hyatt JP, Roy RR, Baldwin KM, Edgerton VR. 2003. Nerve activity-independent regulation of skeletal muscle atrophy: role of MyoD and myogenin in satellite cells and myonuclei. *Am J Physiol Cell Physiol* 285: C1161-73

Ishido M, Kami K, Masuhara M. 2004a. In vivo expression patterns of MyoD, p21, and Rb proteins in myonuclei and satellite cells of denervated rat skeletal muscle. *Am J Physiol Cell Physiol* 287: C484-93

Ishido M, Kami K, Masuhara M. 2004b. Localization of MyoD, myogenin and cell cycle regulatory factors in hypertrophying rat skeletal muscles. *Acta Physiol Scand* 180: 281-9

Jackman RW, Kandarian SC. 2004. The molecular basis of skeletal muscle atrophy. *Am J Physiol Cell Physiol* 287: C834-43

Jagoe RT, Lecker SH, Gomes M, Goldberg AL. 2002. Patterns of gene expression in atrophying skeletal muscles: response to food deprivation. *Faseb J* 16: 1697-712

Jefferies HB, Fumagalli S, Dennis PB, Reinhard C, Pearson RB, Thomas G. 1997. Rapamycin suppresses 5'TOP mRNA translation through inhibition of p70s6k. *Embo J* 16: 3693-704

Jejurikar SS, Marcelo CL, Kuzon WM, Jr. 2002. Skeletal muscle denervation increases satellite cell susceptibility to apoptosis. *Plast Reconstr Surg* 110: 160-8

Jin Y, Murakami N, Saito Y, Goto Y, Koishi K, Nonaka I. 2000. Expression of MyoD and myogenin in dystrophic mice, mdx and dy, during regeneration. *Acta Neuropathol (Berl)* 99: 619-27

Juliano RL, Reddig P, Alahari S, Edin M, Howe A, Aplin A. 2004. Integrin regulation of cell signalling and motility. *Biochem Soc Trans* 32: 443-6

Kamei Y, Miura S, Suzuki M, Kai Y, Mizukami J, Taniguchi T, Mochida K, Hata T, Matsuda J, Aburatani H, Nishino I, Ezaki O. 2004. Skeletal muscle FOXO1 (FKHR) transgenic mice have less skeletal muscle mass, down-regulated Type I (slow twitch/red muscle) fiber genes, and impaired glycemic control. *J Biol Chem* 279: 41114-23

Kandarian SC, Jackman RW. 2006. Intracellular signaling during skeletal muscle atrophy. *Muscle Nerve* 33: 155-65

Katoch SS, Sharma K. 2004. Clenbuterol treatment stimulates cell proliferation in denervated chick gastrocnemius muscle. *Indian J Exp Biol* 42: 770-5

Katoch SS, Garg A, Sharma K. 2006. Histological evidences of reparative and regenerative effects of beta-adrenoceptor agonists, clenbuterol and isoproterenol, in denervated rat skeletal muscle. *Indian J Exp Biol* 44(6): 448-58

Katoh M, Katoh M. 2006. FGF signaling network in the gastrointestinal tract (review). *Int J Oncol* 29: 163-8

Kearns CF, McKeever KH, Malinowski K, Struck MB, Abe T. 2001. Chronic administration of therapeutic levels of clenbuterol acts as a repartitioning agent. *J Appl Physiol* 91: 2064-70

Kiely J, Hadcock JR, Bahouth SW, Malbon CC. 1994. Glucocorticoids down-regulate beta 1-adrenergic-receptor expression by suppressing transcription of the receptor gene. *Biochem J* 302 (Pt 2): 397-403

Kilts JD, Gerhardt MA, Richardson MD, Sreeram G, Mackensen GB, Grocott HP, White WD, Davis RD, Newman MF, Reves JG, Schwinn DA, Kwatra MM. 2000. Beta(2)-adrenergic and several other G protein-coupled receptors in human atrial membranes activate both G(s) and G(i). *Circ Res* 87: 705-9

Kim YS, Sainz RD. 1992. Beta-adrenergic agonists and hypertrophy of skeletal muscles. *Life Sci* 50: 397-407

Kline WO, Panaro FJ, Yang H, Bodine SC. 2007. Rapamycin inhibits the growth and muscle-sparing effects of clenbuterol. *J Appl Physiol* 102: 740-7.

Knirsch U, Sturm S, Reuter A, Bachus R, Gosztonyi G, Voelkel H, Ludolph AC. 2001. Calcineurin A and calbindin immunoreactivity in the spinal cord of G93A superoxide dismutase transgenic mice. *Brain Res* 889: 234-8

Kocamis H, Killefer J. 2002. Myostatin expression and possible functions in animal muscle growth. *Domest Anim Endocrinol* 23: 447-54

Kosmidou I, Xagorari A, Roussos C, Papapetropoulos A. 2001. Reactive oxygen species stimulate VEGF production from C(2)C(12) skeletal myotubes through a PI3K/Akt pathway. *Am J Physiol Lung Cell Mol Physiol* 280: L585-92

Krieger C, Hu JH, Pelech S. 2003. Aberrant prtein kinases and phosphoproteins in amyotrophic lateral sclerosis. *Trends Pharm Sci* 24(10): 535-41

Laakmann G, Munz T, Hinz A, Voderholzer U. 1990. Influence of clenbuterol, a b-adrenergic agonist, on desipramine induced growth hormone, prolactin and cortisol stimulation. *Psychoneuroendocrinology* 15: 391-9

Lai KM, Gonzalez M, Poueymirou WT, Kline WO, Na E, Zlotchenko E, Stitt TN, Economides AN, Yancopoulos GD, Glass DJ. 2004. Conditional activation of akt in adult skeletal muscle induces rapid hypertrophy. *Mol Cell Biol* 24: 9295-304

Launay T, Armand AS, Charbonnier F, Mira JC, Donsez E, Gallien CL, Chanoine C. 2001. Expression and neural control of myogenic regulatory factor genes during regeneration of mouse soleus. *J Histochem Cytochem* 49: 887-99

Lawlor MA, Rotwein P. 2000. Coordinate control of muscle cell survival by distinct insulin-like growth factor activated signaling pathways. *J Cell Biol* 151: 1131-40

Lee SJ. 2004. Regulation of muscle mass by myostatin. *Annu Rev Cell Dev Biol* 20: 61-86

Leevers SJ, Weinkove D, MacDougall LK, Hafen E, Waterfield MD. 1996. The Drosophila phosphoinositide 3-kinase Dp110 promotes cell growth. *Embo J* 15: 6584-94

Leger B, Vergani L, Soraru G, Hespel P, Derave W, Gobelet C, D'Ascenzio C, Angelini C, Russell AP. 2006. Human skeletal muscle atrophy in amyotrophic lateral sclerosis reveals a reduction in Akt and an increase in atrogin-1. *Faseb J* 20: 583-5

Lev S, Moreno H, Martinez R, Canoll P, Peles E, Musacchio JM, Plowman GD, Rudy B, Schlessinger J. 1995. Protein tyrosine kinase PYK2 involved in Ca(2+)-induced regulation of ion channel and MAP kinase functions. *Nature* 376: 737-45

Li B, Xu W, Luo C, Gozal D, Liu R. 2003. VEGF-induced activation of the PI3-K/Akt pathway reduces mutant SOD1-mediated motor neuron cell death. *Brain Res Mol Brain Res* 111: 155-64

Li L, Heller-Harrison R, Czech M, Olson EN. 1992. Cyclic AMP-dependent protein kinase inhibits the activity of myogenic helix-loop-helix proteins. *Mol Cell Biol* 12: 4478-85

Lowe DA, Lund T, Alway SE. 1998. Hypertrophy-stimulated myogenic regulatory factor mRNA increases are attenuated in fast muscle of aged quails. *Am J Physiol* 275: C155-62

Lowe DA, Alway SE. 1999. Stretch-induced myogenin, MyoD, and MRF4 expression and acute hypertrophy in quail slow-tonic muscle are not dependent upon satellite cell proliferation. *Cell Tissue Res* 296: 531-9

Lu DX, Huang SK, Carlson BM. 1997. Electron microscopic study of long-term denervated rat skeletal muscle. *Anat Rec* 248: 355-65

Ludolph DC, Konieczny SF. 1995. Transcription factor families: muscling in on the myogenic program. *Faseb J* 9: 1595-604

Lynch GS, Hayes A, Campbell SP, Williams DA. 1996. Effects of beta 2-agonist administration and exercise on contractile activation of skeletal muscle fibers. *J Appl Physiol* 81: 1610-8

Lynch GS, Hinkle RT, Faulkner JA. 2001. Force and power output of diaphragm muscle strips from mdx and control mice after clenbuterol treatment. *Neuromuscul Disord* 11: 192-6

Ma L, Chen Z, Erdjument-Bromage H, Tempst P, Pandolfi PP. 2005. Phosphorylation and functional inactivation of TSC2 by Erk implications for tuberous sclerosis and cancer pathogenesis. *Cell* 121: 179-93

MacLennan PA, Edwards RH. 1989. Effects of clenbuterol and propranolol on muscle mass. Evidence that clenbuterol stimulates muscle beta-adrenoceptors to induce hypertrophy. *Biochem J* 264: 573-9

Maltin CA, Reeds PJ, Delday MI, Hay SM, Smith FG, Lobley GE. 1986. Inhibition and reversal of denervation-induced atrophy by the beta-agonist growth promoter, clenbuterol. *Biosci Rep* 6: 811-8

Maltin CA, Delday MI, Hay SM, Smith FG, Lobley GE, Reeds PJ. 1987. The effect of the anabolic agent, clenbuterol, on overloaded rat skeletal muscle. *Biosci Rep* 7: 143-9

Maltin CA, Hay SM, Delday MI, Reeds PJ, Palmer RM. 1989. Evidence that the hypertrophic action of clenbuterol on denervated rat muscle is not propranolol-sensitive. *Br J Pharmacol* 96: 817-22

Maltin CA, Hay SM, McMillan DN, Delday MI. 1992. Tissue specific responses to clenbuterol; temporal changes in protein metabolism of striated muscle and visceral tissues from rats. *Growth Regul* 2: 161-6

Maltin CA, Delday MI, Campbell GP, Hesketh JE. 1993. Clenbuterol mimics effects of innervation on myogenic regulatory factor expression. *Am J Physiol* 265: E176-8

McCroskery S, Thomas M, Maxwell L, Sharma M, Kambadur R. 2003. Myostatin negatively regulates satellite cell activation and self-renewal. *J Cell Biol* 162: 1135-47

McCroskery S, Thomas M, Platt L, Hennebry A, Nishimura T, McLeay L, Sharma M, Kambadur R. 2005. Improved muscle healing through enhanced regeneration and reduced fibrosis in myostatin-null mice. *J Cell Sci* 118: 3531-41

McElligott MA, Mulder JE, Chaung LY, Barreto A, Jr. 1987. Clenbuterol-induced muscle growth: investigation of possible mediation by insulin. *Am J Physiol* 253: E370-5

McFee IJL. 2005. Retrograde transport rates in the G93A mouse model of amyotrophic lateral sclerosis. M.Sc. (Kinesiology) Thesis, SFU

McKinnell IW, Rudnicki MA. 2004. Molecular mechanisms of muscle atrophy. *Cell* 119: 907-10

McMahon CD, Popovic L, Oldham JM, Jeanplong F, Smith HK, Kambadur R, Sharma M, Maxwell L, Bass JJ. 2003. Myostatin-deficient mice lose more skeletal muscle mass than wild-type controls during hindlimb suspension. *Am J Physiol Endocrinol Metab* 285: E82-7

McPherron AC, Lawler AM, Lee SJ. 1997. Regulation of skeletal muscle mass in mice by a new TGF-beta superfamily member. *Nature* 387: 83-90

Mercier J, Perez-Martin A, Bigard X, Ventura R. 1999. Muscle plasticity and metabolism: effects of exercise and chronic diseases. *Mol Aspects Med* 20: 319-73

Metter EJ, Talbot LA, Schrager M, Conwit R. 2002. Skeletal muscle strength as a predictor of all-cause mortality in healthy men. *J Gerontol A Biol Sci Med Sci* 57: B359-65

Miana-Mena FJ, Munoz MJ, Yague G, Mendez M, Moreno M, Ciriza J, Zaragoza P, Osta R. 2005. Optimal methods to characterize the G93A mouse model of ALS. *Amyotroph Lateral Scler Other Motor Neuron Disord* 6: 55-62

Michel RN, Dunn SE, Chin ER. 2004. Calcineurin and skeletal muscle growth. *Proc Nutr Soc* 63: 341-9

Mitchell PO, Mills ST, Pavlath GK. 2002. Calcineurin differentially regulates maintenance and growth of phenotypically distinct muscles. *Am J Physiol Cell Physiol* 282: C984-92

Mitchell PO, Pavlath GK. 2002. Multiple roles of calcineurin in skeletal muscle growth. *Clin Orthop Relat Res*: S197-202

Moore NG, Pegg GG, Sillence MN. 1994. Anabolic effects of the beta 2-adrenoceptor agonist salmeterol are dependent on route of administration. *Am J Physiol* 267: E475-84

Mozdziak PE, Greaser ML, Schultz E. 1998. Myogenin, MyoD, and myosin expression after pharmacologically and surgically induced hypertrophy. *J Appl Physiol* 84: 1359-64

Murphy RJ, Beliveau L, Seburn KL, Gardiner PF. 1996. Clenbuterol has a greater influence on untrained than on previously trained skeletal muscle in rats. *Eur J Appl Physiol Occup Physiol* 73: 304-10

Musaro A, McCullagh K, Paul A, Houghton L, Dobrowolny G, Molinaro M, Barton ER, Sweeney HL, Rosenthal N. 2001. Localized Igf-1 transgene expression sustains hypertrophy and regeneration in senescent skeletal muscle. *Nat Genet* 27: 195-200

Musaro A, McCullagh KJ, Naya FJ, Olson EN, Rosenthal N. 1999. IGF-1 induces skeletal myocyte hypertrophy through calcineurin in association with GATA-2 and NF-ATc1. *Nature* 400: 581-5

Musaro A, Rosenthal N. 1999. Transgenic mouse models of muscle agin. *Exp Gerontol* 34: 147-56

Myer A, Wagner DS, Vivian JL, Olson EN, Klein WH. 1997. Wild-type myoblasts rescue the ability of myogenin-null myoblasts to fuse in vivo. *Dev Biol* 185: 127-38

Myers MG, Jr., Sun XJ, White MF. 1994. The IRS-1 signaling system. *Trends Biochem Sci* 19: 289-93

Nabeshima Y, Hanaoka K, Hayasaka M, Esumi E, Li S, Nonaka I, Nabeshima Y. 1993. Myogenin gene disruption results in perinatal lethality because of severe muscle defect. *Nature* 364: 532-5

Nader GA, Esser KA. 2001. Intracellular signaling specificity in skeletal muscle in response to different modes of exercise. *J Appl Physiol* 90: 1936-42

Nakae J, Kitamura T, Silver DL, Accili D. 2001. The forkhead transcription factor Foxo1 (Fkhr) confers insulin sensitivity onto glucose-6-phosphatase expression. *J Clin Invest* 108: 1359-67

Naya FJ, Mercer B, Shelton J, Richardson JA, Williams RS, Olson EN. 2000. Stimulation of slow skeletal muscle fiber gene expression by calcineurin in vivo. *J Biol Chem* 275: 4545-8

Oishi Y, Imoto K, Ogata T, Taniguchi K, Matsumoto H, Fukuoka Y, Roy RR. 2004. Calcineurin and heat-shock proteins modulation in clenbuterol-induced hypertrophied rat skeletal muscles. *Pflugers Arch* 448: 114-22

Oliveira AS, Corbo M, Duigou G, Gabbai AA, Hays AP. 1993. Expression of a cell death marker (Clusterin) in muscle target fibers. *Arq Neuropsiquiatr* 51: 371-6

Olson EN. 1992. Proto-oncogenes in the regulatory circuit for myogenesis. *Semin Cell Biol* 3: 127-36

Pachter BR, Eberstein A. 1992. Long-term effects of partial denervation on sprouting and muscle fiber area in rat plantaris. *Exp Neurol* 116: 246-55

Pallafacchina G, Calabria E, Serrano AL, Kalhovde JM, Schiaffino S. 2002. A protein kinase B-dependent and rapamycin-sensitive pathway controls skeletal muscle growth but not fiber type specification. *Proc Natl Acad Sci U S A* 99: 9213-8

Pan SJ, Hancock J, Ding Z, Fogt D, Lee M, Ivy JL. 2001. Effects of clenbuterol on insulin resistance in conscious obese Zucker rats. *Am J Physiol Endocrinol Metab* 280: E554-61

Parkington JD, Siebert AP, LeBrasseur NK, Fielding RA. 2003. Differential activation of mTOR signaling by contractile activity in skeletal muscle. *Am J Physiol Regul Integr Comp Physiol* 285: R1086-90

Pellegrino MA, D'Antona G, Bortolotto S, Boschi F, Pastoris O, Bottinelli R, Polla B, Reggiani C. 2004. Clenbuterol antagonizes glucocorticoid-induced atrophy and fibre type transformation in mice. *Exp Physiol* 89: 89-100

Perry RLS, Rudnicki MA. 2000. Molecular mechanisms regulating myogenic determination and differentiation. *Front Biosci* 5: d750-67

Pesce L, Guerrero C, Comellas A, Ridge KM, Sznajder JI. 2000. beta-agonists regulate Na,K-ATPase via novel MAPK/ERK and rapamycin-sensitive pathways. *FEBS Lett* 486: 310-4

Picquet F, De-Doncker L, Falempin M. 2004. Enhancement of hybrid-fiber types in rat soleus muscle after clenbuterol administration during hindlimb unloading. *Can J Physiol Pharmacol* 82: 311-8

Polla B, Cappelli V, Morello F, Pellegrino MA, Boschi F, Pastoris O, Reggiani C. 2001. Effects of the beta(2)-agonist clenbuterol on respiratory and limb muscles of weaning rats. *Am J Physiol Regul Integr Comp Physiol* 280: R862-9

Potter CJ, Pedraza LG, Huang H, Xu T. 2003. The tuberous sclerosis complex (TSC) pathway and mechanism of size control. *Biochem Soc Trans* 31: 584-6

Price RD, Yamaji T, Matsuoka N. 2003. FK506 potentiates NGF-induced neurite outgrowth via the Ras/Raf/MAP kinase pathway. *Br J Pharmacol* 140: 825-9

Psilander N, Damsgaard R, Pilegaard H. 2003. Resistance exercise alters MRF and IGF-I mRNA content in human skeletal muscle. *J Appl Physiol* 95: 1038-44

Puri PL, Sartorelli V. 2000. Regulation of muscle regulatory factors by DNA-binding, interacting proteins, and post-transcriptional modifications. *J Cell Physiol* 185: 155-73

Rabinovsky ED, Gelir E, Felir S, Lui H, Kattash M, Demayo RJ, Shenaq SM, Schwartz RJ. 2002. Targeted expression of IGF-1 transgene to skeletal muscle accelerates muscle and motor neuron regeneration. *FASEB* 17: 53-5

Reeds PJ, Hay SM, Dorward PM, Palmer RM. 1988. The effect of beta-agonists and antagonists on muscle growth and body composition of young rats (Rattus sp.). *Comp Biochem Physiol C* 89: 337-41

Rennie MJ, Wackerhage H, Spangenburg EE, Booth FW. 2004. Control of the size of the human muscle mass. *Annu Rev Physiol* 66: 799-828

Rescan PY. 2001. Regulation and functions of myogenic regulatory factors in lower vertebrates. *Comp Biochem Physiol B Biochem Mol Biol* 130: 1-12

Riaz SS, Tomlinson DR. 1999. Clenbuterol stimulates neurotrophic support in streptozotocin-diabetic rats. *Diabetes Obes Metab* 1: 43-51

Ricart-Firinga C, Stevens L, Canu MH, Nemirovskaya TL, Mounier Y. 2000. Effects of beta(2)-agonist clenbuterol on biochemical and contractile properties of unloaded soleus fibers of rat. *Am J Physiol Cell Physiol* 278: C582-8

Rommel C, Bodine SC, Clarke BA, Rossman R, Nunez L, Stitt TN, Yancopoulos GD, Glass DJ. 2001. Mediation of IGF-1-induced skeletal myotube hypertrophy by PI(3)K/Akt/mTOR and PI(3)K/Akt/GSK3 pathways. *Nat Cell Biol* 3: 1009-13

Roth SM, Martel GF, Ferrell RE, Metter EJ, Hurley BF, Rogers MA. 2003. Myostatin gene expression is reduced in humans with heavy-resistance strength training: a brief communication. *Exp Biol Med (Maywood)* 228: 706-9

Roth SM, Walsh S. 2004. Myostatin: a therapeutic target for skeletal muscle wasting. *Curr Opin Clin Nutr Metab Care* 7: 259-63

Rothwell NJ, Stock MJ. 1985. Modification of body composition by clenbuterol in normal and dystrophic (mdx) mice. *Biosci Rep* 5: 755-60

Rudnicki MA, Braun T, Hinuma S, Jaenisch R. 1992. Inactivation of MyoD in mice leads to up-regulation of the myogenic HLH gene Myf-5 and results in apparently normal muscle development. *Cell* 71: 383-90

Sabourin LA, Rudnicki MA. 2000. The molecular regulation of myogenesis. *Clin Genet* 57: 16-25

Sabri A, Pak E, Alcott SA, Wilson BA, Steinberg SF. 2000. Coupling function of endogenous alpha(1)- and beta-adrenergic receptors in mouse cardiomyocytes. *Circ Res* 86: 1047-53

Sakamoto K, Goodyear LJ. 2002. Invited review: intracellular signaling in contracting skeletal muscle. *J Appl Physiol* 93: 369-83

Sakuma K, Watanabe K, Sano M, Uramoto I, Sakamoto K, Totsuka T. 1999. The adaptive response of MyoD family proteins in overloaded, regenerating and denervated rat muscles. *Biochim Biophys Acta* 1428: 284-92

Sakuma K, Watanabe K, Sano M, Uramoto I, Totsuka T. 2000. Postnatal profiles of myogenic regulatory factors and the receptors of TGF-beta 2, LIF and IGF-I in the gastrocnemius and rectus femoris muscles of dy mouse. *Acta Neuropathol (Berl)* 99: 169-76

Sakuma K, Nishikawa J, Nakao R, Watanabe K, Totsuka T, Nakano H, Sano M, Yasuhara M. 2003. Calcineurin is apotent regulator for skeletal muscle regeneration by association with NFATc1 and GATA-2. *Acta Neuropathol* 105: 271-80

Sandri M, Sandri C, Gilbert A, Skurk C, Calabria E, Picard A, Walsh K, Schiaffino S, Lecker SH, Goldberg AL. 2004. Foxo transcription factors induce the atrophy-related ubiquitin ligase atrogin-1 and cause skeletal muscle atrophy. *Cell* 117: 399-412

Sartorelli C, Fulco M. 2004. Molecular and cellular determinants of skeletal muscle atrophy and hypertrophy. *Sci STKE* 244: re11

Scheid MP, Woodgett JR. 2001. PKB/AKT: functional insights from genetic models. *Nat Rev Mol Cell Biol* 2: 760-8

Schiaffino S, Serrano A. 2002. Calcineurin signaling and neural control of skeletal muscle fiber type and size. *Trends Pharmacol Sci* 23: 569-75

Schoser BGH, Wehling S, Blottner D. 2001. Cell death and apoptosis-related proteins in muscle biopsies of sporadic amyotrophic lateral sclerosis and polyneuropathy. *Muscle Nerve* 24: 1083-9

Schuelke M, Wagner KR, Stolz LE, Hubner C, Riebel T, Komen W, Braun T, Tobin JF, Lee SJ. 2004. Myostatin mutation associated with gross muscle hypertrophy in a child. *N Engl J Med* 350: 2682-8

Semkova I, Schilling M, Henrich-Noack P, Rami A, Krieglstein J. 1996. Clenbuterol protects mouse cerebral cortex and rat hippocampus from ischemic damage and attenuates glutamate neurotoxicity in cultured hippocampal neurons by induction of NGF. *Brain Res* 717: 44-54

Semkova I, Krieglstein J. 1999. Neuroprotection mediated via neurotrophic factors and induction of neurotrophic factors. *Brain Res Rev* 30: 176-88

Semsarian C, Sutrave P, Richmond DR, Graham RM. 1999a. Insulin-like growth factor (IGF-I) induces myotube hypertrophy associated with an increase in anaerobic glycolysis in a clonal skeletal-muscle cell model. *Biochem J* 339 (Pt 2): 443-51

Semsarian C, Wu MJ, Ju YK, Marciniec T, Yeoh T, Allen DG, Harvey RP, Graham RM. 1999b. Skeletal muscle hypertrophy is mediated by a Ca2+-dependent calcineurin signalling pathway. *Nature* 400: 576-81

Serrano AL, Murgia M, Pallafacchina G, Calabria E, Coniglio P, Lomo T, Schiaffino S. 2001. Calcineurin controls nerve activity-dependent specification of slow skeletal muscle fibers but not muscle growth. *Proc Natl Acad Sci U S A* 98: 13108-13

Shah OJ, Anthony JC, Kimball SR, Jefferson LS. 2000a. 4E-BP1 and S6K1: translational integration sites for nutritional and hormonal information in muscle. *Am J Physiol Endocrinol Metab* 279: E715-29

Shah OJ, Kimball SR, Jefferson LS. 2000b. Among translational effectors, p70S6k is uniquely sensitive to inhibition by glucocorticoids. *Biochem J* 347: 389-97

Shavlakadze T, Winn N, Rosenthal N, Grounds MD. 2005. Reconciling data from transgenic mice that overexpress IGF-1 specifically in skeletal muscle. *Growth Horm IGF Res* 15(1): 4-18

Shi H, Zeng C, Ricome A, Hannon K, Grant A, Gerrard DE. 2006. Extracellular Signal-regulated Kinase Pathway is Differentially Involved in Beta Agonist-induced Hypertrophy in Slow and Fast Muscles. *Am J Physiol Cell Physiol* Dec 6; [Epub ahead of print]

Shi X, Garry DJ. 2006. Muscle stem cells in development, regeneration, and disease. *Genes Dev* 20: 1692-708

Sillence MN, Matthews ML, Moore NG, Reich MM. 1995. Effects of BRL-47672 on growth, beta 2-adrenoceptors, and adenylyl cyclase activation in female rats. *Am J Physiol* 268: E159-67

Smith WN, Dirks A, Sugiura T, Muller S, Scarpace P, Powers SK. 2002. Alteration of contractile force and mass in the senescent diaphragm with beta(2)-agonist treatment. *J Appl Physiol* 92: 941-8

Sneddon AA, Delday MI, Maltin CA. 2000. Amelioration of denervation-induced atrophy by clenbuterol is associated with increased PKC-alpha activity. *Am J Physiol Endocrinol Metab* 279: E188-95

Sneddon AA, Delday MI, Steven J, Maltin CA. 2001. Elevated IGF-II mRNA and phosphorylation of 4E-BP1 and p70(S6k) in muscle showing clenbuterol-induced anabolism. *Am J Physiol Endocrinol Metab* 281: E676-82

Solomon AM, Bouloux PM. 2006. Modifying muscle mass - the endocrine perspective. *J Endocrinol* 191: 349-60

Spangenburg EE, Booth FW. 2003. Molecular regulation of individual skeletal muscle fibre types. *Acta Physiol Scand* 178: 413-24

Spurlock DM, McDaneld TG, McIntyre LM. 2006. Changes in skeletal muscle gene expression following clenbuterol administration. *BMC Genomics* 7:320

Stewart CE, Rittweger J. 2006. Adaptive processes in skeletal muscle: molecular regulators and genetic influences. *J Musculoskelet Neuronal Interact* 6: 73-86

Stupka N, Gregorevic P, Plant DR, Lynch GS. 2004. The calcineurin signal transduction pathway is essential for successful muscle regeneration in mdx dystrophic mice. *Acta Neuropathol (Berl)* 107: 299-310

Sugiura T, Abe N, Nagano M, Goto K, Sakuma K, Naito H, Yoshioka T, Powers SK. 2005. Changes in PKB/Akt and calcineurin signaling during recovery in atrophied soleus muscle induced by unloading. *Am J Physiol Regul Integr Comp Physiol* 288: R1273-8

Taylor WE, Bhasin S, Artaza J, Byhower F, Azam M, Willard DH, Jr., Kull FC, Jr., Gonzalez-Cadavid N. 2001. Myostatin inhibits cell proliferation and protein synthesis in C2C12 muscle cells. *Am J Physiol Endocrinol Metab* 280: E221-8

Tee AR, Fingar DC, Manning BD, Kwiatkowski DJ, Cantley LC, Blenis J. 2002. Tuberous sclerosis complex-1 and -2 gene products function together to inhibit mammalian target of rapamycin (mTOR)-mediated downstream signaling. *Proc Natl Acad Sci U S A* 99: 13571-6

Teng YD, Choi H, Huang W, Onario RC, Frontera WR, Snyder EY, Sabharwal S. 2006. Therapeutic effects of clenbuterol in a murine model of amyotrophic lateral sclerosis. *Neurosci Lett* 397: 155-8

Theys PA, Peeters E, Robberecht W. 1999. Evolution of motor and sensory deficits in amyotrophic lateral sclerosis estimated by neurophysiological techniques. *J Neurol* 246: 438-42

Thomas CK, Zijdewind I. 2006. Fatigue of muscles weakened by death of motoneurons. *Muscle Nerve* 33: 21-41

Toker A, Newton AC. 2000. Cellular signaling: pivoting around PDK-1. *Cell* 103: 185-8

Van Eyk JE, Arrell DK, Foster DB, Strauss JD, Heinonen TY, Furmaniak-Kazmierczak E, Cote GP, Mak AS. 1998. Different molecular mechanisms for Rho family GTPase-dependent, Ca2+-independent contraction of smooth muscle. *J Biol Chem* 273: 23433-9

Veldink JH, Bar PR, Joosten EAJ, Otten M, Wokke JHJ, van den Berg LH. 2003. Sexual differences in onset of disease and response to exercise in a transgenic model of ALS. *Neuromusc Disord* 13: 737-43

Venuti JM, Morris JH, Vivian JL, Olson EN, Klein WH. 1995. Myogenin is required for late but not early aspects of myogenesis during mouse development. *J Cell Biol* 128: 563-76

von Deutsch DA, Abukhalaf IK, Wineski LE, Roper RR, Aboul-Enein HY, Paulsen DF, Potter DE. 2002. Distribution and muscle-sparing effects of clenbuterol in hindlimb-suspended rats. *Pharmacology* 65: 38-48

von Deutsch DA, Abukhalaf IK, Wineski LE, Silvestrov NA, Bayorh MA, Potter DE. 2003. Changes in muscle proteins and spermidine content in response to unloading and clenbuterol treatment. *Can J Physiol Pharmacol* 81: 28-39

Voytik SL, Przyborski M, Badylak SF, Konieczny SF. 1993. Differential expression of muscle regulatory factor genes in normal and denervated adult rat hindlimb muscles. *Dev Dyn* 198: 214-24

Wagner KR, McPherron AC, Winik N, Lee SJ. 2002. Loss of myostatin attenuates severity of muscular dystrophy in mdx mice. *Ann Neurol* 52: 832-6

Walters EH, Stickland NC, Loughna PT. 2000. The expression of the myogenic regulatory factors in denervated and normal muscles of different phenotypes. *J Muscle Res Cell Motil* 21: 647-53

Wang HG, Pathan N, Ethell IM, Krajewski S, Yamaguchi Y, Shibasaki F, McKeon F, Bobo T, Franke TF, Reed JC. 1999. Ca2+-induced apoptosis through calcineurin dephosphorylation of BAD. *Science* 284: 339-43

Wang L, Gout I, Proud CG. 2001. Cross-talk between the ERK and p70 S6 kinase (S6K) signaling pathways. MEK-dependent activation of S6K2 in cardiomyocytes. *J Biol Chem* 276: 32670-7

Wehling M, Cai B, Tidball JG. 2000. Modulation of myostatin expression during modified muscle use. *Faseb J* 14: 103-10

Weinkove D, Leevers SJ. 2000. The genetic control of organ growth: insights from Drosophila. *Curr Opin Genet Dev* 10(1): 75-80

Weinstein RB, Slentz MJ, Webster K, Takeuchi JA, Tischler ME. 1997. Lysosomal proteolysis in distally or proximally denervated rat soleus muscle. *Am J Physiol* 273: R1562-5

Weydt P, Hong SY, Kliot M, Moller T. 2003. Assessing disease onset and progression in the SOD1 mouse model of ALS. *Neuroreport* 14: 1051-4

Widegren U, Wretman C, Lionikas A, Hedin G, Henriksson J. 2000. Influence of exercise intensity on ERK/MAP kinase signalling in human skeletal muscle. *Pflugers Arch* 441: 317-22

Widegren U, Ryder JW, Zierath JR. 2001. Mitogen-activated protein kinase signal transduction in skeletal muscle: effects of exercise and muscle contraction. *Acta Physiol Scand* 172: 227-38

Williamson D, Gallagher P, Harber M, Hollon C, Trappe S. 2003. Mitogen-activated protein kinase (MAPK) pathway activation: effects of age and acute exercise on human skeletal muscle. *J Physiol* 547: 977-87

Williamson DL, Kubica N, Kimball SR, Jefferson LS. 2006. Exercise-induced alterations in extracellular signal-regulated kinase 1/2 and mammalian target of rapamycin (mTOR) signalling to regulatory mechanisms of mRNA translation in mouse muscle. *J Physiol* 573: 497-510

Wineski LE, von Deutsch DA, Abukhalaf IK, Pitts SA, Potter DE, Paulsen DF. 2002. Muscle-specific effects of hindlimb suspension and clenbuterol in mature male rats. *Cells Tissues Organs* 171: 188-98

Wooley CM, Sher RB, Kale A, Frankel WN, Cox GA, Seburn KL. 2005. Gait analysis detects early changes in transgenic SOD1(G93A) mice. *Muscle Nerve* 32: 43-50

Woscholski R, Kodaki T, Parker PJ. 1995. The lipid kinase activity of the phosphatidylinositol 3-kinase is affected by its intrinsic protein kinase activity. *Biochem Soc Trans* 23: 14S

Wu Z, Jin H, Gu Y. 2002. [The effect of MyoD family proteins on muscular atrophy induced by brachial plexus injury in rats]. *Zhonghua Yi Xue Za Zhi* 82: 561-3

Xu F, Salpeter MM. 1995. Protein kinase A regulates the degradation rate of Rs acetylcholine receptors. *J Cell Physiol* 165: 30-9

Yamaguchi A, Ishii H, Morita I, Oota I, Takeda H. 2004. mRNA expression of fibroblast growth factors and hepatocyte growth factor in rat plantaris muscle following denervation and compensatory overload. *Pflugers Arch* 448: 539-46

Yang E, Zha J, Jockel J, Boise LH, Thompson CB, Korsmeyer SJ. 1995. Bad, a heterodimeric partner for Bcl-XL and Bcl-2, displaces Bax and promotes cell death. *Cell* 80: 285-91

Yang Y, MCElligott M. 1989. Multiple actions of beta-adrenergic agonists on skeletal muscle and adipose tissue. *Biochem J.* 261: 1-10

Young OA, Watkins S, Oldham JM, Bass JJ. 1995. The role of insulin-like growth factor I in clenbuterol-stimulated growth in growing lambs. *J Anim Sci* 73: 3069-77

Zeman RJ, Ludemann R, Etlinger JD. 1987. Clenbuterol, a beta 2-agonist, retards atrophy in denervated muscles. *Am J Physiol* 252: E152-5

Zeman RJ, Ludemann R, Easton TG, Etlinger JD. 1988. Slow to fast alterations in skeletal muscle fibers caused by clenbuterol, a beta 2-receptor agonist. *Am J Physiol* 254: E726-32

Zeman RJ, Feng Y, Peng H, Etlinger JD. 1999. Clenbuterol, a beta(2)-adrenoceptor agonist, improves locomotor and histological outcomes after spinal cord contusion in rats. *Exp Neurol* 159: 267-73

Zeman RJ, Peng H, Danon MJ, Etlinger JD. 2000. Clenbuterol reduces degeneration of exercised or aged dystrophic (mdx) muscle. *Muscle Nerve* 23: 521-8

Zeman RJ, Peng H, Etlinger JD. 2004. Clenbuterol retards loss of motor function in motor neuron degeneration mice. *Exp Neurol* 187: 460-7

Zhu WZ, Zheng M, Koch WJ, Lefkowitz RJ, Kobilka BK, Xiao RP. 2001. Dual modulation of cell survival and cell death by beta(2)-adrenergic signaling in adult mouse cardiac myocytes. *Proc Natl Acad Sci U S A* 98: 1607-12

Zimmers TA, Davies MV, Koniaris LG, Haynes P, Esquela AF, Tomkinson KN, McPherron AC, Wolfman NM, Lee SJ. 2002. Induction of cachexia in mice by systemically administered myostatin. *Science* 296: 1486-8